Hmi1p and UvrD: Two Superfamily I Helicases and their Respective Roles in *S. cerevisiae* mtDNA Maintenance and *E. coli* Methyl-Directed Mismatch Repair

Danny Scott Monroe Jr.

A dissertation submitted to the faculty of the University of North Carolina at Chapel Hill in partial fulfillment of the requirements for the degree of Doctor of Philosophy in the Department of Biology.

Chapel Hill
2008

Approved by:

Steven Matson

William Copeland

William Marzluff

Thomas Petes

Jeff Sekelsky

ABSTRACT

Danny Scott Monroe Jr.

Hmi1p and UvrD: Two Superfamily I Helicases and their Respective Roles in *S. cerevisiae* mtDNA Maintenance and *E. coli* Methyl-Directed Mismatch Repair

(Under the direction of Steven Matson)

Helicases are vital to all aspects of genomic maintenance. Double-stranded DNA, DNA/RNA hybrids, and self-annealed RNA require the action of this class of proteins to separate into single-stranded components that can be manipulated for cellular function and survival.

Hmi1p, a Superfamily I helicase shown to localize to the mitochondria, is required to maintain mtDNA in *Saccharomyces cerevisiae*. Through biochemical studies, we are able to show that Hmi1p is a nucleic acid stimulated NTPase that unwinds DNA in a 3'→5' direction. Furthermore, we show that site-directed mutagenesis of the conserved lysine residue of the Walker A box effectively obliterates ATP hydrolysis and, therefore, helicase activity. Suprisingly, genetic analyses indicate that this ATP hydrolysis mutant is able to partially complement the petite phenotype associated with Δ*hmi1* mutants. A possible structural role as part of the mtDNA replication machinery and future experimentation is discussed.

The *Escherichia coli* Superfamily I helicase, UvrD, is involved in replication, nucleotide excision repair, and methyl-directed mismatch repair (MMR). The role of UvrD in MMR is well-defined but the mechanism of unwinding stimulation by the protein MutL is

poorly understood. We have constructed and tested a substrate designed to track relative distances of MutL and UvrD along a dsDNA region through the use of single-molecule FRET (smFRET) and total internal reflection microscopy (TIRM). We show that UvrD and MutL bind the substrate separately and, when combined, enhance the binding of both proteins to the DNA. An in-depth discussion of necessary controls and experiments is expanded upon to unravel this mechanism.

For Stephen and Austin

ACKNOWLEDGEMENTS

From the outset, I would like to thank my advisor, Steve Matson, and my committee for overseeing my graduate career. Their guidance has shaped me into a better scientist capable of critical thought and analysis. This work is the representative culmination of the 20+ years behind my formal education and, for that, an immense amount of praise and thanks is due to all of the teachers that have contributed to my development.

Special thanks are extended to my maternal grandparents and the Cope family for being there for me at every turn and having very direct, nurturing roles in my growth. My wife, Sarah, also receives special thanks for keeping me focused and sane through the numerous mental trials that accompany all graduate careers. Her support has been invaluable through this journey.

All of my accomplishments and achievements are products of a loving and supportive upbringing. I am among the fortunate few having been blessed with parents that put their children above themselves. My mother and father always have (and still do) sacrifice aspects of their own lives for my brother and me. They have been exemplary role models as providers and parents, sacrificing time and money for the growth and development of their children. This piece of work is but a small token of the fruits of their labor and I hope and pray that their example will give me the strength and resolve to do the same for my family.

TABLE OF CONTENTS

LIST OF TABLES

Table

LIST OF FIGURES

LIST OF ABBREVIATIONS

AMP-PNP	Adenosine-5'-(β,γ-imido) triphosphates
ATP	Adenosine-5'-triphosphate
ATP-γ-S	Adenosine-5'-O-(3-thiotriphosphate)
BSA	Bovine serum albumin
CBD	Chitin binding domain
dATP	Deoxyadenosine triphosphate
DMSO	Dimethyl Sulfoxide
DNA	Deoxyribonucleic acid
dsDNA	Double-stranded deoxyribonucleic acid
DTT	Dithiothreitol
dTTP	2'-Deoxythymine-5'-Triphosphate
EDTA	Ethylenediamine tetraacetic acid
EGTA	Ethylene glycol tetraacetic acid
FRET	Forster resonance energy transfer
GLUCOT	Glucose and 1,3,5,7-cyclooctatetraene
GOXCAT	Glucose oxidase and catalase
GST	Glutathione-S-transferase
HEPES	N-[2-Hydroxyethyl] piperazine-N'-[2-Ethanesulfonic acid]
IDL	Insertion-deletion loop
IPTG	Isopropyl-β-D-thiogalactopyranoside
K32A	32nd amino acid, lysine, changed to an alanine
K32M	32nd amino acid, lysine, changed to a methionine

K32S	32nd amino acid, lysine, changed to a serine
LB	Luria-Bertani broth
LC20	MutL carboxyl terminal 183 amino acids
LN40	MutL amino terminal331 aminoacids
MBP	Maltose binding protein
MMR	Methyl-directed mismatch repair
mtDNA	Mitochondria deoxyribonucleic acid
NaPi	Sodium Phosphate
NTP	Nucleoside triphosphates
NTP	Nucleotide Triphosphate
OD	Optical density
PCA	Protochatecuic acid
PCD	protochatecuate-3,4-dioxygenase
PCR	Polymerase chain reaction
PMSF	Phenylmethanesulfonyl fluoride
PNK	Polynucleotide kinase
rATP	Riboadenosine triphosphates
RNA	Ribonucleic acid
rRNA	Ribosomal ribonucleic acid
SD	Selective dropout media
SDS	Sodium dodecyl sulfate
SDS-PAGE	Sodium dodecyl sulfate polyacrylamide gel electrophoresis
smFRET	Single-molecule Forster resonance energy transfer

SSB	Single-strand binding protein
ssDNA	Single-stranded deoxyribonucleic acid
TAMRA	Tetramethyl-6-carboxyrhodamine
TBE	Tris base, boric acid, and EDTA
TIR	Total internal reflection
TIRM	Total internal reflection microscopy
Tris	Tris [hydroxymethyl] aminomethane
TRITC	Tetramethyl rhodamine iso-thiocyanate
trp	Tryptophan
ura	Uracil
YPD	Yeast extract, peptone, dextrose
YPEG	Yeast extract, peptone, ethanol, glycerol
α-[^{32}P]dCTP	2'Deoxycytidine-5'-triphosphate ^{32}P labeled on the α phosphate
β-ME	2-mercaptoethanol
γ-[^{32}P]ATP	Adenosine-5'-triphosphate ^{32}P labeled on the γ phosphate

Chapter 1

Concerning helicases and their diversity

From bacteria and yeast to plants and animals, all living things must maintain and interpret their DNA to ensure organism viability and long term species survival. Maintenance and interpretation tasks include but are not limited to DNA replication, transcription, translation, recombination, and DNA repair. Each of these processes is a very precise and controlled operation where a jack-of-all-trades protein just isn't feasible. Rather, each process requires a host of enzymes that work together to perform very specialized functions in order to maintain a great deal of control.

Consider the diversity among polymerases in eukaryotes. This class of proteins has the vital role of synthesizing chains of nucleic acids and some act on DNA while others act on RNA. There are three nuclear RNA polymerases, each associated with transcription beginning at a particular type of promoter. RNA polymerase II is charged with transcribing the genes for the majority of the cell's proteins while RNA polymerase I and III transcribe large rRNA and catalytic/structural RNA, respectively (1-4). When considering DNA polymerases, the high-fidelity A and B families are most familiar. The A family polymerase, Polγ, functions as the mitochondrial polymerase while the three family B polymerases (Pol α, Pol δ, and Pol ε) are involved in nuclear genome replication and repair (reviewed in (5)). Beyond these well-known polymerases there are the more error-prone Y-family polymerases (η, κ, and ι) that are involved in translesion synthesis (reviewed in (6)) and the X-family of polymerases (β, λ, and μ) that are involved in repair and recombination (reviewed in (7)).

The eukaryotic cell even has a specific polymerase in place charged with regenerating telomere length (8). Because DNA is the very soul of the cell (without which propagation and survival would not be possible), it is easy to understand why there exists such a diversity of proteins involved in the numerous aspects of genome maintenance.

This same idea also applies to helicases. Helicases are instrumental to all aspects of genomic maintenance and are responsible for separating double-stranded nucleic acids (DNA, RNA, or DNA/RNA hybrids) into two complementary single-stranded counterparts. This seemingly simple duty is absolutely imperative because the single-stranded form of DNA has roles in recombination and must be available for polymerases to gain access to the genetic sequence.

For three decades helicases have been identified and studied from a myriad of cell types including bacteria, yeast, plant, animal, and even viruses, mitochondria, and chloroplasts. Not unlike polymerases, helicases are found in many forms and are specialized for particular duties. They have multiple tasks during DNA replication alone including unwinding of the replication fork, facilitating replication restart at stalled forks, initiating recombination and assisting in repair of replication errors (Table 1). In fact, some of these roles are so critical that there is homology between helicases from organisms as simple as *Escherichia coli* to the complex eukaryotic human cell. RecQ from *E. coli*, for example, is the founding member of the RecQ family of helicases involved in recombination and replication fork stabilization (9, 10). Yeast have one RecQ family helicase, Sgs1, which shares the same roles as the *E. coli* protein while humans contain four RecQ family helicases: RECQ1, RECQ5, BLM, and WRN (five if you count the ATPase RECQ4) (9-12). Table 1 illustrates the vast diversity of helicases and compares them across three species: *E. coli,*

Saccharomyces cerevisiae, and Homo sapiens. In addition to the helicases listed in Table 1 there are also many RNA helicases. However, our focus here concerns DNA helicases and their roles in genomic maintenance.

Structure and Function of Helicases

Enzymatic unwinding of double-stranded DNA and RNA is a process in which helicases couple the energy released by the hydrolysis of NTPs with the disruption of the hydrogen bonds holding the two complementary strands of nucleic acid together (reviewed in (13-15)). There are many different types of helicases and they function in different ways to accomplish this task. Helicases were first divided into families based on sequence similarity twenty years ago (16-18). The most recent family breakdown describes each helicase as being from one of six different groups: superfamilies 1 (SF1) and 2 (SF2) and families 3 (F3), 4 (F4), 5 (F5) and 6 (F6) (14, 19). SF1 and SF2 are the largest of the six and each member has a set of seven conserved amino acid motifs that are implicated in the helicase unwinding reaction (Figure 1). Generally, helicases in SF1 and SF2 actively unwind as dimers, whereas F3-F6 helicases form and unwind as hexameric rings (Figure 1) (19). However, there are apparent exceptions to this simple classification. There are fewer family members in F3 – F6 and these enzymes lack the seven conserved amino acid motifs found in SF1 and SF2. However, F3 – F6 do contain conserved motifs that presumably have analogous roles in unwinding to the SF1 and SF2 seven conserved motifs. Interestingly, some of these F3-F6 helicases do not contain NTP binding sites in monomeric form but upon oligomerizaton NTP binding sites are generated at the interfaces between the subunits (Figure 1) (19).

	Organism	Cellular role	Referenced works
RecQ	*E. coli*	recombination, fork stabilization	(9, 10)
DnaB	*E. coli*	lagging strand replicative helicase	(20, 21)
PriA	*E. coli*	replication restart	(22-25)
Rep	*E. coli*	replication restart	(24, 25)
UvrD	*E. coli*	DNA repair	(25-27)
RecBCD	*E. coli*	homologous recombination for double strand break repair	(19, 28)
RecG	*E. coli*	facilitates stalled fork into a Holliday junction	(19, 29)
TraI	*E. coli*	bacterial conjugation	(30)
Rad3	*S. cerevisiae*	DNA excision repair	(31, 32)
Rad25	*S. cerevisiae*	nucleotide excision repair, transcription	(31, 32)
Srs2	*S. cerevisiae*	recombination inhibition	(33, 34)
Pif1	*S. cerevisiae*	mtDNA repair, nuclear DNA telomere maintenance	(35-38)
Rrm3	*S. cerevisiae*	fork progression and stability, telomere maintenance	(38-40)
Sgs1	*S. cerevisiae*	coordinates replication restart and recombination	(9, 11, 33, 34)
Hmi1p	*S. cerevisiae*	mtDNA maintenance	(41-43)
XPB	*H. sapiens*	nucleotide excision repair, transcription	(44, 45)
XPD	*H. sapiens*	nucleotide excision repair, transcription	(44, 45)
RECQ1	*H. sapiens*	homologous recombination repair	(46)
WRN	*H. sapiens*	recombination, fork stabilization	(9, 10, 12)
BLM	*H. sapiens*	functional homolog of yeast Sgs1, replication restart	(9, 10)
TWINKLE	*H. sapiens*	mtDNA replicative helicase	(47, 48)

Table 1: Example helicases and their roles from *E. coli*, *S. cerevisiae*, and *H. sapiens.* This list is a sampling of common helicases from three different systems. It is non-exhaustive and should serve only to illustrate the diverse role of helicases within and amongst organisms.

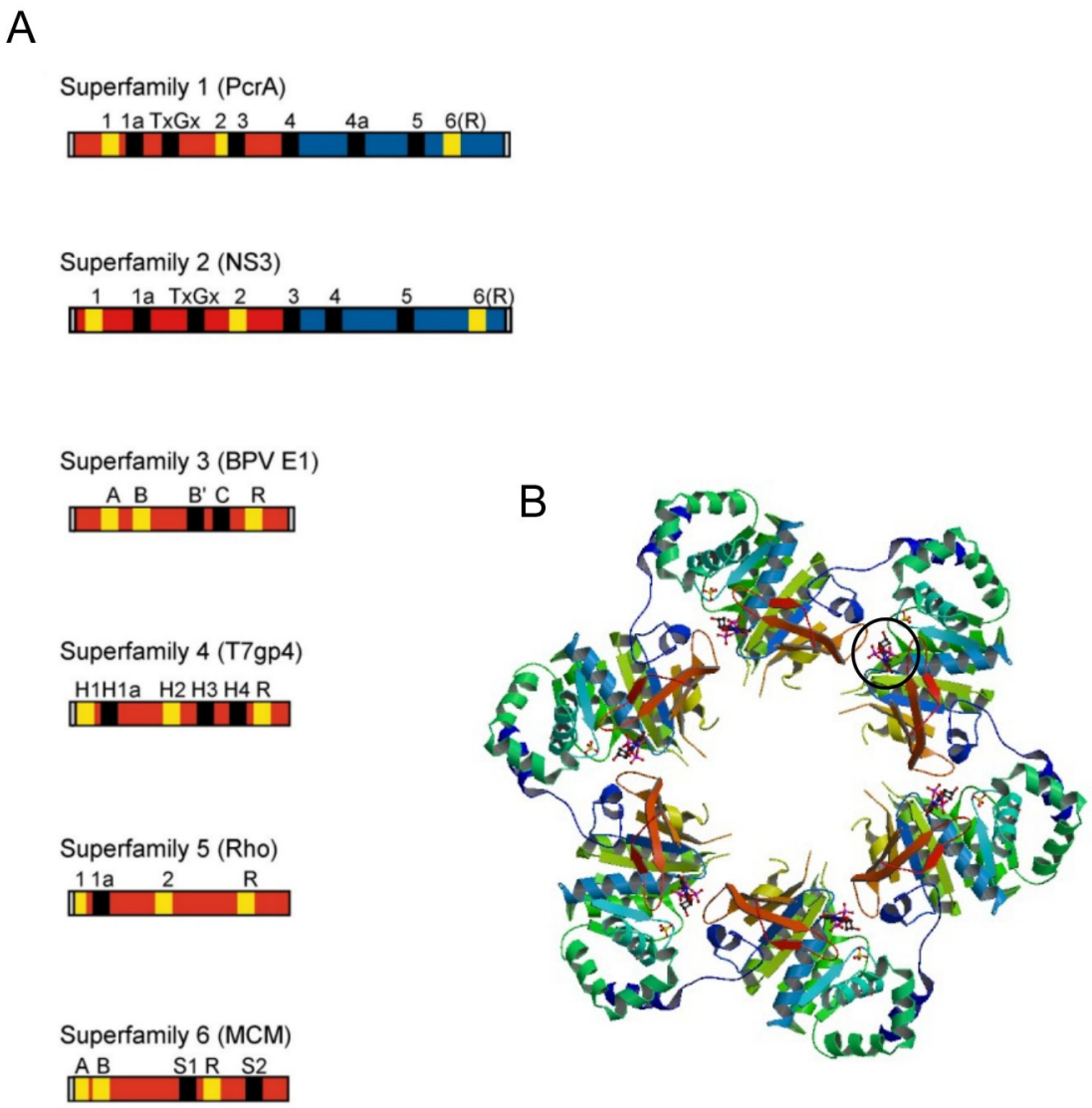

Figure 1: Superfamily motif comparison and ring-shaped helicase NTP binding sites

A. Comparison of amino acid motifs and structures across the six helicase superfamilies. The representative of each superfamily is shown in parentheses. The motifs are depicted by yellow and black squares with the yellow ones being common structural forms found in all helicases that are involved in NTP binding, hydrolysis, and the coupling of hydrolysis to conformational changes. (modified from (19))

B. An example of a ring-shaped helicase. This quaternary structure of six monomers forms the hexameric helicase of gene 4 from the bacteriophage T7. This structure was co-crystallized with dTTP (encircled) which can be found at each subunit interface. (crystal structure from Protein Database (PDB): 1cr1 described in (49))

The seven conserved helicase motifs are also present in other nucleic acid translocases. This group of proteins includes, but is not exclusive to, helicases and can be defined as any protein that actively moves along DNA in an energy-dependent manner. An example of this is Rad54p from *S. cerevisiae* which contains the seven helicase motifs and is involved in homologous recombination yet possesses no unwinding activity (50). The seven conserved helicase motifs work in conjunction to allow translocases to bind and couple the hydrolysis of NTPs to protein conformational shifts on the DNA backbone, resulting in translocation and, in the case of helicases, unwinding (15, 19). Motifs I and II (also referred to as the Walker A and B boxes, respectively) provide the necessary local chemistry to facilitate NTP hydrolysis (14). The Walker A and B boxes are found in many NTP-hydrolyzing proteins and numerous single-site mutational analyses have shown the conserved lysine of the Walker A box to be crucial in NTP hydrolysis, as Walker A point mutants display poor utilization of NTPs (51-54). Mutational analysis and crystal structure studies have shown that motifs III-VI do not have discrete roles. Rather, these motifs work together to bind NTP and the DNA backbone to induce conformation changes based upon nucleotide binding and hydrolysis (14, 55-58). Since the first description of the seven conserved helicase domains, a TxGx domain (Figure 1) has also been identified and implicated in ssDNA binding (59).

A molecular model for unwinding, derived from analyses of multiple co-crystals of an SF1 protein, describes a helicase binding the dsDNA at the fork and forcing a negatively charged domain onto the duplex, thereby making the complementary base-pairing of the nucleotides energetically less favorable (60, 61). This ultimately causes the complementary bases to flip away from each other allowing the helicase to continue translocation and

unwinding. This particular mechanism is an example of active unwinding, in which the DNA is forced apart. When working as a machine, an SF1/SF2 helicase uses the energy derived from hydrolyzed ATP to drive itself forward on a single strand of dsDNA while displacing the two strands through local environment chemistry manipulation.

The focus of my work has been to understand the roles of two related superfamily I helicases and their mechanisms in two distinct DNA maintenance pathways. My most recent work concerns helicase II (UvrD) from the prokaryote, *E. coli*, where I examined the stimulatory effect of MutL on the unwinding processivity of UvrD in the methyl-directed mismatch repair pathway. My study of helicases began with an analysis of the biochemical characteristics of Hmi1p, a helicase required to maintain mitochondrial DNA (mtDNA) in the eukaryote, *S. cerevisiae*.

Mitochondria DNA replication

The mode of replication and inheritance of mitochondrial DNA has been extensively studied for its biological implications ranging from metabolism and aging to genetic disorders and human evolution (47, 62, 63). The model organism *S. cerevisiae* has been pivotal in studies concerning all facets of mitochondrial function and has lent insight to the understanding of human mitochondria. Genes and proteins required for respiration can be extensively studied in yeast due to the ability of yeast to remain viable in the absence of cellular respiration (64, 65). However, studies addressing metabolism of mtDNA were pioneered through efforts in mammalian cells.

The small and compact nature of animal mtDNA combined with the novelty of a circular genome present in humans, made it an attractive system in which to study mtDNA

metabolism. There are two models explaining the replication of mtDNA in humans (Fig. 2, taken from (66)). The traditional model is referred to as the "strand asynchronous" model and describes replication initiating at the heavy strand origin (O_H) via an D-loop and synthesis proceeding unidirectionally (red arrow in Fig 2a) (67). Once the "replication bubble" travels 2/3 of the circle, the light strand origin is revealed and allows replication to initiate (presumably in the same manner as the O_H) on the light strand in the opposite direction. The new model, termed "bidirectional strand-coupled replication" describes an initiation event at the O_H followed by bidirectional replication. The light strand synthesis (black arrow in Fig 2b) is quickly halted as it arrives at the termination site (just upstream of the O_H) but the heavy strand replication (red arrow in Fig 2b) continues, giving the appearance that the mechanism is unidirectional (68). The light strand is replicated in fragments similar to that of nuclear replication.

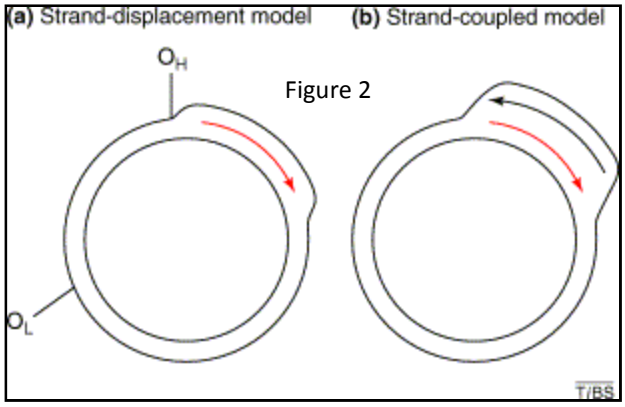

Figure 2

The story is much less clear in the case of yeast mtDNA replication, due to the structure of the genome. The yeast mitochondrial genome is approximately five-fold larger than the mammalian mitochondrial genome (80 kbp vs. 16 kbp) and the majority is found in a linear concatemeric form, the structure of which had eluded scientists until the early 1990's. Current replication themes for *S. cerevisiae* mtDNA involve both rolling circle and recombination models (69-71). Studies by Maleszka et al. (1991) in a similar yeast, *Candida (Torulopsis) glabrata*, found that a small portion of the mtDNA genome is present as circular structures which suggest that the linear mtDNA undergoes replication in a rolling circle

manner (although not exclusively) which is initiated via a recombination event (72). Electron microscopy of the mtDNA also reveals rolling circle intermediates such as circular molecules that have single-stranded tail or lariat structures. Studies of *MHR1*, whose gene product is involved in partitioning mtDNA into bud cells, have shown that the predominant form of mtDNA in bud cells is in a circular monomeric form (73). This may suggest that the concatemeric mtDNA found within the mother cells is a rolling-circle replication intermediate similar to that of *E. coli* phages. Subsequently, these concatemeric forms may be cleaved into monomeric circles (representing the heritable units) that are transmitted to the bud cell.

Recombination in yeast mtDNA replication is also supported by the fact that Holliday junction resolving and stabilizing proteins, Cce1 and Abf2 respectively, are important for maintenance of the mtDNA and that [rho$^-$] (i.e. truncated/incomplete mtDNA) mitochondria don't require origins of replication to replicate (74-76). This may suggest that the rolling circle mechanism is initiated by a recombination event or that recombination based replication may involve intermediates that resemble rolling circle structures. Mhr1p has the ability to generate D-loop structures by pairing dsDNA with homologous ssDNA and it is this activity that may play a role in initiating the recombination event used to begin rolling circle replication (73).

Proteins Involved in Yeast mtDNA Maintenance

Several of the proteins presumed to play a role in the replication of the mtDNA genome have been studied, yet the replication machine and mechanism remains elusive. *MIP1* was shown to encode the mitochondrial DNA polymerase in yeast (77) and *RIM1*

encodes the mtDNA single stranded binding protein (78). Both are required for the maintenance of mtDNA. There is no known homologue to the mammalian twinkle helicase and a replicative helicase for *S. cerevisiae* mtDNA has yet to be demonstrated, despite the presence of two known helicases that localize to the mitochondria. The *PIF1* gene has been shown to encode a nuclear and mitochondrial helicase via alternative splicing, the latter having roles in yeast mtDNA repair, recombination, and protection of the mtDNA from double-stranded breaks (37, 79-81). *pif1* mutant cells still contain functional mitochondria and are able to respire at normal temperatures, but they are very susceptible to DNA damage due to the importance of Pif1 in mtDNA repair (80, 82). For these reasons Pif1p is not thought to be the primary helicase involved in mtDNA replication.

Helicase of the Mitochondria 1 (*HMI1*)

The other known yeast mtDNA helicase, the product of the *HMI1* gene, was identified as a protein with significant sequence homology with the *E. coli uvrD* gene, which encodes DNA helicase II (42). Hmi1p is a *S. cerevisiae* superfamily 1 helicase and has been shown to localize to the mitochondria and is required for the maintenance of the yeast mitochondrial genome (42). When *HMI1* is disrupted, the resulting cell progeny display a petite colony phenotype that is associated with mitochondrial malfunction and the inability to generate ATP via oxidative phosphorylation. This mitochondrial defect is further demonstrated by the failure of these colonies to grow on media lacking a fermentable carbon source, since yeast are facultative anaerobes and do not require functional mitochondria for growth (reviewed in(83)). Hmi1p has been shown to unwind duplex DNA and has no role in the transcription of mtDNA genes (42). Furthermore, cells lacking *HMI1* "lose" their

mitochondrial DNA and become rho° (42, 43). Despite these characteristics, Hmi1p is not believed to be the yeast mtDNA replicative helicase because rho$^-$ genomes can be maintained in *hmi1*Δ strains (42). Recently, it has been demonstrated that *hmi1*Δ rho$^-$ strains suffer significant shortening of the concatemeric mtDNA compared to *HMI1* rho$^-$ strains (41). In addition, genetic studies show that a mutant form of Hmi1p, in which a conserved Walker A box residue has been altered, complements a *hmi1*Δ mutant (43). From these data it was concluded that Hmi1p stimulates the formation of concatemeric mtDNA, although the mechanism by which this occurs remains unknown.

With implications from genetic diseases to aging, mtDNA studies are vital to our understanding of cellular respiration and apoptosis. Yeast is an ideal system in which to study mitochondrial function due to the ability of yeast to maintain viability without functional mitochondria. The current data paints a very incomplete picture of yeast mtDNA replication and there is much to be uncovered before a working model of this mechanism can be pieced together.

Helicase II from *E. coli*

As previously stated, *HMI1* was identified in the yeast genome based on its sequence similarity to *E. coli uvrD*. Helicase II (UvrD) was identified as the *uvrD* gene product in *E. coli* 25 years ago by Hickson et al. and has been shown to have major roles in methyl-directed mismatch repair (MMR), replication, recombination, and nucleotide excision repair (25-27). UvrD is an 82 kDa superfamily I helicase that unwinds DNA as a dimer in a 3'-5' direction (84-87). UvrD has ssDNA-stimulated ATPase activity and ATP-dependent helicase activity (26). As a translocase on ssDNA, a UvrD monomer has a processivity on

the order of 2.5 kb, however, when unwinding dsDNA, the processivity of the dimer is drastically reduced to approximately 45 bp (86, 88).

E. coli UvrD seems to participate in many aspects of replication and recombination, and as result, its precise roles in these processes are unclear. What we do know is based on *uvrD* deletion studies. Double mutations in *uvrD* and either *polA* (polymerase I) or *rep* helicase are lethal, suggesting that UvrD is involved in lagging-strand synthesis and/or fork progression, respectively (89, 90). It was previously shown that *uvrD* deletion mutants have an increased rate of recombination but it wasn't until recently that studies demonstrated that UvrD is involved in regulating recombination by hindering recombination proteins (27, 91, 92). Although UvrD is involved in replication and recombination, it is most well-known for its role in the *E. coli* MMR pathway.

Methyl-Directed Mismatch Repair in *E. coli*

So-called "high-fidelity" polymerases are quite efficient at replicating DNA with minimal errors (reviewed in (93)). However, even with proofreading subunits, errors can occur in the form of incorrect base pairing or insertion-deletion loops (IDL) that can result in unpaired bases. Such errors have been reported to occur at a rate of 1×10^{-6} in *E. coli* (94). Without a reliable repair mechanism in place, these errors give rise to mutations that can be deleterious to the organism (94). The methyl-directed mismatch repair pathway is charged with identifying, removing, and replacing non-complementary base pairs and IDLs to maintain the integrity of the *E. coli* genome. The following research focuses on aspects of the *E. coli* MMR system, which is triggered when a mismatched base or IDL is missed by the high-fidelity polymerase III proofreading complex, resulting in a warped DNA backbone.

Aberrations in DNA, such as mismatched bases, can generate an irregularity along the backbone that results in kinking and local flexibility attributed to poor base stacking (reviewed in (95)). Recognition of these irregularities by the MutS homodimer is the first step in the mismatch repair process (figure 3). Atomic force microscopy and crystal structure studies have shown that MutS bends the DNA at the mismatch site and, through conformational changes, is able to stabilize the base stacking and unkink the DNA (96).

In *E. coli*, mismatch-bound MutS recruits a MutL homodimer to the repair site which, in turn, stimulates MutH endonuclease-catalyzed nicking of the DNA backbone at the nearest hemi-methylated d(GATC) site (reviewed in (96)). These methylation modifications are performed by Dam methyltransferase which attaches a methyl group at all d(GATC) sites in the *E. coli* genome in a post-replication event. Hemi-methylated sites occur during DNA replication and are composed of one parent strand and a newly replicated daughter strand. The parent strand is methylated from a previous replication event while methylation of the nascent strand occurs subsequent to the DNA being replicated. MutH uses this signal to discriminate between the strands and specifically nicks the nascent strand. The MutH-bound hemi-methylated site can be up to 3 kb away from the mismatch. It is believed that the stimulation of MutH nicking activity is made possible by local looping of DNA, permitting MutL to interact with MutS and MutH simultaneously (Figure 1) (96).

MutL binds the MutH-generated nick and loads UvrD onto the DNA so that it may unwind in a 3'-5' direction toward the mismatch site. UvrD is able to translocate on ssDNA for approximately 2.5 kb, however, translocation through dsDNA is severely retarded (86, 88). Several reports have indicated that UvrD can only unwind ~45 bp in a single unwinding event before dissociation. To account for the discrepancy in repair tract length and the

limited processivity of UvrD, it is currently hypothesized that MutL continuously loads several dimers of UvrD to unwind the repair tract in its entirety (97).

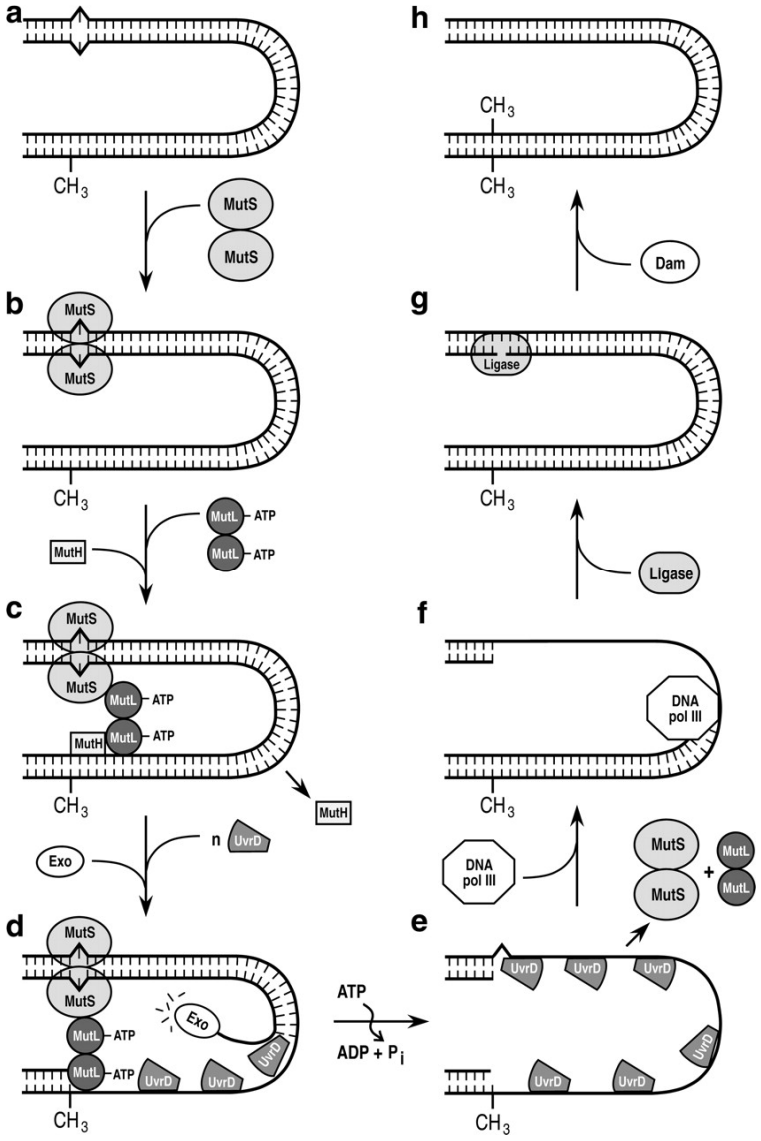

Figure 3: Model for *E. coli* methyl-directed mismatch repair (taken from (98))

During unwinding, several exonucleases (RecJ, ExoI, ExoVII, and Exo X) can function to digest the displaced strand as it is being unwound. The UvrD helicase continues to work until it has displaced (presumably) the MutS/MutL complex from the DNA and has unwound approximately 100 bp beyond the mismatch site. The ssDNA is protected and stabilized by single-stranded binding protein (SSB) until DNA polymerase III completes synthesis of the complementary strand. Ligase repairs the remaining nick site restoring the DNA to a continuous double-stranded form free of mispaired bases.

Here, I take a closer look at the MMR repair tract unwinding by UvrD. Specifically, I investigate the mechanism by which MutL promotes UvrD unwinding of the repair tract. First, we must consider the structure and function of the *E. coli* MutL protein.

MutL

MutL is a DNA-stimulated ATPase required for MMR in *E. coli*. It functions only as a dimer and has a non-specific ssDNA and dsDNA binding affinity that is stimulated through the binding of ATP. Recent crystal structure analyses have shown that MutL is comprised of two separate domains: the N-terminal ATPase domain and the C-terminal domain (99). These are referred to as LN40 (MutL N-terminal 40 kDa) and LC20 (MutL C-terminal 20 kDa). The LN40 and LC20 regions are connected by a linker that is made up of ~100 amino acids that is too variable to generate a resolvable structure. The linker is speculated to be present to allow the MutL dimer to encompass 2-4 dsDNA molecules at once. Upon dimerization, positively charged clefts, which are implicated in DNA binding, are formed between both LN40 and both LC20 domains. Both the LN40 and LC20 domains have

arginine residues in their clefts that, when mutated, result in a MutL dimer with drastically reduced DNA affinity, resulting in an increased mutation rate *in vivo* (99).

ATP has been shown to be required for MutL to function in the MMR pathway through elegant mutation studies that suggest MutL uses ATP binding and slow hydrolysis as a switch (98). Size-exclusion experiments show the ATP-bound form of MutL to be more compact than the ATP-unbound form, suggesting that the LN40 domains dimerize upon ATP binding. This open and closed conformation model is corroborated by a marked increase in MutL affinity for DNA in the presence of ATP and supports the idea that MutL could completely encompass the diameter of the DNA and then clamp around it following ATP binding. Here, subsequent ATP hydrolysis results in an opening of the protein and DNA dissociation. Although the role of ATP binding in MutL activity has been examined through biochemical and physical means, we still do not have a detailed understanding of its control.

Single-molecule FRET

An experimental design utilizing Forster Resonance Energy Transfer (FRET) technology will be used to study the mechanism of unwinding by UvrD and MutL. Fluorescent molecules absorb photons at a specific wavelength and then emit nonradiative energy at a higher wavelength (lower energy) (100). FRET is the transfer of energy from one fluorophore to another: from the donor to an acceptor. It is ideal to use an acceptor that absorbs energy at the wavelength that the donor emits. As a result, an input of light at the donor's wavelength would result in transfer (or FRET) of energy to the acceptor molecule. The acceptor molecule then emits light at an even lower energy level than the donor. In an experiment, if the donor absorbs the input wavelength but the wavelength of the acceptor is

emitted, then FRET has been achieved. This becomes useful because FRET requires an intimate association between the two fluorophore partners and the efficiency is reduced exponentially with increased distance. As a result, this technology is used widely to demonstrate close associations between two partners on the angstrom scale. For our purposes here, we take advantage of FRET technology to show a change in position of a protein along a DNA strand. In order to assay this, we have utilized a relatively new method referred to as single-molecule FRET (smFRET).

Traditional single-molecule microscopy studies have involved the use of a tethered or trapped bead attached to a DNA strand >10 kb in length (101). UvrD, a helicase that unwinds in the 30-45 bp range, necessitated an approach that could be analyzed on the level of a few base pairs. T. Ha's lab has pioneered the use of smFRET to show the unwinding of small duplex substrates (reviewed in (102)). By tagging two oligonucleotides with FRET partners onto complementary bases, the DNA substrate shows high levels of FRET when annealed. Unwinding could be demonstrated by the loss of FRET as the two oligos unwound and separated.

Single molecule FRET technology is based upon total internal reflection microscopy (TIRM) (102). Total internal reflection (TIR) is an optical event that results when a ray of light strikes the boundary between two different mediums and all of the light is reflected away from the boundary (Fig 4D). Normally when light goes from one medium to another it refracts and reflects a portion of the light (Fig 4A). Refraction is a change in the direction of light based upon a change in the speed of the light (Fig 4B). In order to achieve TIR the ray of light must strike the medium boundary at an angle greater than the 'critical angle' (Fig 4C). The critical angle is defined as the angle at which the ray of light is refracted by the

second medium to travel along the boundary of the two mediums. Any greater angle will result in the light being reflected back into the first medium (Fig 4D).

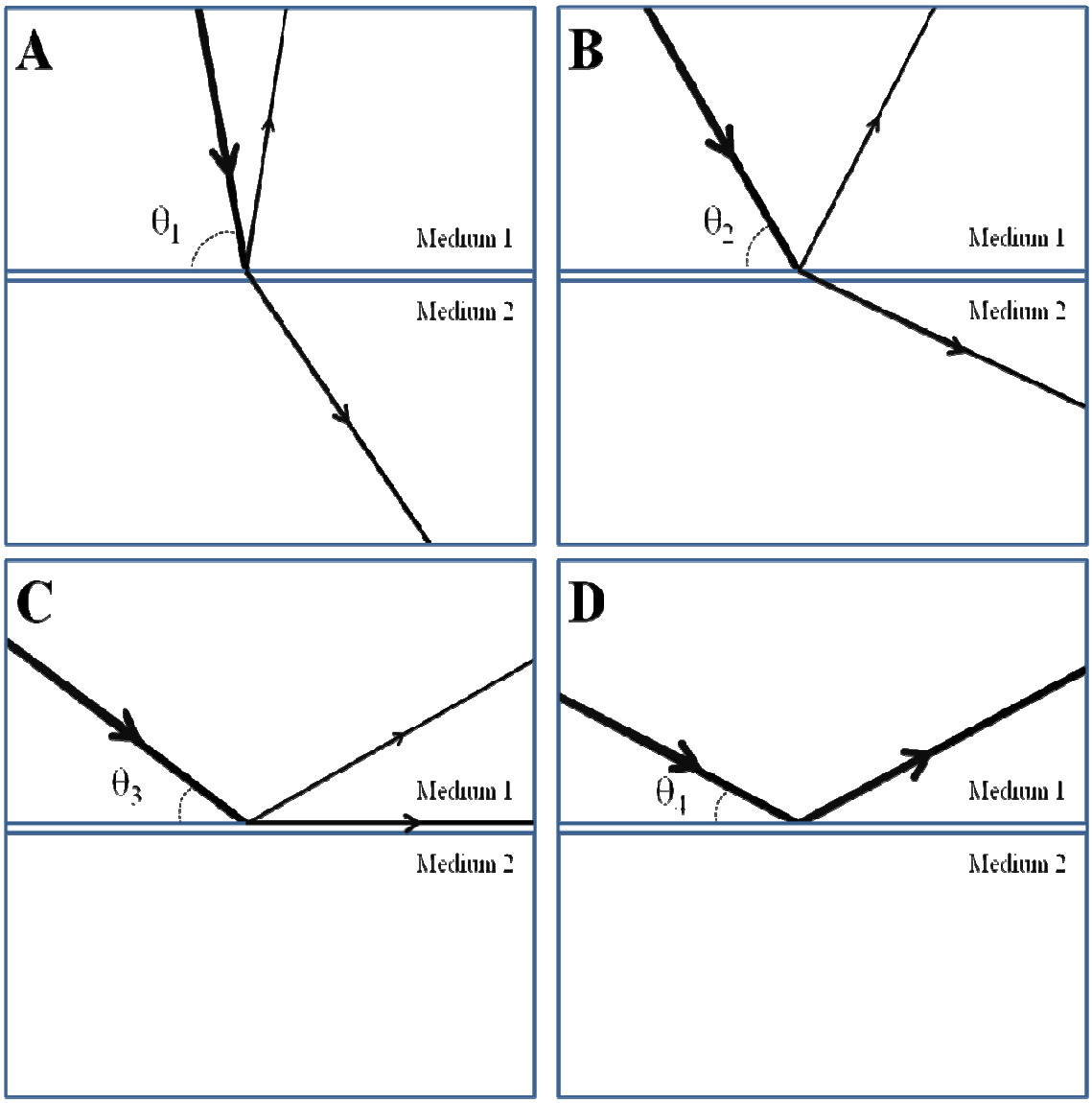

Figure 4: Light Refraction and Total Internal Reflection

A, When light strikes the boundary of two different media, some light reflects and some refracts. *B,* As the angle to normal increases, the light refracts at a smaller angle to the boundary. *C,* θ_3 is the critical angle: the angle at which light refracts along the boundary. *D,* A greater angle to normal than the critical angle results in total internal reflection.

Now consider a conventional light microscope setup: light travels through air and the slide before coming out on the other side to be refracted through lenses to magnify the image. If you polarize the light source and then direct that light onto the slide at an angle greater than the critical angle, you will achieve TIR. Of course, if TIR is achieved then the slide will reflect all of the light and nothing will be seen through the objective. However, there is slight anomaly that occurs during TIR that is referred to as the evanescent wave which allows the viewer to visualize a small portion of the slide. An evanescent wave is a nearfield wave emitted from the reflected light at the boundary and decays exponentially with distance. This comes in handy when doing fluorescent microscopy because in three-dimensional samples such as cells or flow channels, the objective gets overloaded with background fluorescent molecules. The evanescent wave allows the observer to view a very finite region attached directly to the slide (Fig 5). In the experiments conducted here, a set amount of fluorescent DNA is attached to the slide and the restrictions of the evanescent wave permit viewing of this region without any background fluorescence.

This dissertation will address the role of two related superfamily I helicases, Hmi1 and UvrD, in two very different DNA maintenance pathways, one eukaryotic the other prokaryotic. Chapter 2 describes the overexpression, purification, and characterization of the yeast helicase, Hmi1p. Chapter 3 addresses the mechanism by which MutL stimulates the dsDNA processivity of UvrD in MMR through *in vitro* experiments based upon single-molecule FRET microscopy. The final chapter will be a discussion of each of these helicases and their respective roles in DNA maintenance, in addition to proposed experiments and future research concerning these proteins.

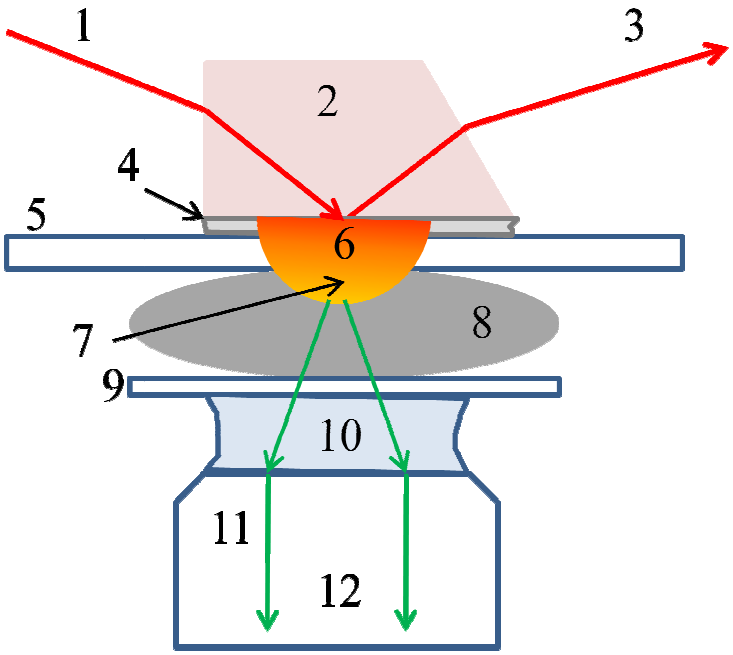

Figure 5: TIRM and the Evanescent Wave setup for this study (not to scale)

1. Laser excitation wave length 635 nm
2. Prism
3. Reflected light
4. Immersion oil
5. Slide
6. Evanescent wave
7. Portion of sample being excited at 635 nm
8. Flow channel sample
9. Cover slip
10. Water
11. FRET emission wavelength at 532 nm
12. Objective

References

1. Sims RJ,3rd, Belotserkovskaya R, Reinberg D. Elongation by RNA polymerase II: The short and long of it. Genes Dev. 2004 Oct 15;18(20):2437-68.

2. Asturias FJ. RNA polymerase II structure, and organization of the preinitiation complex. Current Opinion in Structural Biology. 2004 4;14(2):121-9.

3. Grummt I. Life on a planet of its own: Regulation of RNA polymerase I transcription in the nucleolus. Genes Dev. 2003 July 15;17(14):1691-702.

4. Paule MR, White RJ. Survey and summary: Transcription by RNA polymerases I and III. Nucleic Acids Res. 2000 Mar 15;28(6):1283-98.

5. Bebenek K, Kunkel TA. Functions of DNA polymerases. In: Wei Yang, editor. Advances in Protein Chemistry, Academic Press; 2004. p. 137-65.

6. McCulloch SD, Kunkel TA. The fidelity of DNA synthesis by eukaryotic replicative and translesion synthesis polymerases. Cell Res. 2008 Jan;18(1):148-61.

7. Moon AF, Garcia-Diaz M, Batra VK, Beard WA, Bebenek K, Kunkel TA, et al. The X family portrait: Structural insights into biological functions of X family polymerases. DNA Repair. 2007 12/1;6(12):1709-25.

8. Harrington L. Biochemical aspects of telomerase function. Cancer Lett. 2003 May 15;194(2):139-54.

9. Wu L, Hickson ID. DNA helicases required for homologous recombination and repair of damaged replication forks. Annu Rev Genet. 2006 12/33;40(1):279-306.

10. Hickson ID. RecQ helicases: Caretakers of the genome. Nat Rev Cancer. 2003 Mar;3(3):169-78.

11. Schmidt KH, Wu J, Kolodner RD. Control of translocations between highly diverged genes by Sgs1, the saccharomyces cerevisiae homolog of the bloom's syndrome protein. Mol Cell Biol. 2006 July 15;26(14):5406-20.

12. Brosh RM,Jr, Orren DK, Nehlin JO, Ravn PH, Kenny MK, Machwe A, et al. Functional and physical interaction between WRN helicase and human replication protein A. J Biol Chem. 1999 Jun 25;274(26):18341-50.

13. Lohman TM. Helicase-catalyzed DNA unwinding. J Biol Chem. 1993 Feb 5;268(4):2269-72.

14. Hall MC, Matson SW. Helicase motifs: The engine that powers DNA unwinding. Mol Microbiol. 1999 Dec;34(5):867-77.

15. Lohman TM, Tomko EJ, Wu CG. Non-hexameric DNA helicases and translocases: Mechanisms and regulation. Nat Rev Mol Cell Biol. 2008 May;9(5):391-401.

16. Hodgman TC. A new superfamily of replicative proteins. Nature. 1988 May 5;333(6168):22-3.

17. Gorbalenya AE, Koonin EV, Donchenko AP, Blinov VM. A novel superfamily of nucleoside triphosphate-binding motif containing proteins which are probably involved in duplex unwinding in DNA and RNA replication and recombination. FEBS Letters. 1988 8/1;235(1-2):16-24.

18. Singleton MR, Dillingham MS, Wigley DB. Structure and mechanism of helicases and nucleic acid translocases. Annu Rev Biochem. 2007;76:23-50.

19. Singleton MR, Dillingham MS, Wigley DB. Structure and mechanism of helicases and nucleic acid translocases. Annu Rev Biochem. 2007;76:23-50.

20. Corn JE, Berger JM. Regulation of bacterial priming and daughter strand synthesis through helicase-primase interactions. Nucleic Acids Res. 2006;34(15):4082-8.

21. Belle JJ, Casey A, Courcelle CT, Courcelle J. Inactivation of the DnaB helicase leads to the collapse and degradation of the replication fork: A comparison to UV-induced arrest. J Bacteriol. 2007 August 1;189(15):5452-62.

22. Cadman CJ, Lopper M, Moon PB, Keck JL, McGlynn P. PriB stimulates PriA helicase via an interaction with single-stranded DNA. J Biol Chem. 2005 December 2;280(48):39693-700.

23. Marians KJ. PriA-directed replication fork restart in escherichia coli. Trends in Biochemical Sciences. 2000 4/1;25(4):185-9.

24. Heller RC, Marians KJ. Unwinding of the nascent lagging strand by rep and PriA enables the direct restart of stalled replication forks. J Biol Chem. 2005 October 7;280(40):34143-51.

25. Heller RC, Marians KJ. Non-replicative helicases at the replication fork. DNA Repair. 2007 7/1;6(7):945-52.

26. Hickson ID, Arthur HM, Bramhill D, Emmerson PT. The E. coli uvrD gene product is DNA helicase II. Mol Gen Genet. 1983;190(2):265-70.

27. Kang J, Blaser MJ. UvrD helicase suppresses recombination and DNA damage-induced deletions. J Bacteriol. 2006 Aug;188(15):5450-9.

28. Kowalczykowski SC. Initiation of genetic recombination and recombination-dependent replication. Trends in Biochemical Sciences. 2000 4/1;25(4):156-65.

29. McGlynn P, Lloyd RG. Genome stability and the processing of damaged replication forks by RecG. Trends in Genetics. 2002 8/1;18(8):413-9.

30. Matson SW, Sampson JK, Byrd DRN. F plasmid conjugative DNA transfer. THE TraI HELICASE ACTIVITY IS ESSENTIAL FOR DNA STRAND TRANSFER. J Biol Chem. 2001 January 19;276(4):2372-9.

31. Prakash S, Prakash L. Nucleotide excision repair in yeast. Mutation Research/Fundamental and Molecular Mechanisms of Mutagenesis. 2000 6/30;451(1-2):13-24.

32. Deschavanne PJ, Harosh I. The Rad3 protein from saccharomyces cerevisiae: A DNA and DNA:RNA helicase with putative RNA helicase activity. Mol Microbiol. 1993 Mar;7(6):831-5.

33. Spell RM, Jinks-Robertson S. Examination of the roles of Sgs1 and Srs2 helicases in the enforcement of recombination fidelity in saccharomyces cerevisiae. Genetics. 2004 December 1;168(4):1855-65.

34. Ira G, Malkova A, Liberi G, Foiani M, Haber JE. Srs2 and Sgs1–Top3 suppress crossovers during double-strand break repair in yeast. Cell. 2003 11/14;115(4):401-11.

35. Boule J, Zakian VA. Roles of Pif1-like helicases in the maintenance of genomic stability. Nucl Acids Res. 2006 September 10;34(15):4147-53.

36. Cheng X, Dunaway S, Ivessa AS. The role of Pif1p, a DNA helicase in saccharomyces cerevisiae, in maintaining mitochondrial DNA. Mitochondrion. 2007 5;7(3):211-22.

37. Lahaye A, Leterme S, Foury F. PIF1 DNA helicase from saccharomyces cerevisiae. biochemical characterization of the enzyme. J Biol Chem. 1993 Dec 15;268(35):26155-61.

38. O'Rourke TW, Doudican NA, Zhang H, Eaton JS, Doetsch PW, Shadel GS. Differential involvement of the related DNA helicases Pif1p and Rrm3p in mtDNA point mutagenesis and stability. Gene. 2005 7/18;354:86-92.

39. Torres JZ, Schnakenberg SL, Zakian VA. Saccharomyces cerevisiae Rrm3p DNA helicase promotes genome integrity by preventing replication fork stalling: Viability of rrm3 cells requires the intra-S-phase checkpoint and fork restart activities. Mol Cell Biol. 2004 April 15;24(8):3198-212.

40. Schmidt KH, Kolodner RD. Requirement of Rrm3 helicase for repair of spontaneous DNA lesions in cells lacking Srs2 or Sgs1 helicase. Mol Cell Biol. 2004 April 15;24(8):3213-26.

41. Sedman T, Joers P, Kuusk S, Sedman J. Helicase Hmi1 stimulates the synthesis of concatemeric mitochondrial DNA molecules in yeast saccharomyces cerevisiae. Curr Genet. 2005 Apr;47(4):213-22.

42. Sedman T, Kuusk S, Kivi S, Sedman J. A DNA helicase required for maintenance of the functional mitochondrial genome in saccharomyces cerevisiae. Mol Cell Biol. 2000 Mar;20(5):1816-24.

43. Kuusk S, Sedman T, Joers P, Sedman J. Hmi1p from saccharomyces cerevisiae mitochondria is a structure-specific DNA helicase. J Biol Chem. 2005 Jul 1;280(26):24322-9.

44. Coin F, Oksenych V, Egly J. Distinct roles for the XPB/p52 and XPD/p44 subcomplexes of TFIIH in damaged DNA opening during nucleotide excision repair. Molecular Cell. 2007 4/27;26(2):245-56.

45. Lehmann AR. DNA repair-deficient diseases, xeroderma pigmentosum, cockayne syndrome and trichothiodystrophy. Biochimie. 2003 11;85(11):1101-11.

46. Sharma S, Brosh RM,Jr. Human RECQ1 is a DNA damage responsive protein required for genotoxic stress resistance and suppression of sister chromatid exchanges. PLoS ONE. 2007 Dec 12;2(12):e1297.

47. Copeland WC. Inherited mitochondrial diseases of DNA replication. Annu Rev Med. 2008;59:131-46.

48. Falkenberg M, Larsson N, Gustafsson CM. DNA replication and transcription in mammalian mitochondria. Annu Rev Biochem. 2007 07/18;76(1):679-99.

49. Sawaya MR, Guo S, Tabor S, Richardson CC, Ellenberger T. Crystal structure of the helicase domain from the replicative helicase-primase of bacteriophage T7. Cell. 1999 10/15;99(2):167-77.

50. Heyer W, Li X, Rolfsmeier M, Zhang X. Rad54: The swiss army knife of homologous recombination? Nucl Acids Res. 2006 September 10;34(15):4115-25.

51. Barnett ME, Zolkiewski M. Site-directed mutagenesis of conserved charged amino acid residues in ClpB from escherichia coli. Biochemistry. 2002 Sep 17;41(37):11277-83.

52. George JW, Brosh RM, Matson SW. A dominant negative allele of the escherichia coli uvrD gene encoding DNA helicase II : A biochemical and genetic characterization. Journal of Molecular Biology. 1994 1/13;235(2):424-35.

53. Monroe DS,Jr, Leitzel AK, Klein HL, Matson SW. Biochemical and genetic characterization of Hmi1p, a yeast DNA helicase involved in the maintenance of mitochondrial DNA. Yeast. 2005 Dec;22(16):1269-86.

54. Powe AC,Jr, Al-Nakkash L, Li M, Hwang TC. Mutation of walker-A lysine 464 in cystic fibrosis transmembrane conductance regulator reveals functional interaction between its nucleotide-binding domains. J Physiol. 2002 Mar 1;539(Pt 2):333-46.

55. Hall MC, Matson SW. Mutation of a highly conserved arginine in motif IV of escherichia coli DNA helicase II results in an ATP-binding defect. J Biol Chem. 1997 Jul 25;272(30):18614-20.

56. Cordin O, Banroques J, Tanner NK, Linder P. The DEAD-box protein family of RNA helicases. Gene. 2006 2/15;367:17-37.

57. Satapathy AK, Pavankumar TL, Bhattacharjya S, Sankaranarayanan R, Ray MK. ATPase activity of RecD is essential for growth of the antarctic pseudomonas syringae Lz4W at low temperature. FEBS J. 2008 Apr;275(8):1835-51.

58. Zittel MC, Keck JL. Coupling DNA-binding and ATP hydrolysis in escherichia coli RecQ: Role of a highly conserved aromatic-rich sequence. Nucleic Acids Res. 2005 Dec 9;33(22):6982-91.

59. Korolev S, Hsieh J, Gauss GH, Lohman TM, Waksman G. Major domain swiveling revealed by the crystal structures of complexes of E. coli rep helicase bound to single-stranded DNA and ADP. Cell. 1997 8/22;90(4):635-47.

60. Soultanas P, Wigley DB. Unwinding the 'gordian knot' of helicase action. Trends Biochem Sci. 2001 Jan;26(1):47-54.

61. Velankar SS, Soultanas P, Dillingham MS, Subramanya HS, Wigley DB. Crystal structures of complexes of PcrA DNA helicase with a DNA substrate indicate an inchworm mechanism. Cell. 1999 4/2;97(1):75-84.

62. Laun P, Bruschi CV, Dickinson JR, Rinnerthaler M, Heeren G, Schwimbersky R, et al. Yeast mother cell-specific ageing, genetic (in)stability, and the somatic mutation theory of ageing. Nucl Acids Res. 2007 December 3;35(22):7514-26.

63. Mishmar D, Ruiz-Pesini E, Golik P, Macaulay V, Clark AG, Hosseini S, et al. Natural selection shaped regional mtDNA variation in humans. Proceedings of the National Academy of Sciences. 2003 January 7;100(1):171-6.

64. Contamine V, Picard M. Maintenance and integrity of the mitochondrial genome: A plethora of nuclear genes in the budding yeast. Microbiol Mol Biol Rev. 2000 Jun;64(2):281-315.

65. EPHRUSSI B, SLONIMSKI PP. Subcellular units involved in the synthesis of respiratory enzymes in yeast. Nature. 1955 Dec 24;176(4495):1207-8.

66. Bogenhagen DF, Clayton DA. The mitochondrial DNA replication bubble has not burst. Trends Biochem Sci. 2003 Jul;28(7):357-60.

67. Clayton DA. Transcription and replication of mitochondrial DNA. Hum Reprod. 2000 Jul;15 Suppl 2:11-7.

68. Reyes A, Yang MY, Bowmaker M, Holt IJ. Bidirectional replication initiates at sites throughout the mitochondrial genome of birds. J Biol Chem. 2005 Feb 4;280(5):3242-50.

69. Bendich AJ. Structural analysis of mitochondrial DNA molecules from fungi and plants using moving pictures and pulsed-field gel electrophoresis. J Mol Biol. 1996 Feb 2;255(4):564-88.

70. Ling F, Hori A, Yoshida M, Shibata T. Rolling circle replication: A universal model for controlling mechanisms of mitochondrial DNA copy number. Tanpakushitsu Kakusan Koso. 2007 Jul;52(8):886-92.

71. Lockshon D, Zweifel SG, Freeman-Cook LL, Lorimer HE, Brewer BJ, Fangman WL. A role for recombination junctions in the segregation of mitochondrial DNA in yeast. Cell. 1995 Jun 16;81(6):947-55.

72. Maleszka R, Skelly PJ, Clark-Walker GD. Rolling circle replication of DNA in yeast mitochondria. EMBO J. 1991 Dec;10(12):3923-9.

73. Ling F, Shibata T. Recombination-dependent mtDNA partitioning: In vivo role of Mhr1p to promote pairing of homologous DNA. EMBO J. 2002 Sep 2;21(17):4730-40.

74. Kleff S, Kemper B, Sternglanz R. Identification and characterization of yeast mutants and the gene for a cruciform cutting endonuclease. EMBO J. 1992 Feb;11(2):699-704.

75. Lecrenier N, Foury F. New features of mitochondrial DNA replication system in yeast and man. Gene. 2000 Apr 4;246(1-2):37-48.

76. MacAlpine DM, Perlman PS, Butow RA. The high mobility group protein Abf2p influences the level of yeast mitochondrial DNA recombination intermediates in vivo. Proc Natl Acad Sci U S A. 1998 Jun 9;95(12):6739-43.

77. Foury F. Cloning and sequencing of the nuclear gene MIP1 encoding the catalytic subunit of the yeast mitochondrial DNA polymerase. J Biol Chem. 1989 Dec 5;264(34):20552-60.

78. Van Dyck E, Foury F, Stillman B, Brill SJ. A single-stranded DNA binding protein required for mitochondrial DNA replication in S. cerevisiae is homologous to E. coli SSB. EMBO J. 1992 Sep;11(9):3421-30.

79. Foury F, Kolodynski J. Pif mutation blocks recombination between mitochondrial rho+ and rho- genomes having tandemly arrayed repeat units in saccharomyces cerevisiae. Proc Natl Acad Sci U S A. 1983 Sep;80(17):5345-9.

80. Lahaye A, Stahl H, Thines-Sempoux D, Foury F. PIF1: A DNA helicase in yeast mitochondria. EMBO J. 1991 Apr;10(4):997-1007.

81. Cheng X, Dunaway S, Ivessa AS. The role of Pif1p, a DNA helicase in saccharomyces cerevisiae, in maintaining mitochondrial DNA. Mitochondrion. 2007 May;7(3):211-22.

82. Doudican NA, Song B, Shadel GS, Doetsch PW. Oxidative DNA damage causes mitochondrial genomic instability in saccharomyces cerevisiae. Mol Cell Biol. 2005 June 15;25(12):5196-204.

83. Shadel GS. Yeast as a model for human mtDNA replication. Am J Hum Genet. 1999 Nov;65(5):1230-7.

84. Matson SW. Escherichia coli helicase II (urvD gene product) translocates unidirectionally in a 3' to 5' direction. J Biol Chem. 1986 Aug 5;261(22):10169-75.

85. Matson SW, George JW. DNA helicase II of escherichia coli. characterization of the single-stranded DNA-dependent NTPase and helicase activities. J Biol Chem. 1987 Feb 15;262(5):2066-76.

86. Maluf NK, Ali JA, Lohman TM. Kinetic mechanism for formation of the active, dimeric UvrD helicase-DNA complex. J Biol Chem. 2003 Aug 22;278(34):31930-40.

87. Maluf NK, Fischer CJ, Lohman TM. A dimer of escherichia coli UvrD is the active form of the helicase in vitro. J Mol Biol. 2003 Jan 31;325(5):913-35.

88. Fischer CJ, Maluf NK, Lohman TM. Mechanism of ATP-dependent translocation of E.coli UvrD monomers along single-stranded DNA. J Mol Biol. 2004 Dec 10;344(5):1287-309.

89. Moolenaar GF, Moorman C, Goosen N. Role of the escherichia coli nucleotide excision repair proteins in DNA replication. J Bacteriol. 2000 October 15;182(20):5706-14.

90. Washburn BK, Kushner SR. Construction and analysis of deletions in the structural gene (uvrD) for DNA helicase II of escherichia coli. J Bacteriol. 1991 Apr;173(8):2569-75.

91. Lestini R, Michel B. UvrD controls the access of recombination proteins to blocked replication forks. EMBO J. 2007 Aug 22;26(16):3804-14.

92. Lestini R, Michel B. UvrD and UvrD252 counteract RecQ, RecJ and RecFOR in the rep mutant. J Bacteriol. 2008 June 20.

93. McCulloch SD, Kunkel TA. The fidelity of DNA synthesis by eukaryotic replicative and translesion synthesis polymerases. Cell Res. 2008 Jan;18(1):148-61.

94. Schaaper R. Base selection, proofreading, and mismatch repair during DNA replication in escherichia coli. J Biol Chem. 1993 November 15;268(32):23762-5.

95. Tuteja N, Tuteja R. Unraveling DNA helicases. motif, structure, mechanism and function. Eur J Biochem. 2004 May;271(10):1849-63.

96. Kunkel TA, Erie DA. DNA MISMATCH REPAIR*. Annu Rev Biochem. 2005 07/18;74(1):681-710.

97. Matson SW, Robertson AB. The UvrD helicase and its modulation by the mismatch repair protein MutL. Nucleic Acids Res. 2006;34(15):4089-97.

98. Robertson AB, Pattishall SR, Gibbons EA, Matson SW. MutL-catalyzed ATP hydrolysis is required at a post-UvrD loading step in methyl-directed mismatch repair. J Biol Chem. 2006 Jul 21;281(29):19949-59.

99. Guarne A, Ramon-Maiques S, Wolff EM, Ghirlando R, Hu X, Miller JH, et al. Structure of the MutL C-terminal domain: A model of intact MutL and its roles in mismatch repair. EMBO J. 2004 Oct 27;23(21):4134-45.

100. Clegg RM. [18] fluorescence resonance energy transfer and nucleic acids. In: David M.J. Lilley and James E. Dahlberg, editor. Methods in Enzymology, Academic Press; 1992. p. 353-88.

101. Kimura Y, Bianco PR. Single molecule studies of DNA binding proteins using optical tweezers. Analyst. 2006 Aug;131(8):868-74.

102. Roy R, Hohng S, Ha T. A practical guide to single-molecule FRET. Nat Methods. 2008 Jun;5(6):507-16.

Chapter 2

Biochemical and genetic characterization of Hmi1p, a yeast DNA helicase involved in the maintenance of mitochondrial DNA.

The *HMI1* gene encodes a DNA helicase that localizes to the mitochondria and is required for maintenance of the mitochondrial DNA (mtDNA) genome of *Saccharomyces cerevisiae*. Identified based on its homology with *E. coli uvrD*, the *HMI1* gene product, Hmi1p, has been presumed to be involved in the replication of the 80 kb linear *S. cerevisiae* mtDNA genome. Here we report the purification of Hmi1p to apparent homogeneity and provide a characterization of the helicase reaction and the ATPase reaction with regard to NTP preference, divalent cation preference and the stimulatory effects of different nucleic acids on Hmi1p-catalysed ATPase activity. Genetic complementation assays indicate that mitochondrial localization of Hmi1p is essential for its role in mtDNA metabolism. The helicase activity, however, is not essential. Point mutants that lack ATPase/helicase activity partially complement a strain lacking Hmi1p. We suggest several possible roles for Hmi1p in mtDNA metabolism.

Introduction

The 80 kilobase pair (kb) *Saccharomyces cerevisiae* mitochondrial DNA (mtDNA) genome exists within the organelle in a predominantly linear concatemeric form and encodes several proteins required for oxidative phosphorylation and ATP synthesis (1, 2). Loss of the mitochondrial genome or of crucial mtDNA genes results in respiration deficiency and, therefore, mechanisms must exist to maintain the integrity of the mitochondrial genome (3). One method by which the mitochondrial genome can be lost is through failure to replicate mtDNA. Alternatively a failure in transmission of the mtDNA to daughter cells can result in loss of the mitochondrial genome. Although well understood in terms of its genetic contribution to the cell, little is known regarding the mechanism by which this linear genome is replicated and maintained in yeast.

Current mechanisms proposed for *S. cerevisiae* mtDNA replication involve both rolling circle and recombination models (4-6). Studies by Maleszka et al. (2) in a similar yeast, *Torulopsis glabrata,* suggest that mtDNA undergoes replication via a rolling circle mechanism (although not exclusively). Electron microscopy reveals putative rolling circle intermediates in which circular molecules have a single-stranded tail or lariat structure (2). However, these studies do not address the mechanism by which replication is initiated. Studies of *MHR1*, whose gene product is involved in partitioning mtDNA into bud cells, have shown that the predominant form of mtDNA in bud cells is a circular monomer suggesting that a circular form of the mtDNA genome is transmitted from the mother cell to the daughter cell (6, 7). This may suggest that the concatemeric mtDNA found within the mother cell is the rolling circle replication intermediate that will subsequently be cleaved to yield monomeric circular molecules (representing the heritable units) that are transmitted to

the bud cell. How this may occur remains unknown. There is also evidence to suggest that recombination events play an important role in mtDNA replication. For example, the Holliday junction resolving and stabilizing proteins, Cce1p and Abf2p respectively, are important for maintenance of mtDNA (8-10). Furthermore rho$^-$ mitochondria do not require specific origins of replication to propagate their genome (8, 9, 11). This may suggest that a rolling circle replication mechanism can be initiated by a recombination event or that recombination-based replication involves intermediates that resemble rolling circle structures. Mhr1p has been shown to participate in the generation of D-loop structures by pairing duplex DNA with homologous single-stranded DNA (ssDNA) and this activity may play a role in initiating rolling circle replication (6).

Several of the proteins that are believed to be directly involved in the replication of the mtDNA genome have been purified and described biochemically. *MIP1* was shown to encode the mitochondrial DNA polymerase and *RIM1* encodes the mitochondrial ssDNA binding protein (12, 13). Both gene products are required for the maintenance of mtDNA as evidenced by deletion studies (13, 14). A DNA helicase directly involved in replication of *S. cerevisiae* mtDNA has yet to be established despite the presence of two helicases that appear to have a role in mtDNA metabolism. The *PIF1* gene has been shown to encode a helicase with roles in yeast mtDNA repair and recombination (15). However, *pif1*Δ cells still contain functional mitochondria and are able to respire at normal temperatures (16). For these reasons Pif1p is not believed to function as the primary helicase involved in mtDNA replication although it apparently has an ancillary role in mtDNA metabolism. Indeed, recent data indicates that Pif1p is involved in the repair of DNA damage induced by reactive oxygen species in a role that apparently does not involve recombination (17, 18).

The other known mtDNA helicase, *HMI1*, was identified as a protein with significant sequence homology with the *E. coli uvrD* gene encoding DNA helicase II (19). The *S. cerevisiae* superfamily 1 helicase encoded by *HMI1* has been shown to localize to the mitochondria and is required for the maintenance of the yeast mitochondrial genome (19). When this nuclear gene is disrupted, the resulting cell progeny display a petite colony phenotype. This phenotype is generally associated with mitochondrial malfunction and the inability to generate ATP via oxidative phosphorylation (reviewed in (3)). This mitochondrial defect can further be demonstrated by the failure of these colonies to grow on media lacking a fermentable carbon source since yeast are facultative anaerobes and do not require functional mitochondria for growth (reviewed in (20)). Hmi1p has been shown to unwind duplex DNA and has no role in the transcription of mtDNA genes (19). Furthermore, cells lacking *HMI1* "lose" their mitochondrial DNA to become rho° (19, 21). Despite these characteristics, Hmi1p is not believed to be the yeast mtDNA replicative helicase because rho$^-$ genomes can be maintained in *hmi1*Δ strains (19). Recently, it has been demonstrated that *hmi1*Δ rho$^-$ strains suffer significant shortening of the concatemeric mtDNA compared to *HMI1* rho$^-$ strains (22). In addition, genetic studies show that a mutant form of Hmi1p in which a conserved residue found within the Walker A box, and known to be necessary for ATPase activity in other helicases, has been altered, complements an *hmi1*Δ mutant (22). From these data it was concluded that Hmi1p stimulates the formation of concatemeric mtDNA although the mechanism by which this occurs remains unknown.

To further elucidate the precise functions of Hmi1p in the cell and its role in mtDNA maintenance, we have purified Hmi1p and characterized its helicase and ATPase activities. In addition, single point mutants designed to eliminate ATP hydrolysis have been engineered

and the mutant proteins were purified to test their activity *in vitro* and *in vivo* in comparison to the wild type. Complementation assays using a point mutant lacking ATPase/helicase activity and a mutant lacking the mitochondrial localization signal indicate that Hmi1p is essential for maintenance of mtDNA but the helicase activity of the protein appears to be at least partially dispensable.

Materials and Methods

Bacterial strains, plasmids, and nucleic acids – E. coli RDK1896(DE3) is an exoI$^-$, exoIII$^-$, endoI$^-$, and recJ$^-$ strain kindly provided by Richard Kolodner (University of California at San Diego, Ludwig Institute). *E. coli* DH5α was from Invitrogen and was used in all cloning steps. The expression plasmid, pTYB4, was from New England Biolabs and modified as described below. Poly(dT) was from US Biochemical, Inc. M13mp18 ssDNA was prepared as previously described (23). rRNA was from Boehringer Mannheim and nucleotides were from Amersham Pharmacia Biotech.

To construct pEG(KG)*HMI1*, *HMI1* was amplified by polymerase chain reaction (PCR) from CBOO1 genomic DNA prepared as described (23) using primers AKL01 and AKL02 which provided BamH1 sites at each end of the gene (Table 1). The amplified *HMI1* gene was then inserted into pEG(KG) at the BamH1 site and orientation was determined by restriction site analysis. pEG(KG) was the kind gift of R. Deschenes (24). pYE*HMI1* was obtained by excising *HMI1* from pEG(KG)*HMI1* with BamHI and inserting the *HMI1* fragment into pYE12. pYE12 was constructed by digestion of pEG(KG) with SacI to remove the GST gene and the multiple cloning site. The resulting plasmid, pYE12, retains

the BamH1 and HindIII restriction sites and allows galactose-inducible expression of a gene without a GST tag.

pYE12*hmi1K32M* was constructed using Quikchange Site Directed Mutagenesis (Stratagene) and primers AKL03 and AKL04 (Table 1). Amplification of the *HMI1* gene using pMal*HMI1*as the target with AKL03 and AKL04, DpnI treatment, and transformation were performed according to the manufacturer's recommended protocol. Primers AKL03 and AKL04 change codon 32 from AAA (K) to ATG (M) and introduce a SmaI site 5' to codon 32. The introduction of a SmaI site allowed rapid screening of transformants by restriction digest to identify plasmids containing *HMI1* with the desired mutation. The *hmi1K32M* gene was excised from pMal*hmi1K32M* using BamHI and inserted into pYE12 at the unique BamHI site. Orientation was determined by restriction site analysis.

The pYE12*hmi1Δmls* plasmid, which contains *HMI1* lacking the mitochondrial localization signal (mls), was obtained by amplification of *HMI1* from CBOO1 genomic DNA with primers AKL01 and AKL05 (Table 1). AKL05 replaces R691 with a stop codon to truncate Hmi1p 16 residues from the C-terminus which removes the mls. AKL05 also introduced a BamH1 site on the 3' end of the gene. The amplified DNA was digested with BamH1 and inserted into pYE12 to generate pYE12*hmi1ΔMLS.*

Oligonucleotide	Oligonucleotide Sequence (5’ → 3’)
HK1	AGATCTTTAACAACATTATG
HK2	CATGGTTATAATGTGCAGCG
HK5	TACTATCAACTGCTTTGTTT
HK6	GGTGTTGGAACGTACTTGCA
AKL01	TGTGGATCCATGGACAAGCTAACTCCATC
AKL02	GTGGGATCCTATATACGTCTGAAAACGC
AKL03	GCGGGCCCGGGCTCAGGAATGACGCTAACGCT
AKL04	AGCGTTAGCGTCATTCCTGAGCCCGGGCCCGC
AKL05	AAAGGATCCTCAATAAAATCCAAAATTTTTACG
pET11d Sequencing Primer	GGAATTGTGAGCGGATAACAATTCCCC
8xHIS for Intein	AATCTGCAGTCAGTGATGGTGATGGTGATGGTGATGT
CtermHmi1dmls	TGTGTCCAGCTGTGCTCTATAAAATCCAAA
Hmi1Nco18His	TTTTTTCCATGGCTCATCACCATCACCATCACCATCAC
20-mer	ATTCAAAAGGGTGAGAAAGG
40-mer	CAGGAGGCCGATTAAAGGGATTTTAGACAGGAACGGTAC G
91-mer	AGTAGCACCATTACCATTAGCAAGGCCGGAAACGTCACCA ATGAAACCATCGATAGCAGCACCGTAATCAGTAGCGACAG AATCAAGTTTG
K32S FOR	CGGGCCCGGGCTCAGGAAGCACGCTAACGCTAC
K32S REV	GTAGCGTTAGAGTGCTTCCTGAGCCCGGGCCCG
K32A FOR	CGGGCCCGGGCTCAGGAGCAACGCTAACGCTAC
K32A REV	GTAGCGTTAGCGTTGCTCCTGAGCCCGGGCCCG

Table 1: Oligonucleotides

Yeast strains – Saccharomyces cerevisiae KCY3-2D was derived from W303 by single step gene replacement (25). Primers HK6 and HK5 (Table 1) were used to amplify the region from -300 to 181 of YOL095c. Primers HK2 and HK1 (Table 1) were used to amplify the region from 2081 to +65 3' to the YOL095c sequence. These fragments were inserted into a YIp (yeast integrating plasmid) carrying *TRP1*. The inserted fragments target the YIp to the *HMI1* sequence without disrupting the first 66 amino acid residues of Hmi1p. 104 bp from the 3' end of *HMI1* also remain in the genome. After integration of the linearized YIp, KCY1 was sporulated and tetrads were dissected to obtain KCY3-2D. KCY3-2D was crossed with W303a to obtain the heterozygous diploid strain (ALY01) used in complementation experiments. Heterozygosity at the *HMI1* locus was confirmed by Southern blots probed with a [^{32}P]DNA fragment containing *HMI1* and 249 base pairs upstream of the *HMI1* gene. pYE12, pYE12*HMI1*, pYE12*hmi1Δmls* and pYE12*hmi1K32M* were transformed into ALY01 and selected on SD-ura to generate ALY02, ALY03, ALY05 and ALY04 respectively. Plasmids were transformed into yeast using the lithium acetate procedure, as described (23). Yeast strains were grown on standard yeast media. SD was 6.7 g yeast nitrogen base without amino acids, with ammonium sulfate and 20 g dextrose per liter plus the appropriate drop-out mixture of amino acids. Mitochondrial function was assessed on YPEG (10 g yeast extract, 20 g peptone, 20 ml ethanol, 20 ml glycerol, 20 g agar/liter). Modified SGE (6.7 g Yeast Nitrogen Base without amino acids, with ammonium sulfate, 3% glycerol, 2% ethanol, 0.1% dextrose plus the appropriate amino acids) or SR (6.7 g yeast nitrogen base without amino acids, with ammonium sulfate, 20 g raffinose per liter plus the appropriate amino acids) media were used for induction of protein expression in yeast.

Table 2: Yeast Strains

Genotype and source of yeast strains used in this study are indicated.

Yeast Strains	Genotype	Source
CBOO1	MATa, *leu2-3, trp1-1, ura3-52, prb1, pep4::URA3*	A. Sugino
W303	MATa/MATα, *leu2-3,112/leu2-3,112 ura3-3/ura3-3 ade2-101/ade2-101 can1-100/can1-100 his3Δ-11,15/his3Δ-11,15 trp1-1/trp1 -1*	T. Petes
W303a	W303 MATa	T. Petes
KCY1	W303 MATa/α, *HMI1/hmi1::TRP1*	H. Klein, this study
KCY3-2D	W303 MATα, *hmi1::TRP1*; obtained by dissection from KCY1	H. Klein, this study
ALY01	KCY3-2D X W303a; *HMI1/hmi1::TRP1*	This study
ALY02	ALY01/pYE	This study
ALY03	ALY01/pYE*HMI1*	This study
ALY04	ALY01/pYE*hmi1K32M*	This study
ALY05	ALY01/pYE*hmi1ΔMLS*	This study

Antibody Preparation – Anti-MBPHmi1p antiserum was prepared by Covance, Inc. using a maltose binding protein Hmi1p fusion protein (MBP-Hmi1p). The fusion protein was expressed in *E. coli* and purified by ammonium sulfate precipitation, amylose affinity chromatography and Superose 12 chromatography. The partially purified protein was resolved from contaminants on a SDS-polyacrylamide gel and used directly as antigen. We observe cross reaction with a variety of yeast proteins using this antiserum.

Expression Vector Construction – The pTYB4 expression plasmid was modified at nucleotide 7330 by the addition of a sequence encoding eight histidines for use as an extra

purification tag. This was accomplished by amplifying the 1.7 kbp region of the intein-chitin binding domain on pTYB4 with the pET11d sequencing primer and a primer complementary to the end of the chitin binding domain (CBD) containing the engineered 8 histidine sequence and a *Pst*I restriction site to clone into the vector's *PstI* site at base 7330 (Table 1). The amplified product and the unmodified pTYB4 vector were digested with *Hind*III and *Pst*I. The fragment was inserted into the vector and verified by sequencing. *HMI1* was amplified from yeast genomic DNA via PCR using primers that contained an *Nco*I site and *Xho*I site to clone into pTYB4 (Table 1). The primer used to amplify the C-terminal end of the gene was constructed to remove the last 48 nucleotides which correspond to the termination codon and the predicted C-terminal mls (26). The amplification product was digested with *Nco*I and *Xho*I, purified on an agarose gel, and ligated between the *Nco*I and *Xho*I sites on pTYB4-8His. The point mutants K32S, K32A and K32M were generated through PCR-facilitated Quikchange Site Directed Mutagenesis (Stratagene; see primers in Table 1). The mutated alleles of *hmi1* were inserted in the corresponding region on the pTYB4-8His *Hmi1*Δmls through a simple fragment replacement utilizing two restriction sites within the gene. All genes were verified by direct DNA sequencing to insure the absence of unintended mutations.

Protein Purification – All purification steps were conducted at 4°C. The pTYB4-8His *HMI*Δmls plasmid was used to express recombinant Hmi1Δmls protein in RDK1896(DE3). The cultures were grown to OD_{600} ~1.0 in LB media containing 100 μg/ml ampicillin and 10 μg/ml tetracyline. Cells were induced for 24 hours at 16°C with 0.3 mM isopropyl-β, D-thiogalactopyranoside (IPTG). The lower temperature was required to maintain the solubility of the expressed protein. Cells were harvested by centrifugation and

suspended in a lysis buffer containing 50 mM Hepes-NaOH (pH 7.0), 1 mM EDTA, 200 mM NaCl and 10% sucrose. The suspended cells were lysed by the addition of 150 μg/mL lysozyme for 1 hour followed by the addition of Triton X-100 to a final concentration of 0.1%. The NaCl concentration was raised to 500 mM and the cell suspension was sonicated to reduce the viscosity (3 bursts at 14 second intervals). The lysate was clarified by centrifugation at 47,800 g for 60 minutes. Polymin P was added to the soluble cell lysate to a final concentration of 0.3% (w/v) by the slow addition of 10% polymin P (pH 6.8) to precipitate nucleic acids. The polymin P precipitate was collected by centrifugation at 26,890 g for 20 minutes. Solid ammonium sulfate was added to the supernatant to 33% saturation. The $(NH_4)_2S0_4$ precipitate was collected by centrifugation and suspended in a buffer containing 50 mM Hepes-NaOH (pH 7.0), 10 mM imidazole, and 10% glycerol (buffer A). NaCl was added to a final concentration of 500 mM. The solution was batch bound to 2 ml TALON metal affinity resin (BD Biosciences) for 1 hour and the column was washed to baseline with buffer A containing 500 mM NaCl (buffer B). The column was eluted with buffer B containing 350 mM imidazole and fractions containing the Hmi1-CBP-intein fusion protein were identified by SDS-polyacrylamide gel electrophoresis and western blotting using antibodies directed against Hmi1p. The fractions were pooled and batch bound to 2 mls chitin bead resin (New England Biolabs) for 1 hour, poured into a column and washed to baseline with the chitin wash buffer (buffer C): 50 mM Hepes-NaOH (pH 7.0), 500 mM NaCl, 0.1 mM EDTA, and 10% glycerol. The column was then quickly washed with 2 column volumes of buffer C containing 50 mM dithiothreitol (DTT) and incubated for ~40 hours at 4°C to induce intein cleavage. The column was eluted using buffer C and fractions containing Hmi1p were identified by SDS-polyacrylamide gel electrophoresis and

western blotting. Appropriate fractions were combined and dialyzed against a storage solution containing 25 mM Hepes-NaOH (pH 7.0), 200 mM NaCl, 0.1 mM EDTA, 1 mM DTT, and 50% glycerol. The protein was judged to be greater than 95% pure by SDS-polyacrylamide gel electrophoresis (see Fig. 1) and was stored at –20^{o}C.

Partial Duplex Substrates – Partial duplex DNA substrates containing 22 bp, 25 bp, 30 bp, 35 bp, 42 bp or 93 bp of duplex DNA were prepared by mixing M13mp18 ssDNA with the appropriate oligonucleotide at equimolar concentrations of M13 ssDNA and oligonucleotide. The mixture was boiled for 5 minutes followed by slow cooling to promote annealing of the oligonucleotides to the M13 ssDNA. Products were 3'-end labeled using the Klenow fragment of DNA polymerase I and [γ-^{32}P]dCTP. Products of the extension reaction were phenol/chloroform extracted and the DNA was purified on an A5M (Biorad) column equilibrated with 10 mM Tris-HCl (pH 8.0), 100 mM NaCl, and 1 mM EDTA. Fractions were collected drop wise to separate the partial duplex DNA substrate from unincorporated nucleotides. Fractions containing the partial duplex substrate were pooled and used directly in helicase activity assays. The final concentration of the pooled fractions was estimated at 20 µM DNA-Pi. Partial duplex substrates containing 25 bp, 30 bp and 35 bp of duplex DNA were prepared by mixing the appropriate oligonucleotide, labeled at the 5'-end using [γ-^{32}P]ATP and polynucleotide kinase, with an equimolar concentration of M13 ssDNA. Annealing and purification of the partial duplex substrate were as described above.

Helicase Directionality Substrate – The substrate used to determine the polarity of the Hmi1p unwinding reaction (see Fig. 3A) was constructed by annealing the 91 base oligonucleotide to the M13mp18 ssDNA. This oligonucleotide anneals to the region between bases 2490 and 2581 on M13mp18 ssDNA. The 91 bp partial duplex DNA was digested to

completion with *Cla*I and DNA polymerase I (Klenow fragment) was used to extend all available 3'-OH ends in the presence of [α-^{32}P]dCTP and dGTP. The final product was purified as described above for the partial duplex substrates and resulted in a DNA molecule with a long internal ssDNA region and short (43 bp on the 3'-end and 52 bp on the 5' end) duplex regions on each end.

Helicase Assays – Helicase reaction mixtures (20 µl) contained 25 mM Tris-HCl (pH 7.5), 6 mM $MgCl_2$, 20 mM NaCl, 1 mM DTT, 50 µg/ml bovine serum albumin, 2 mM ATP, the indicated amount of enzyme, and partial duplex substrate (2 µM DNA-Pi or ~ 0.25 nM circular molecules). The reactions were incubated at 30°C for 10 min and quenched with 10 µl stop buffer containing 38% glycerol, 50 mM EDTA, 0.3% sodium dodecyl sulfate and dyes. The reaction products were resolved on 8% non-denaturing polyacrylamide gels and visualized using a PhosphorImager (Molecular Dynamics).

ATPase Assays – Assays designed to measure the ATP hydrolysis reaction catalyzed by Hmi1p were set up in the same manner as helicase assays substituting partial duplex DNA with 30 µM M13mp18 ssDNA and ATP with the indicated concentration of [γ-^{32}P]ATP. The reactions were incubated at 30°C for 10 minutes unless otherwise stated. Reactions were quenched with 280 µl of a 20 mM phosphoric acid solution containing 1 mM EDTA and 5% Norit® activated carbon. Mixtures were incubated on ice for 15 minutes before centrifugation at 16,110 g for 10 minutes. A 200 µl aliquot of each supernatant was removed and added to 3 ml of scintillation fluid for quantification in a scintillation counter.

Genetic Analysis – ALY01 was sporulated using standard procedures (23) and tetrads were dissected onto YPD and YPEG to determine mitochondrial phenotype. The sporulation

media was modified from standard sporulation media by the addition of 0.0005% adenine (23).

For complementation studies the plasmids pYE12, pYE12*HMI1*, pYE12*hmi1Δmls*, pYE12*hmi1K32M* were transformed into ALY01, a diploid strain heterozygous at the *HMI1* locus, to generate ALY02, ALY03, ALY05 and ALY04. ALY02, ALY03, ALY04, ALY05 were sporulated and dissected onto YPD. After dissection on YPD, plates were incubated at 30°C for 48 hours, shifted to 4°C for 48 hours and scored for red/white color. The dissection plates were then replica plated to YPD, SD-ura, SD-trp and YPEG media. After overnight incubation at 30°C, the tetrads were scored for growth on the respective media. Growth on media lacking tryptophan revealed spores that contained the *Δhmi1::TRP1* allele. Growth in the absence of uracil indicated spore colonies that contained pYE12 derived plasmids. *Δhmi1::TRP1* spores containing pYE12-derived plasmids were scored for retention of functional mitochondria as indicated by their ability to grow on YPEG media.

Results

Purification of Recombinant Hmi1p

The *HMI1* gene was amplified from yeast genomic DNA using PCR primers that excluded the last 48 bp of the gene which encodes the mitochondria localization signal (MLS). Since the MLS is cleaved *in vivo* to generate the mature protein product upon entrance into the mitochondrial matrix (26), it was not included in the protein purified and analyzed here. The purification of Hmi1p was a three-step process that utilized two affinity columns. A fusion of Hmi1p with an intein-chitin binding domain (CBD) containing a C-terminal eight histidine affinity tag was precipitated from the cell lysate using ammonium

sulfate and was partially purified using a TALON metal affinity column (BD Biosciences) as described under "Materials and Methods". The peak fractions containing the fusion protein were pooled and bound to chitin resin. A 40 hour incubation with 50 mM DTT induced cleavage of the intein-CBP affinity tag and resulted in the release of the Hmi1Δmls product. We will refer to this protein as Hmi1p. The purified protein had a relative molecular mass of 80 kDa, consistent with the predicted molecular weight of the *HMI1* gene product and was judged to be greater than 95% pure based on analysis of an SDS-polyacrylamide gel stained with Coomassie blue. The protein was confirmed to be the product of the *HMI1* gene using a polyclonal antibody generated against Hmi1p (Fig. 1). The protein preparation used in the studies described below was substantially more pure than previous preparations of Hmi1p (see refs. (19, 22, 27) for representative SDS-polyacrylamide gels of previous purifications).

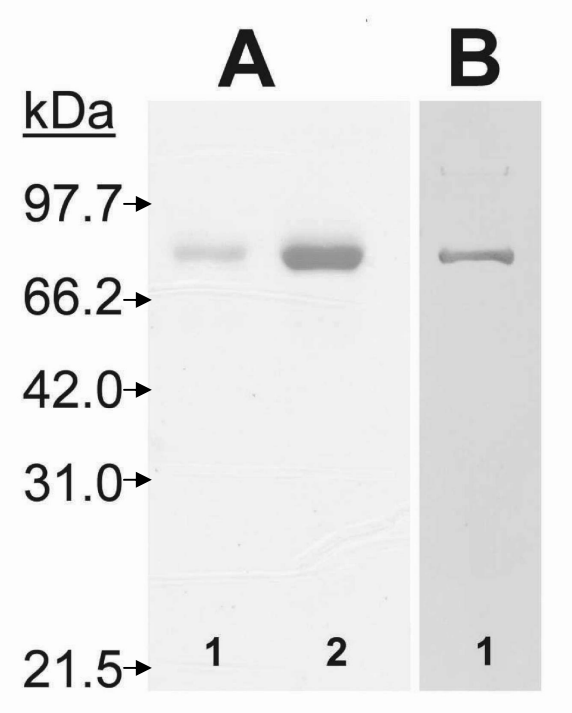

Figure 1. Analysis of purified Hmi1p.

A, Purified Hmi1p was resolved on a 9.6% SDS-polyacrylamide gel and stained with Coomassie blue. *Lane 1*, 1 µg purified Hmi1p; *lane 2*, 3 µg purified Hmi1p. *B*, 1 µg of purified Hmi1p was resolved on an identical gel and then transferred to nitrocellulose and probed with antibody directed against Hmi1p. The position of the MW standards (Biorad), resolved in an adjacent lane on the gel, are indicated on the left.

Hmi1p Helicase Activity

Prior to this study the helicase activity associated with Hmi1p had not been thoroughly characterized due to the lack of significant amounts of protein. We also note that a more rigorous characterization of Hmi1p was recently published using recombinant protein (22,). With significant amounts of purified recombinant protein available, we sought to provide an initial characterization of both the helicase reaction and the ATPase reaction catalyzed by Hmi1p. Initially, helicase activity was measured using a series of partial duplex DNA substrates containing duplex regions with lengths of 22 bp, 42 bp, and 93 bp (Fig. 2A). Purified Hmi1p effectively unwound the 22 bp partial duplex substrate. Complete unwinding of this DNA substrate was observed in a ten minute incubation with 20 nM Hmi1p. At the same protein concentration, Hmi1p was able to unwind only ~35% of the 42 bp and less than 10% of the 93 bp partial duplex substrates. Time course reactions (Fig. 2B) using 20 nM Hmi1p and the 22 bp partial duplex substrate suggested that unwinding of this duplex was complete in less than 15 minutes. Similar experiments with the 42 bp and 93 bp partial duplex substrates indicated that increasing the length of the incubation did not dramatically improve the fraction of the substrate unwound. It is interesting to note that unwinding of the 93 bp partial duplex was only slightly less than unwinding of the 42 bp partial duplex suggesting that once a critical length of duplex DNA is encountered unwinding is reduced dramatically. This is in contrast to the proportional decrease in unwinding as duplex length increases that has been reported for the UvrD helicase from *E. coli* (28). The significance of this observation is not understood at present. Apparently, the protein encounters some barrier to unwinding of longer partial duplex substrates that cannot be overcome by increasing either the length of the incubation or the protein concentration.

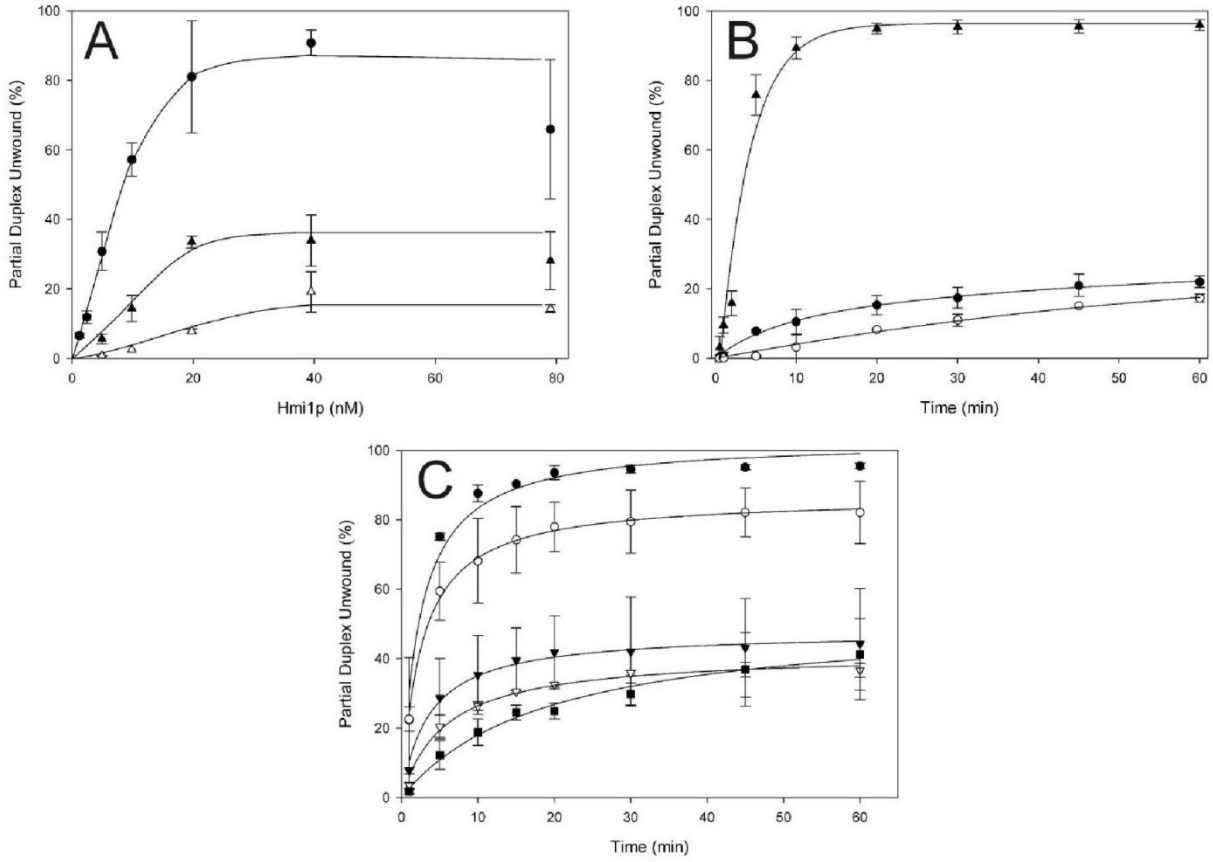

Figure 2. Hmi1p-catalyzed unwinding of partial duplex substrates. *A*. Helicase activity assay showing a titration of Hmi1p from 1 nM to 80 nM on 22 (*closed circles*), 42 (*closed triangles*) and 93 bp (*open triangles*) partial duplex DNA substrates. Reactions were incubated for 10 minutes under standard helicase reaction conditions (see "Materials and Methods") and products were resolved on native polyacrylamide gels. *B*. Helicase assay showing the unwinding activity of 20 nM Hmi1p over the course of 60 minutes. *Closed triangles*, 22 bp partial duplex; *closed circles*, 42 bp partial duplex; *open circles*, 93 bp partial duplex. *C*. Helicase assay testing the unwinding activity of 40 nM Hmi1p on partial duplexes ranging from 22-42 bp in length over a period of 60 minutes. *Closed circles*, 22 bp partial duplex; *open circles*, 25 bp partial duplex; *closed inverted triangle*, 30 bp partial duplex; *open inverted triangle*, 35 bp partial duplex; *closed square*, 42 bp partial duplex. The curves represent the best fit of the data to a rectangular hyperbola. The error bars represent the deviation about the mean in at least three separate experiments.

To more accurately determine the length dependence of the steady state unwinding reaction, helicase assays were conducted using partial duplex DNA substrates containing 25 bp, 30 bp and 35 bp of duplex DNA (Fig. 2C). In terms of sequence, these substrates represent 5 bp incremental decreases in the length of the 40 bp oligonucleotide used in construction of the 42 bp partial duplex substrate. We observed significant unwinding of the 25 bp partial duplex DNA but unwinding of both the 30 and 35 bp partial duplex DNAs was reduced to levels comparable to that of the 42 bp substrate. Thus a kinetic barrier to unwinding duplex regions greater than about 25 bp seems to exist. The reason for this is unknown but could reflect protein dissociation from the substrate allowing reannealing of the two strands to occur. Alternatively, the protein might be blocked in some way and unable to progress farther than 25-30 bp as it translocates through duplex DNA. Efforts to unwind longer partial duplex DNAs in the presence of the mitochondrial single-stranded DNA binding protein RIM1 or the related *E. coli* SSB have not been successful (data not shown).

Hmi1p shares significant similarity (23% identical, 39% similar) at the amino acid level with *E. coli* UvrD. UvrD, also known as DNA helicase II, catalyzes the 3' → 5' unwinding of duplex DNA (29). For this reason, Hmi1p has been assumed to catalyze an unwinding reaction with a 3' → 5' polarity but this has not been directly demonstrated. To directly determine the polarity of the Hmi1p-catalyzed helicase reaction the partial duplex substrate shown in Fig. 3A was constructed. This linear DNA contains a long internal region of ssDNA (>7100 nucleotides), on which the protein can load, and duplex regions of different length at each end. A helicase that binds the internal ssDNA and translocates 3' → 5' will catalyze unwinding of the 43 bp duplex at the 5'-end of the linear molecule. A

helicase that binds and translocates 5' → 3' will catalyze displacement of the 52 nucleotide DNA fragment.

The polarity of the unwinding reaction catalyzed by Hmi1p was tested using this substrate. As controls, two helicases, helicase I, an enzyme with 5' → 3' polarity and helicase II, an enzyme with 3' → 5' polarity were also tested using this DNA substrate. As expected, helicase I catalyzed the unwinding of the 52 nucleotide DNA fragment indicating a 5' → 3' polarity. Helicase II catalyzed the unwinding of the 43 bp duplex region consistent with its known 3' → 5' polarity. Hmi1p catalyzed the unwinding of the 43 bp duplex region consistent with unwinding of duplex DNA in a 3'→ 5' direction (Figure 3B, lane 5). We conclude that Hmi1p translocates in a 3' → 5' direction with respect to the DNA strand on which it is bound as it catalyzes the unwinding of duplex DNA.

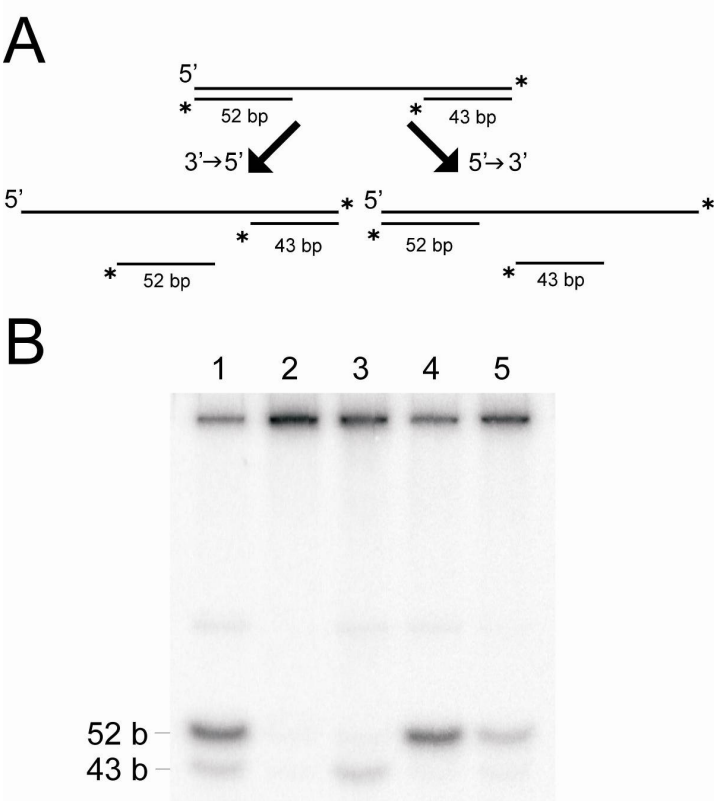

Figure 3. Hmi1p unwinds DNA with a 3'→5' polarity. *A*, Schematic depicting the substrate and the possible products generated as a result of the helicase polarity experiment. The substrate was prepared as described under "Materials and Methods". The asterisks represent radioactive label at each 3'-end. *B*, Helicase reaction mixtures were as described under "Materials and Methods". *Lanes 1 and 2*, no enzyme. *Lane 1*, boiled to denature the substrate. *Lanes 3, 4, and 5* contained TraI (10 nM), UvrD (10 nM), and Hmi1 (40 nM) respectively. The reactions were incubated at 30°C for 10 minutes and the products were resolved on a 6% non-denaturing polyacrylamide gel.

We also tested a series of reaction conditions and different cofactors to determine an optimal set of conditions for measuring the helicase activity of Hmi1p in vitro. A helicase, by definition, catalyzes the unwinding of double stranded nucleic acid in a reaction that requires NTP hydrolysis. The unwinding activity of Hmi1p was measured in the presence of each of the eight canonical (d)NTPs individually using the 22 bp partial duplex substrate (Fig. 4). As expected, no unwinding was detected in the absence of an NTP. Both ATP and dATP supported the unwinding reaction and, under these conditions, resulted in the unwinding of approximately 65% of the DNA substrate. Even though there was no significant difference between dATP and ATP, ATP consistently supported the helicase reaction slightly better than dATP. UTP and both forms of CTP were poor cofactors in the helicase reaction supporting the unwinding of approximately 10% of the DNA substrate. No unwinding was observed with dTTP or either form of GTP.

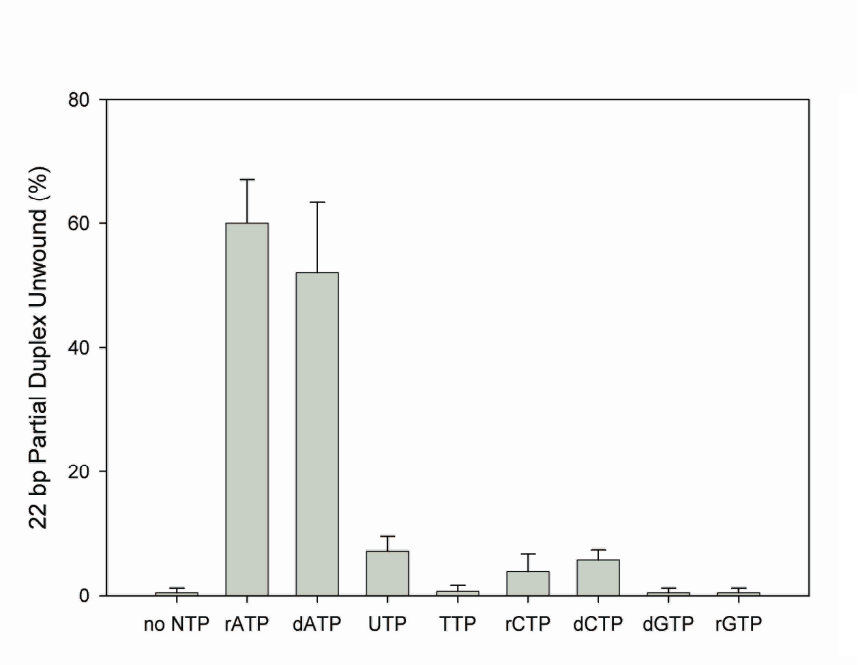

Figure 4. Nucleotide preference of Hmi1p. Helicase activity assays were conducted as described under "Materials and Methods" using the 22 bp partial duplex substrate. Each reaction contained 40 nM Hmi1p and one of the eight (d)NTPs at a final concentration of 2 mM. The error bars represent the standard deviation about the mean of two experiments.

The dependence of the Hmi1p-catalyzed unwinding reaction on ATP concentration was investigated using the 22 bp partial duplex substrate and it revealed an apparent K_M for ATP of 90 μM with optimal unwinding at a final ATP concentration of 2 mM (Fig. 5). For this reason all subsequent experiments have been conducted using 2 mM ATP as the energy cofactor.

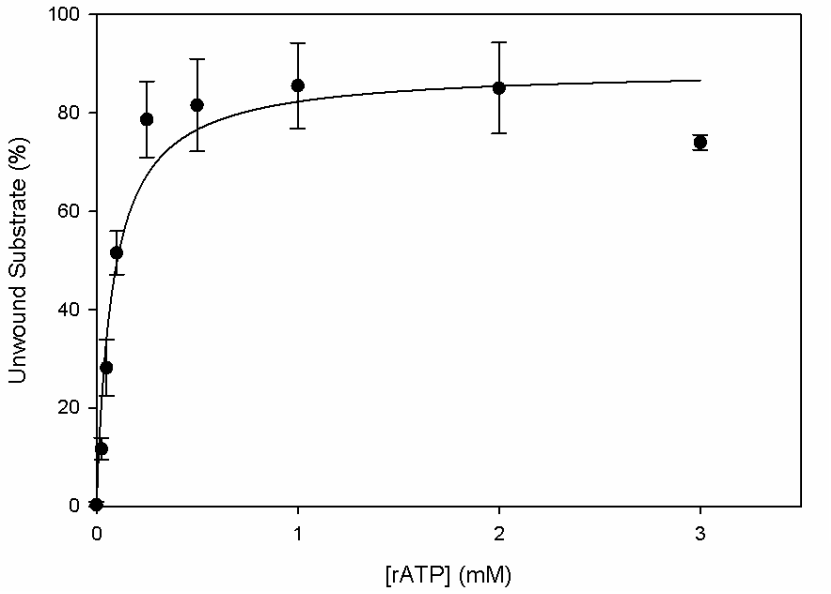

Figure 5. rATP titration and Hmi1p unwinding**.** Helicase assays were conducted as described under "Materials and Methods" using the 22 bp partial duplex substrate. The rectangular hyperbola has been fit to the data and the error bars represent the standard deviation about the mean of three experiments.

To demonstrate directly the dependence of the Hmi1p-catalzyed unwinding reaction on the hydrolysis of ATP, several ATP analogs were evaluated for their ability to support or inhibit the helicase reaction (Fig. 6). Each of these ATP analogs is either poorly hydrolyzed (ATP(γ)S) or is non-hydrolyzable (AMP-PNP and AMP-PCP). The helicase reaction was dependent on the presence of ATP as expected (Fig. 6, lane 3) and none of the ATP analogs supported the unwinding reaction (Fig. 6, lanes 6, 8 and 10) suggesting that ATP hydrolysis was essential. In addition, each of the analogs inhibited the helicase reaction when the analog was added to a reaction that contained ATP.

We chose to explore further the impact of ATP(γ)S on the ATPase reaction catalyzed by Hmi1p. To insure that the protein bound this ATP analog the mechanism of inhibition was determined. An inhibitor that binds the protein at the active site is expected to demonstrate competitive inhibition which was the case for ATP(γ)S (data not shown). To determine an apparent K_i for inhibition by ATP(γ)S, this analog was titrated into an Hmi1p-catalyzed ATPase reaction (Fig. 6B). The data were well described by a hyperbolic decay curve with an apparent K_i of 170 μM in the presence of 2 mM ATP. Thus, ATP(γ)S is an effective competitive inhibitor of both the unwinding and ATPase reactions catalyzed by Hmi1p and ATP hydrolysis is required for unwinding.

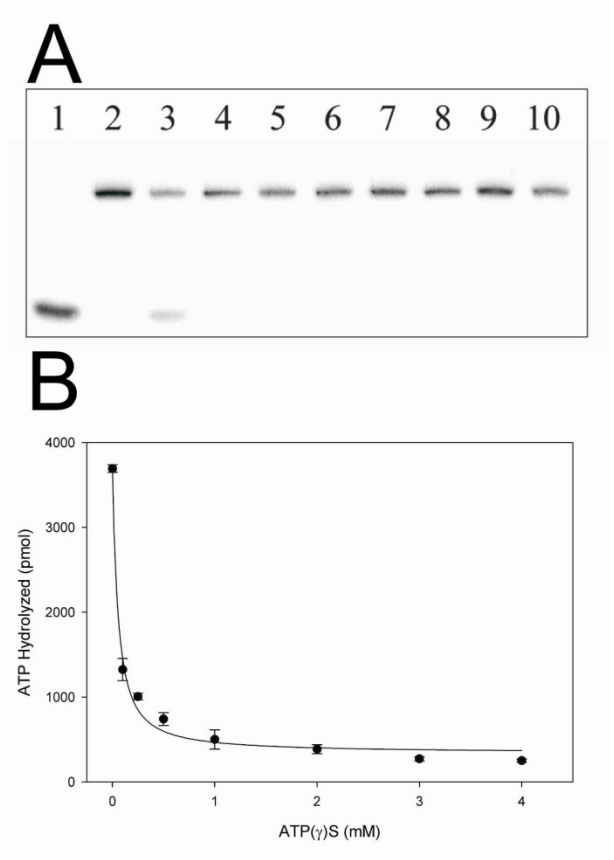

Figure 6. ATP(γ)S, AMP-PNP, and AMP-PCP are inhibitors of Hmi1p ATPase activity. *A*, All reactions were for 10 minutes and contained 40 nM Hmi1p unless otherwise indicated. *Lane 1*, No enzyme and boiled for 3 minutes; *Lane 2*, No enzyme; *Lane 3*, 2 mM ATP; *Lane 4*, no ATP; *Lane 5*, 2 mM ATP and 2 mM ATP(γ)S; *Lane 6*, 2 mM ATP(γ)S; *Lane 7*, 2 mM ATP and 2 mM AMP-PNP; *Lane 8*, 2 mM AMP-PCP; *Lane 9*, 2mM ATP and 2 mM AMP-PCP; *Lane 10*, 2 mM AMP-PCP. *B*, Titration of ATP(γ)S from 0 mM to 4 mM in an ATPase assay containing 2 mM ATP and 160 nM Hmi1p. A hyperbolic decay curve was fit to the data. The error bars represent the standard deviation about the mean of two experiments.

Helicase reactions also typically require the presence of a divalent cation cofactor. A titration of $MgCl_2$ from 0 mM to 27 mM in a helicase reaction using the 22 bp partial duplex substrate revealed that upon addition of $MgCl_2$ there was a pronounced increase in unwinding as the $MgCl_2$ concentration was increased with maximal helicase activity between 6 and 12 mM $MgCl_2$ (data not shown). However, since there was no significant difference between 6 mM and 12 mM $MgCl_2$, 6mM $MgCl_2$ was used for all subsequent reactions. No activity was observed in the absence of $MgCl_2$ suggesting that this is an essential cofactor.

The ATPase Activity of Hmi1p

The unwinding reaction catalyzed by a helicase requires energy which is usually supplied by the hydrolysis of an NTP. In addition, nucleic acid cofactors often stimulate the NTPase activity of helicases. To evaluate the effect of various nucleic acid cofactors on the ATPase activity of Hmi1p, ATP hydrolysis was measured in the presence of several nucleic acid cofactors with differing secondary structure and at varying concentrations (Fig. 7). The nucleic acid cofactors tested were circular M13mp18 ssDNA, supercoiled plasmid DNA, rRNA, linear dsDNA, and poly(dT). Each cofactor was added to an Hmi1p-catalyzed ATPase reaction at concentrations ranging from 0 to 30 μM nucleotide phosphate. Both M13mp18 ssDNA and poly(dT) stimulated the Hmi1p-catalzyed ATPase reaction to similar extent. The DNA concentration required for half-maximal stimulation of ATP hydrolysis was 2.2 μM DNA for M13mp18 ssDNA and 0.6 μM DNA for poly(dT) suggesting that both a circular DNA and a linear DNA were good ATPase activators. Hmi1p-catalyzed ATPase activity was not supported by rRNA, linear dsDNA, or supercoiled dsDNA suggesting that the protein does not productively interact with RNA or with duplex DNA (data not shown).

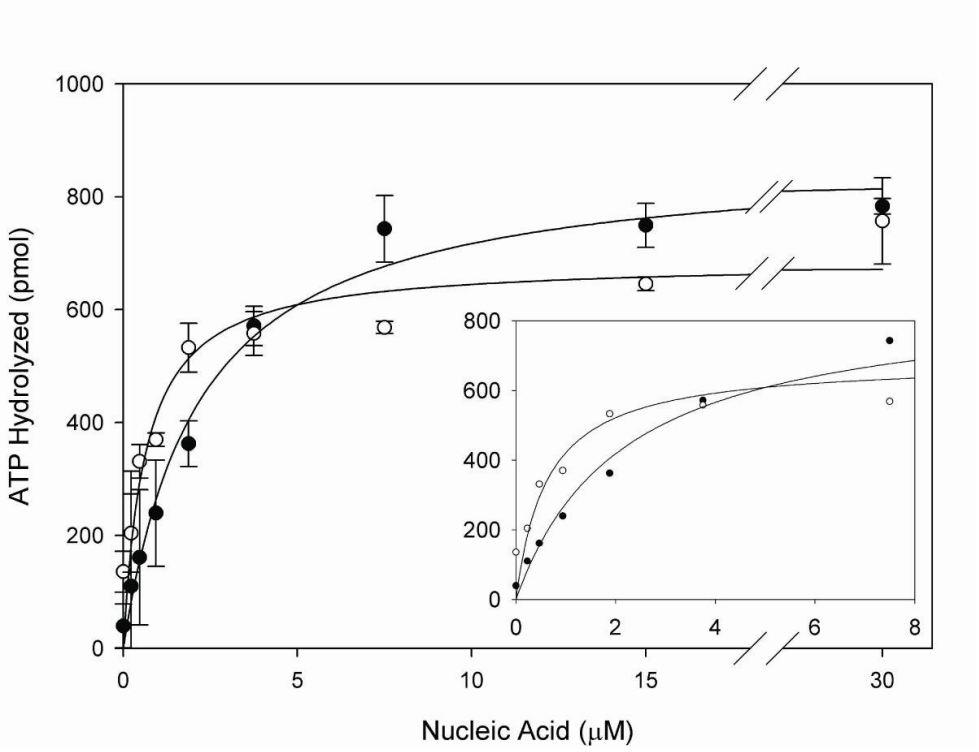

Figure 7. ssDNA stimulates Hmi1p ATPase activity. *A*, ATPase assays were conducted as described under "Materials and Methods" using the indicated concentrations of either M13 mp18 ssDNA (*closed circles*) or poly (dT) (*open circles*). Reactions were incubated for 10 minutes and contained 50 nM Hmi1p. *Inset*: The region from 0.2 μM to 7.5 μM M13 and poly(dT) is shown. Error bars represent the standard deviation about the mean. Rectangular hyperbolas have been fit to the data.

Several divalent cations were also tested in ATPase reactions using Hmi1p and M13 ssDNA as the nucleic acid cofactor (Fig. 8). A total of five divalent cations were tested as Hmi1p cofactors: $MgCl_2$, $MnCl_2$, $CaCl_2$, $ZnCl_2$, and $CuCl_2$. Each divalent cation was tested in an ATPase reaction at a final concentration of 8 mM (Fig 8). ATP hydrolysis in the presence of $MgCl_2$ was two-fold higher than in the presence of either $MnCl_2$ or $CaCl_2$. $ZnCl_2$ and $CuCl_2$ were poor divalent cation cofactors in the Hmi1p-catalyzed ATPase reaction.

ATPase reactions containing M13mp18 ssDNA were used to determine the steady state kinetic parameters for DNA-stimulated ATP hydrolysis catalyzed by Hmi1p (Fig 9). The dependence of the ATP hydrolysis reaction on ATP concentration was well described by

a rectangular hyperbola. Assuming Michealis-Menten kinetics for this reaction, the K_m value was 150 μM ATP and a k_{cat} of 72.7 min^{-1} was observed.

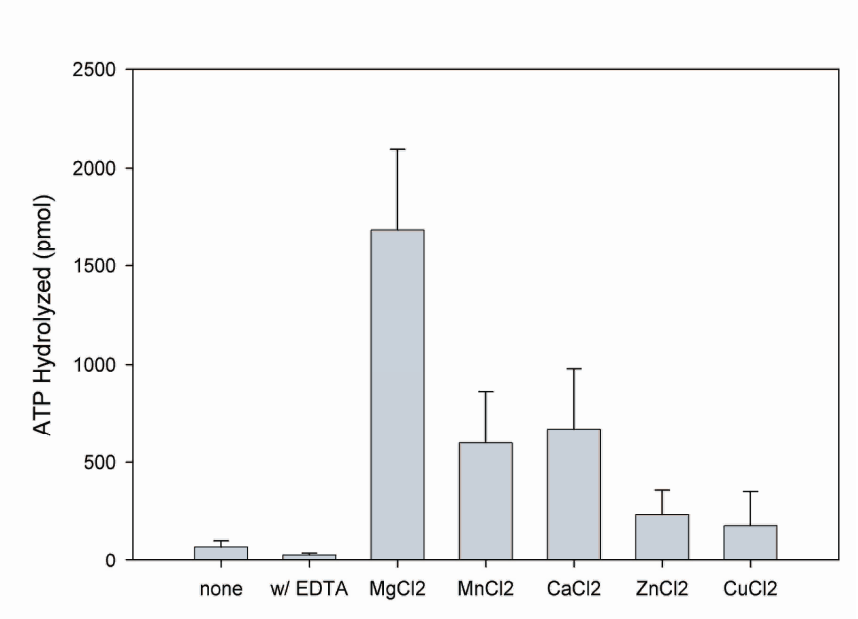

Fig. 8. Divalent metal ion cofactor effects on Hmi1p activity. ATPase assay testing the ability of Hmi1p to hydrolyze ATP based on the presence of differing divalent metal cations. Conditions identical to ATPase assay (Materials and Methods) except Hmi1p present at 62 nM and metal cations present at 8 mM in place of 6 mM $MgCl_2$.

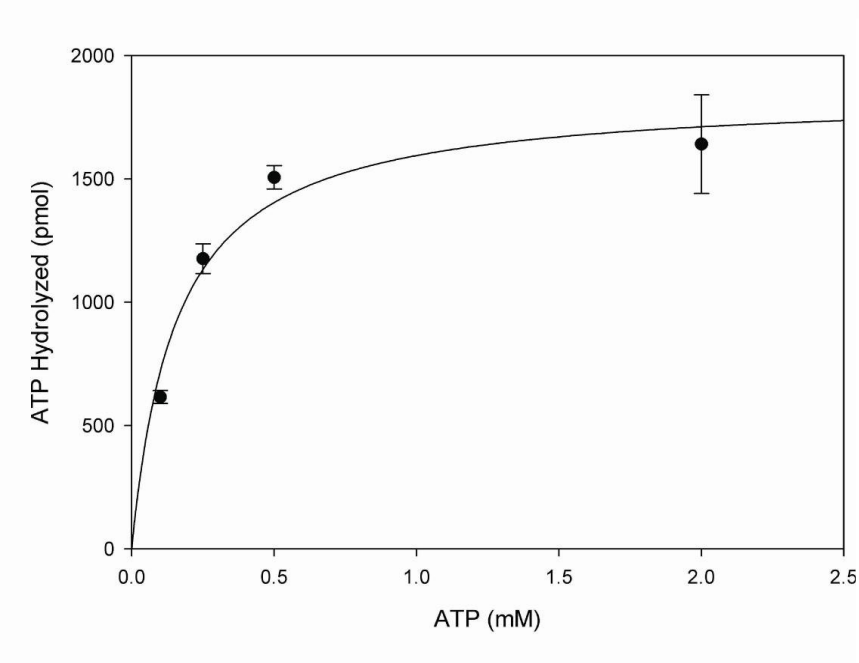

Figure 9. Dependence of the ATPase reaction on ATP concentration. ATPase assays were conducted as described under "Materials and Methods" using 98 nM Hmi1p and the indicated concentrations of ATP. Error bars represent the standard deviation about the mean of three independent experiments. A rectangular hyperbola as described by the Michealis-Menten equation was fit to the data.

Genetic characterization of hmi1 mutants

The haploid W303a*Δhmi1::TRP1*strain, KCY3-2D, formed petite colonies on rich media and failed to grow on YPEG media (data not shown). Together, these phenotypes suggest a lack of mitochondrial function similar to results reported by others (19, 26). KCY3-2D and W303α cells were stained with DAPI to determine if disruption of *HMI1* caused an observable effect on mtDNA (data not shown). When KCY3-2D cells were stained with DAPI the strain appeared to completely lack mtDNA (i.e. the strain was rho^{o}). The mtDNA was clearly present in W303α cells as evidenced by the punctate DAPI staining pattern around the perimeter of the cells.

Since the loss of mtDNA is an irreversible event, it was not possible to simply introduce a plasmid carrying *HMI1* into *hmi1*Δ haploid cells to evaluate the ability of various mutants to complement the *HMI1* deletion. Complementation experiments must be performed under circumstances in which mtDNA is available for Hmi1p or mutant forms of Hmi1p to maintain. Therefore, KCY3-2D and W303α were mated to obtain ALY01, a diploid strain heterozygous (*HMI1*/*hmi1*Δ) at the *HMI1* locus. ALY01 formed grande colonies on rich media and exhibited a wild-type growth phenotype when streaked on YPEG media. The W303 background is *ade2* and respiring *ade2* colonies are red. The red coloration depends on active respiration and, in the absence of respiration, white colonies are formed. This color phenotype allowed for a rapid assay of mitochondrial function on rich media (30, 31). Since the heterozygous diploid grew on YPEG media and developed the red coloration indicative of active respiration, one copy of the wild-type allele of *HMI1* is sufficient to ensure the presence of functional mitochondria. Thus, the petite phenotype associated with *hmi1Δ* strains is recessive to *HMI1*.

When the heterozygote was sporulated and the tetrads dissected, the *hmi1Δ* spore colonies exhibited the expected mitochondrial defect as evidenced by the 2:2 segregation of red and white colonies on YPD. To confirm the genotype of each spore colony, the tetrads were replica plated to media lacking tryptophan to score for the *hmi1::TRP1* deletion allele. The tetrads were also replica plated to media lacking a fermentable carbon source to determine which spore colonies were capable of respiration. Of 48 ALY01 tetrads dissected, the ability to grow on medium lacking tryptophan and the ability to grow on medium lacking a fermentable carbon source were never observed in the same haploid colony. These results indicate that disruption of the *HMI1* gene is responsible for the petite phenotype.

The heterozygote ALY01 was also sporulated and dissected directly onto YPEG media. In this case, two spores in each tetrad were expected to be respiration competent and to grow normally on YPEG media. This is exactly what was observed. The remaining two spores formed microcolonies. Even after extensive incubation at 30°C the microcolonies did not grow into normal sized colonies. The number of cells in the colonies was determined as described under "Materials and Methods." The microcolonies contained an average of 4700 cells while the grande colonies contained an average of 1.3 X 10^6 cells.

As indicated above, the grande spores that grew on the YPEG plates were respiration proficient. When cells from these spore colonies were stained with DAPI, mtDNA was clearly visible (Fig. 10A). The cells from the microcolonies, on the other hand, appeared heterogeneous with respect to the presence of mtDNA (Fig. 10B). Some cells in each microcolony contained mtDNA while others did not. Since all the cells in the microcolony are respiration deficient, the mtDNA present in a subpopulation of the microcolony cells is likely to be rho^-. Therefore, the cells in the microcolonies were either rho^o or rho^- with

respect to the mitochondrial genome. In either case the cells lack a fully functional mitochondrial genome. However, it is important to note that some rho$^-$ mtDNA genomes must be able to replicate in the absence of Hmi1p. Similar data has been reported by others (19, 27).

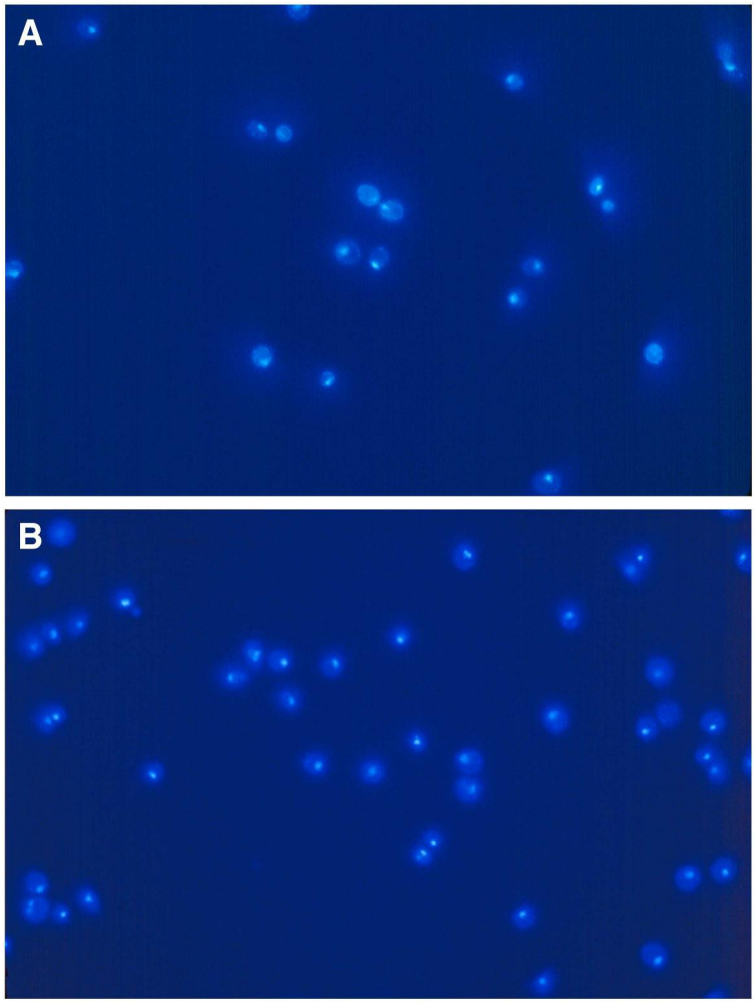

Figure 10. Examination of the spore products from the tetrad dissection of *HMI1/hmi1::TRP1* yeast cells on YPEG media by DAPI staining. *A*. The heterozygous strain was sporulated and directly dissected onto YPEG media. The resulting spore colonies were dispersed in H_2O and plated onto YPD. HMI1 spores form grande colonies and the mtDNA is visible as punctuate staining at the cell periphery when stained with DAPI. *B*. When the microcolonies were stained with DAPI, rho$^-$ and rho^o cells were visible.

The importance of mitochondrial localization and the role of the helicase activity associated with Hmi1p were tested in genetic complementation assays using plasmids expressing *HMI1* and *hmi1* mutants in the strain heterozygous at the *HMI1* locus. Maintenance of functional mtDNA was evaluated by examining the spore products of a heterozygous strain containing plasmid copies of wild-type *HMI1* or the appropriate mutant. When ALY03, the heterozygous strain carrying pYE12*HMI1* (wild-type *HMI1*), was sporulated and dissected on YPD media, the four spores were two red and one or two sectored or red. The sectored pattern observed in one or two of the spore colonies presumably resulted from the loss of plasmid-borne *HMI1* since there was no selection for maintenance of the plasmid. Loss of pYE*HMI1* results in loss of the ability to respire and the concomitant loss of the ability to produce the red coloration. Therefore, plasmid loss is seen as a variegated pattern in the spore colony. When the dissected tetrads were replica plated to YPEG media to directly assess mitochondrial function, all four spore colonies were able to grow (Table 3). The tetrads segregated 2:2 for growth on SD-Trp indicating that two spores were *Δhmi1::TRP1* and two spores were *HMI1*. Spore colonies that grew on SD-Ura retained the pYE*HMI1* plasmid. Thus, the presence of pYE*HMI1* allowed *Δhmi1::TRP1* spore colonies to retain mitochondrial function. When ALY02 containing pYE12 (vector plasmid) was sporulated and dissected on YPD, the red and white phenotype segregated 2:2 as expected. Trp+, Ura+ spores from ALY02 failed to grow on YPEG indicating that the empty vector does not allow *Δhmi1::TRP1* cells to retain functional mitochondria (Table 3).

Table 3: Plasmid Dependent Retention of Functional Mitochondria in *Δhmi1::TRP1* Spores

Strain	YPEG+	YPEG-	Total	Complementation
ALY02(pYE12)	0	150	150	no
ALY03(*HMI*1)	113	19	132	yes
ALY04(K32M)	22	62	84	partial
ALY05(ΔMLS)	2	128	130	no

Strains heterozygous at the *HMI1* locus and carrying the indicated plasmid (pYE12, pYE12*HMI1*, pYE12*hmi1K32M*, pYE12*hmi1ΔMLS)* were generated as described under "Materials and Methods". The strains were sporulated and dissected on YPD media. Spore colonies were replica plated to SD-trp, SD-ura and YPEG media. Spores that grew on SD-trp, indicating that they were *Δhmi1::TRP1*, and on SD-ura, indicating that they contained the plasmid were scored for their ability to grow on YPEG media. The total number of Trp+, Ura+ spores scored for functional mitochondria for each strain is indicated. The number of respiration proficient and respiration deficient spores from the strains were compared using the Fisher exact test method. Two-tailed P values greater than 0.05 were not considered significant. The two-tailed P value for the number of YPEG+ spores from ALY02 (the negative control) and ALY03 (*HMI1*) is less than 0.0001. The two-tailed P value for the number of YPEG+ spores from ALY02 (the negative control) and ALY04 (containing pYE*hmi1K32M*) is less than 0.0001. The two-tailed P value for the number of YPEG+ spores from ALY04 (*hmi1K32M*) and ALY03 (*hmi1*) is less than 0.0001. The P value for the number of YPEG+ spores from ALY02 (the negative control) and ALY05 (*hmi1ΔMLS*) was 0.2147.

To test the importance of localization of Hmi1p to the mitochondria, the *HMI1* gene was altered by site-directed mutagenesis to remove the C-terminal MLS. This altered gene, *hmi1ΔMLS*, was introduced into ALY01 (heterozygous at the *HMI1* locus) and its ability to complement the loss of *HMI1* was tested. When ALY05, containing pYE12*hmi1ΔMLS,* was sporulated and dissected on YPD, the spores segregated 2:2 in the red/white assay suggesting that two spores lacked functional mitochondria. When these spore colonies were replica plated to YPEG, the *Δhmi1::TRP1*/pYE*hmi1ΔMLS* spores failed to grow (Table 3). Thus,

pYE12*hmi1ΔMLS* does not complement the mitochondrial defect seen in the *Δhmi1::TRP1* strain. The *HMI1*/pYE12*hmi1ΔMLS* spores formed red colonies and contained functional mitochondria. We conclude that complementation of the mitochondrial defect requires the C-terminal MLS. This, in turn, suggests that Hmi1p must localize to the mitochondria to function.

To evaluate the role of the helicase reaction catalyzed by Hmi1p in maintenance of the mtDNA genome three point mutants were constructed and evaluated. Point mutants were generated at the highly conserved lysine residue (K32) in the Walker A box of *HMI1*. Previous studies have shown that other helicases containing a similar mutation are able to bind the ATP but fail to catalyze ATP hydrolysis which abrogates the helicase reaction (32-35). The conserved lysine at position 32 was changed to an alanine, serine, and methionine as described under "Materials and Methods". Hmi1p-K32M was insoluble when overexpressed in *E. coli*. Two of the mutant proteins, Hmi1p-K32A and Hmi1p-K32S, were soluble when expressed in *E. coli* and were purified in the same manner as the wild type protein. Neither purified protein exhibited significant helicase activity when tested using a partial duplex DNA substrate (data not shown). Thus, as expected, the conserved lysine in the Walker A box is essential for helicase activity. It should also be noted that this result makes it extremely unlikely that a contaminant in our preparation of Hmi1p is responsible for the helicase activity associated with the purified protein.

The *hmi1K32M* allele was introduced into the *HMI1/hmi1*Δ heterozygote on a multicopy plasmid (pYE12*hmi1K32M*) and its ability to complement the loss of *HMI1* was tested. When ALY04 was sporulated and dissected on YPD, the spore colonies were either red or sectored. When the tetrads were replica plated to YPEG, 22 of 84

Δhmi1::TRP1/pYE12*hmi1K32M* spores were able to grow (Table 3). The remaining 62 *Δhmi1::TRP1*/pYE12*hmi1K32M* spores were unable to grow on YPEG. It appears that pYE12*hmi1K32M* partially complements the mitochondrial defect present in the *Δhmi1::TRP1* strain. This suggests that complementation of the mitochondrial defect does not require the helicase activity associated with Hmi1p. However, the number of *Δhmi1::TRP1*/pYE12*hmi1K32M* spores that were capable of growth on YPEG media was significantly different from that seen when pYE12*HMI* was used in the complementation test. This indicates that the active helicase confers some advantage to the cell in terms of mtDNA maintenance. However, an active helicase is apparently not essential for maintenance of mtDNA.

Discussion

Here we report the purification of a yeast DNA helicase, Hmi1p, and provide an initial biochemical characterization of its DNA helicase and ATPase activities. In addition, the results of genetic complementation studies using two *hmi1* mutants are reported. Taken together, the data demonstrate that Hmi1p is a DNA-stimulated ATPase with 3' → 5' DNA helicase activity that is involved in the maintenance of mtDNA. However, the molecular role of this protein in mtDNA metabolism is still not resolved.

A truncated form of Hmi1p lacking the MLS, which is cleaved in vivo, was expressed and purified in *E. coli* providing significant amounts of recombinant protein for biochemical characterization. The helicase activity associated with Hmi1p requires ATP hydrolysis as demonstrated by the inhibition of the unwinding reaction by a poorly hydrolyzed ATP analog, ATP(γ)S. To ensure the protein binds this ATP analog we have shown that ATP(γ)S

is a competitive inhibitor of the DNA-stimulated ATPase reaction catalyzed by Hmi1p. Thus, ATP hydrolysis is essential for Hmi1p-catalyzed DNA unwinding and the purified protein demonstrates optimal unwinding activity at 2 mM rATP with half maximal reaction velocity at an ATP concentration of 90 μM. We have also directly demonstrated a 3' → 5' unwinding polarity using a DNA substrate that is able to detect both 5' → 3' and 3' → 5' unwinding. The unwinding reaction catalyzed by Hmi1p can be characterized as 'limited' based on the ability of the protein to unwind 22 and 25 bp partial duplex DNAs while unwinding of partial duplex substrates in excess of 30 bp is dramatically reduced compared with unwinding of the 22 bp substrate. Increasing the protein concentration or the length of incubation did not significantly improve this result suggesting there is a block of some kind to unwinding of longer duplex regions. Efforts to stimulate the unwinding reaction by including either *E. coli* SSB or the mitochondrial single-stranded DNA binding protein RIM1 did not improve the result. Thus, Hmi1p, in the absence of other proteins, catalyzes the unwinding of a relatively short duplex region. It is possible the protein interacts with other proteins in the mitochondrion and this may stimulate unwinding. Proteins involved in DNA metabolism often form complexes and work in conjunction with other proteins. This may be the case for Hmi1p and further work will be required to identify proteins that interact with, and perhaps modulate the activity of Hmi1p.

The ATPase activity of Hmi1p was strongly stimulated by the addition of a nucleic acid cofactor. Several nucleic acids were tested for their ability to stimulate the Hmi1p-catalyzed ATPase reaction. Both M13 ssDNA and poly(dT) proved to be effective in stimulating the ATPase reaction. RNA and several duplex DNA molecules were not effective. This suggests that Hmi1p does not interact with RNA, consistent with the fact it is

not required for transcription of the mtDNA genome (19). Moreover, both linear and circular ssDNA stimulate the ATPase reaction to the same extent. However, the DNA concentration required for one-half maximal stimulation (K_{eff}) is slightly different for these two effectors of the ATPase reaction. A four-fold lower concentration of the linear poly(dT) was required for one-half maximal stimulation than circular M13 ssDNA. Previous studies with other helicases have suggested that proteins that translocate processively along ssDNA exhibit a lower K_{eff} for circular DNA than for linear DNA (28, 36). This is based on the fact that a processive translocase would not dissociate from a circular molecule as frequently as from a linear molecule. Applying the same interpretation would suggest that Hmi1p is not a processive translocase. This is consistent with the poor unwinding of long duplex regions. Thus, it is possible that this protein exhibits very low processivity as both a translocase and a helicase in the absence of additional proteins. This interpretation is offered with caution since careful kinetic experiments to directly address the issue of processivity have not been performed.

Genetic studies have shown that disruption of the *HMI1* gene resulted in a haploid strain (KCY3-2D) that lacked mitochondrial function. The failure of *hmi1Δ* colonies to grow on non-fermentable carbon sources and lack of visible mtDNA when stained with DAPI augment the conclusion that disruption of *HMI1* affects the maintenance of mtDNA. A diploid strain heterozygous at the *HMI1* locus exhibited no apparent phenotype with regard to mitochondrial function indicating that the *hmi1Δ* allele was recessive to the wild-type allele. Sporulation and tetrad dissection of the *HMI1/hmi1*Δ heterozygote ALY01 on rich media resulted in two grande and two petite colonies. The cells in petite colonies (*hmi1::TRP1*) exhibited one of two patterns with regard to DAPI staining of mtDNA. The

cells were either rho^{o} (i.e. lacked mtDNA) or were a mixture of rho^{o} and rho^{-}. The grande colonies contained mtDNA as evidenced by staining with DAPI. The DAPI results support the conclusion that Hmi1p affects mtDNA metabolism. Without Hmi1p, yeast cells were not able to maintain rho^{+} mitochondrial genomes; however, some rho^{-} mitochondria were present. A similar result has been obtained by others (19, 27). rho^{+} and rho^{-} mitochondrial genomes appear to be maintained differently as many trans-acting factors and cis-acting sequences required for rho^{+} maintenance are not required for maintenance of rho^{-} mitochondrial genomes (9, 19, 37-41).

Although *hmi1*Δ mutant cells cannot support the maintenance of rho^{+} mitochondrial genomes, these cells can sustain rho^{-} mitochondrial genomes at least for some period of time. When ALY01, the strain heterozygous at the *HMI1* locus, was sporulated and dissected on YPEG, *hmi1*Δ spores formed microcolonies. Even after extensive growth at 30°C these remained microcolonies containing an average of 4700 cells while grande colonies grown for the same time contained 1.32 X 10^{6} cells. The cell number can be used to arrive at an estimate of the number of generations required to achieve the cell number present in the colony. Approximately 12 generations were required to generate 4700 cells while approximately 20 generations were required to generate 1.32 X 10^{6} cells. The absence of Hmi1p affects mtDNA maintenance before 12 generations occur as cells from the microcolony are rho^{o} or rho^{-}. The effect of Hmi1p loss on mtDNA is rapid considering the number of mitochondrial genomes in yeast cells varies depending on a variety of conditions with an upper limit of approximately 50 mitochondrial genomes per cell (42). The fast development of the mitochondrial phenotype suggests Hmi1p plays an important, integral role in mtDNA metabolism.

The petite phenotype associated with *hmi1*Δ strains was prevented by expressing *HMI1* from a plasmid. In addition, spore colonies containing the pYE*HMI1* plasmid were able to grow when replica plated to YPEG media indicating normal mitochondrial function. This result confirms that the petite phenotype of *Δhmi1::TRP1* cells is caused by the lack of Hmi1p. DAPI staining of *Δhmi1::TRP1*/pYE*HMI1* cells revealed mtDNA (data not shown) providing further confirmation that Hmi1p is required for maintenance of rho$^+$ mitochondria.

Hmi1p localizes to mitochondria and recent work indicates that the MLS of Hmi1p is located at the C-terminal end of the protein (19, 26). Therefore, a C-terminal truncation of Hmi1p was constructed and tested for full Hmi1p function in *Δhmi1::TRP1* cells. Exogenous *hmi1ΔMLS* supplied on a plasmid did not allow retention of mtDNA by *Δhmi1::TRP1* cells, although exogenous Hmi1p with an intact MLS did allow retention of mtDNA. The failure of *hmi1ΔMLS* to sustain functional mitochondria in *Δhmi1::TRP1* cells indicates that Hmi1p requires the C-terminus for full *in vivo* function, presumably to direct localization of Hmi1p to the mitochondria. To determine the location of the truncated Hmi1p, mitochondrial and cytosolic fractions were isolated from *hmi1::TRP1*/pYE*hmi1Δmls* cells. Hmi1Δmls was present in the cytosolic fraction, but no Hmi1Δmls could be detected in the mitochondrial fraction (data not shown). In simultaneous experiments with *hmi1::TRP1*/pYE*hmi1K32M* and *hmi1::TRP1/*pYE*HMI1*, Hmi1p was found in the mitochondrial fraction from both strains (data not shown). Thus, removal of the C-terminal 16 residues abrogates localization of Hmi1p to the mitochondria. This, in turn, leads to the failure of *Δhmi1::TRP1* cells containing the *hmi1ΔMLS* allele to sustain rho$^+$ mitochondria. In a recent study, deletion of 15 residues, including the putative MPP cleavage site, interfered with the mitochondrial localization of Hmi1p (19). The results presented here, and those previously published, are

entirely consistent and indicate that localization of Hmi1p to the mitochondria requires the C-terminus of Hmi1p. Moreover, the data presented here indicate that mitochondrial localization is essential for function.

The involvement of Hmi1p in rho$^+$ mtDNA maintenance, combined with the *in vitro* helicase activity of Hmi1p, suggests that Hmi1p might affect rho$^+$ mtDNA maintenance through the helicase activity of Hmi1p. To test the importance of the helicase activity in the role played by Hmi1p in mtDNA maintenance, a point mutant was constructed that was designed to eliminate the unwinding activity of the helicase. Unexpectedly, the plasmid encoded Hmi1p-K32M allowed maintenance of functional mitochondria in a significant fraction of the deletion spores as evidenced by their growth on YPEG media. However, when compared with HMI1*, hmi1K32M* did not allow retention of the wild-type phenotype as well as the wild-type gene (see Table 3). The number of spore colonies able to grow on non-fermentable carbon sources (YPEG+) in *Δhmi1::TRP1*/pYE*hmi1K32M* and *Δhmi1::TRP1*/pYE*HMI1* differ significantly. The intermediate ability of Hmi1p-K32M to allow the deletion strain to retain functional mitochondria indicates a partial restoration of function by Hmi1p-K32M. Apparently the unwinding activity of Hmi1p is not essential for rho$^+$ mitochondrial maintenance. However, the ability of Hmi1p to function in rho$^+$ mtDNA maintenance is clearly improved when the protein is fully functional.

Maintenance of the mitochondrial genome depends on several processes including transcription, recombination and replication, and segregation to the daughter cell. Hmi1p does not appear to affect mitochondrial transcription as similar levels of mitochondrial RNA transcripts occur in both wild-type and deletion strains (19). Thus, Hmi1p could impact mtDNA maintenance through a role in recombination or replication. Several possibilities are

considered below. Replication of rho$^+$ mtDNA is thought to be initiated by mitochondrial RNA polymerase-dependent priming similar to that of mammalian mitochondria (43, 44). However, it has also been suggested that replication of mtDNA may be initiated using recombination intermediates (4, 5, 10). Perhaps Hmi1p plays a role in mtDNA recombination. In wild-type cells Hmi1p might regulate mitochondrial recombination by disrupting non-homologous regions and destabilizing the Holliday junction. In the absence of Hmi1p, recombination of the mitochondrial genome would increase to such a level that the mitochondrial genome would be destabilized by the presence of an increased number of unresolved recombination junctions and, in some cases, the mitochondrial genome would be lost resulting in rho^0 cells. In other cases recombination would rapidly generate rho$^-$ genomes consisting of short repeated sequences that present easy targets for recombination. Although attractive, this model seems less likely since it does not readily account for partial restoration of function by the *hmi1K32M* allele. In this model one would predict that a mutant form of Hmi1p, incapable of unwinding, would not be able to retain functional mitochondria or would affect the stability of mtDNA in the heterozygous strain.

Several helicases that function specifically during initiation of replication have been described, including PriA from *E. coli*. PriA binds DNA at primosome assembly sequences (PAS) or D-loops and recruits other components of the primosome to a complex that restarts collapsed replication forks (45-50). It is thought that the helicase activity of PriA allows the proteins to provide the ssDNA required for a more stable replisome or primosome complex (49, 51). However, helicase deficient mutations in motif I of PriA, which bind DNA and recruit other components of the primosome normally, allow almost wild-type levels of function (32). Thus, the helicase activity of PriA is not required for its function *in vivo*.

Both the wild-type *HMI1* and helicase deficient *hmi1K32M* results are consistent with a model in which Hmi1p participates in replication in a manner similar to the function of PriA in replication restart. Wild-type Hmi1p would bind mtDNA and recruit necessary components of replication but would not necessarily participate in the elongation phase of replication. In the absence of Hmi1p some recombination initiated replication would allow establishment of and replication of rho$^-$ genomes. The ability of *hmi1Δ* cells to support rho$^-$ genomes suggests that Hmi1p is unlikely to be directly involved in the elongation phase of mtDNA replication. While initiation of replication or replication restart might occur more efficiently if Hmi1p were able to provide unwound ssDNA, the essential role of Hmi1p in mtDNA maintenance may be in recruiting other proteins necessary for replication. Although deficient in helicase activity, the Hmi1p-K32M mutant would still be capable of binding DNA and assembling replication proteins on either a collapsed replication fork or the origin of replication. A role for Hmi1p in replication restart or in the initiation of mtDNA replication is consistent with the observed results.

The currently available data suggest that Hmi1p is not the replicative helicase in yeast mitochondria. It has been shown that *HMI1* is required for mtDNA maintenance but that the helicase/ATPase function is dispensable. However, fewer cells maintain their mtDNA in the presence of the ATPase-inactive variants. Perhaps the primary role of Hmi1p is to help maintain the integrity of the replication complex. For example, PriA is involved in replication restart at stalled forks in *E. coli* and is able to function in primosome assembly even with disabled ATPase function. Cells lacking Hmi1p may undergo fork stalling during replication and ultimately generate double-stranded breaks resulting in the fragmented genome seen recently by Sedman et al. (27). Furthermore, they observed *HMI1* was not

required for the maintenance of rho$^-$ genomes which might undergo less fork stalling due to the relatively small genome size (often times 1 kb) resulting in a much higher viability rate and giving the impression that Hmi1p is not the replicative helicase.

References

1. Costanzo MC, Fox TD. Control of mitochondrial gene expression in saccharomyces cerevisiae. Annu Rev Genet. 1990;24:91-113.

2. Maleszka R, Skelly PJ, Clark-Walker GD. Rolling circle replication of DNA in yeast mitochondria. EMBO J. 1991 Dec;10(12):3923-9.

3. Chen XJ, Clark-Walker GD. The petite mutation in yeasts: 50 years on. Int Rev Cytol. 2000;194:197-238.

4. Bendich AJ. Structural analysis of mitochondrial DNA molecules from fungi and plants using moving pictures and pulsed-field gel electrophoresis. J Mol Biol. 1996 Feb 2;255(4):564-88.

5. Lockshon D, Zweifel SG, Freeman-Cook LL, Lorimer HE, Brewer BJ, Fangman WL. A role for recombination junctions in the segregation of mitochondrial DNA in yeast. Cell. 1995 Jun 16;81(6):947-55.

6. Ling F, Shibata T. Recombination-dependent mtDNA partitioning: In vivo role of Mhr1p to promote pairing of homologous DNA. EMBO J. 2002 Sep 2;21(17):4730-40.

7. Ling F, Hori A, Yoshida M, Shibata T. Rolling circle replication: A universal model for controlling mechanisms of mitochondrial DNA copy number. Tanpakushitsu Kakusan Koso. 2007 Jul;52(8):886-92.

8. Kleff S, Kemper B, Sternglanz R. Identification and characterization of yeast mutants and the gene for a cruciform cutting endonuclease. EMBO J. 1992 Feb;11(2):699-704.

9. MacAlpine DM, Perlman PS, Butow RA. The high mobility group protein Abf2p influences the level of yeast mitochondrial DNA recombination intermediates in vivo. Proc Natl Acad Sci U S A. 1998 Jun 9;95(12):6739-43.

10. Zelenaya-Troitskaya O, Newman SM, Okamoto K, Perlman PS, Butow RA. Functions of the high mobility group protein, Abf2p, in mitochondrial DNA segregation, recombination and copy number in saccharomyces cerevisiae. Genetics. 1998 Apr;148(4):1763-76.

11. Lecrenier N, Foury F. New features of mitochondrial DNA replication system in yeast and man. Gene. 2000 Apr 4;246(1-2):37-48.

12. Foury F. Cloning and sequencing of the nuclear gene MIP1 encoding the catalytic subunit of the yeast mitochondrial DNA polymerase. J Biol Chem. 1989 Dec 5;264(34):20552-60.

13. Van Dyck E, Foury F, Stillman B, Brill SJ. A single-stranded DNA binding protein required for mitochondrial DNA replication in S. cerevisiae is homologous to E. coli SSB. EMBO J. 1992 Sep;11(9):3421-30.

14. Genga A, Bianchi L, Foury F. A nuclear mutant of saccharomyces cerevisiae deficient in mitochondrial DNA replication and polymerase activity. J Biol Chem. 1986 Jul 15;261(20):9328-32.

15. Foury F, Kolodynski J. Pif mutation blocks recombination between mitochondrial rho+ and rho- genomes having tandemly arrayed repeat units in saccharomyces cerevisiae. Proc Natl Acad Sci U S A. 1983 Sep;80(17):5345-9.

16. Lahaye A, Stahl H, Thines-Sempoux D, Foury F. PIF1: A DNA helicase in yeast mitochondria. EMBO J. 1991 Apr;10(4):997-1007.

17. Doudican NA, Song B, Shadel GS, Doetsch PW. Oxidative DNA damage causes mitochondrial genomic instability in saccharomyces cerevisiae. Mol Cell Biol. 2005 June 15;25(12):5196-204.

18. O'Rourke TW, Doudican NA, Zhang H, Eaton JS, Doetsch PW, Shadel GS. Differential involvement of the related DNA helicases Pif1p and Rrm3p in mtDNA point mutagenesis and stability. Gene. 2005 7/18;354:86-92.

19. Sedman T, Kuusk S, Kivi S, Sedman J. A DNA helicase required for maintenance of the functional mitochondrial genome in saccharomyces cerevisiae. Mol Cell Biol. 2000 Mar;20(5):1816-24.

20. Shadel GS. Yeast as a model for human mtDNA replication. Am J Hum Genet. 1999 Nov;65(5):1230-7.

21. Leitzel AK. Genetic studies with *HMI1*, a yeast mitochondrial helicase.[dissertation]. University of North Carolina at Chapel Hill; 2000.

22. Kuusk S, Sedman T, Joers P, Sedman J. Hmi1p from saccharomyces cerevisiae mitochondria is a structure-specific DNA helicase. J Biol Chem. 2005 Jul 1;280(26):24322-9.

23. Ausubel F., Brent R., Kingston R., Moore D., Seidman J., Smith J., Struhl K. Current protocols in molecular biology. In: New York: Wiley; 1998.

24. Mitchell AH, West SC. Hexameric rings of escherichia coli RuvB protein. cooperative assembly, processivity and ATPase activity. J Mol Biol. 1994 Oct 21;243(2):208-15.

25. Sikorski RS, Hieter P. A system of shuttle vectors and yeast host strains designed for efficient manipulation of DNA in saccharomyces cerevisiae. Genetics. 1989 May;122(1):19-27.

26. Lee CM, Sedman J, Neupert W, Stuart RA. The DNA helicase, Hmi1p, is transported into mitochondria by a C-terminal cleavable targeting signal. J Biol Chem. 1999 Jul 23;274(30):20937-42.

27. Sedman T, Joers P, Kuusk S, Sedman J. Helicase Hmi1 stimulates the synthesis of concatemeric mitochondrial DNA molecules in yeast saccharomyces cerevisiae. Curr Genet. 2005 Apr;47(4):213-22.

28. Matson SW, George JW. DNA helicase II of escherichia coli. characterization of the single-stranded DNA-dependent NTPase and helicase activities. J Biol Chem. 1987 Feb 15;262(5):2066-76.

29. Matson SW. Escherichia coli helicase II (urvD gene product) translocates unidirectionally in a 3' to 5' direction. J Biol Chem. 1986 Aug 5;261(22):10169-75.

30. Greenleaf AL, Kelly JL, Lehman IR. Yeast RPO41 gene product is required for transcription and maintenance of the mitochondrial genome. Proc Natl Acad Sci U S A. 1986 May;83(10):3391-4.

31. Malaney S, Trumpower BL, Deber CM, Robinson BH. The N terminus of the Qcr7 protein of the cytochrome bc1 complex is not essential for import into mitochondria in saccharomyces cerevisiae but is essential for assembly of the complex. J Biol Chem. 1997 Jul 11;272(28):17495-501.

32. Zavitz KH, Marians KJ. ATPase-deficient mutants of the escherichia coli DNA replication protein PriA are capable of catalyzing the assembly of active primosomes. J Biol Chem. 1992 Apr 5;267(10):6933-40.

33. George JW, Brosh RM, Matson SW. A dominant negative allele of the escherichia coli uvrD gene encoding DNA helicase II : A biochemical and genetic characterization. Journal of Molecular Biology. 1994 1/13;235(2):424-35.

34. Budd ME, Choe WC, Campbell JL. DNA2 encodes a DNA helicase essential for replication of eukaryotic chromosomes. J Biol Chem. 1995 Nov 10;270(45):26766-9.

35. Hishida T, Iwasaki H, Yagi T, Shinagawa H. Role of walker motif A of RuvB protein in promoting branch migration of holliday junctions. walker motif a mutations affect atp binding, atp hydrolyzing, and DNA binding activities of ruvb. J Biol Chem. 1999 Sep 3;274(36):25335-42.

36. Lahue EE, Matson SW. Escherichia coli DNA helicase I catalyzes a unidirectional and highly processive unwinding reaction. J Biol Chem. 1988 Mar 5;263(7):3208-15.

37. Fangman WL, Henly JW, Brewer BJ. RPO41-independent maintenance of [rho-] mitochondrial DNA in saccharomyces cerevisiae. Mol Cell Biol. 1990 Jan;10(1):10-5.

38. Piskur J. Inheritance of the yeast mitochondrial genome. Plasmid. 1994 May;31(3):229-41.

39. Lorimer HE, Brewer BJ, Fangman WL. A test of the transcription model for biased inheritance of yeast mitochondrial DNA. Mol Cell Biol. 1995 Sep;15(9):4803-9.

40. Graves T, Dante M, Eisenhour L, Christianson TW. Precise mapping and characterization of the RNA primers of DNA replication for a yeast hypersuppressive petite by in vitro capping with guanylyltransferase. Nucleic Acids Res. 1998 Mar 1;26(5):1309-16.

41. Van Dyck E, Clayton DA. Transcription-dependent DNA transactions in the mitochondrial genome of a yeast hypersuppressive petite mutant. Mol Cell Biol. 1998 May;18(5):2976-85.

42. Ulery TL, Jaehning JA. MTF1, encoding the yeast mitochondrial RNA polymerase specificity factor, is located on chromosome XIII. Yeast. 1994 Jun;10(6):839-41.

43. Lee DY, Clayton DA. Initiation of mitochondrial DNA replication by transcription and R-loop processing. J Biol Chem. 1998 Nov 13;273(46):30614-21.

44. Shadel GS, Clayton DA. Mitochondrial DNA maintenance in vertebrates. Annu Rev Biochem. 1997;66:409-35.

45. Ng JY, Marians KJ. The ordered assembly of the phiX174-type primosome. II. preservation of primosome composition from assembly through replication. J Biol Chem. 1996 Jun 28;271(26):15649-55.

46. Liu J, Marians KJ. PriA-directed assembly of a primosome on D loop DNA. J Biol Chem. 1999 Aug 27;274(35):25033-41.

47. Liu J, Xu L, Sandler SJ, Marians KJ. Replication fork assembly at recombination intermediates is required for bacterial growth. Proc Natl Acad Sci U S A. 1999 Mar 30;96(7):3552-5.

48. Sandler SJ, Marians KJ. Role of PriA in replication fork reactivation in escherichia coli. J Bacteriol. 2000 Jan;182(1):9-13.

49. Jones JM, Nakai H. PriA and phage T4 gp59: Factors that promote DNA replication on forked DNA substrates microreview. Mol Microbiol. 2000 May;36(3):519-27.

50. Jones JM, Nakai H. Duplex opening by primosome protein PriA for replisome assembly on a recombination intermediate. J Mol Biol. 1999 Jun 11;289(3):503-16.

51. Boehmer PE, Lehman IR. Herpes simplex virus DNA replication. Annu Rev Biochem. 1997;66:347-84.

Chapter 3

The use of single molecule FRET to demonstrate the cotranslocation of MutL and UvrD

E. coli methyl-directed mismatch repair tracts can be up to 3 kb long, yet the helicase (UvrD) involved in this pathway has a dsDNA processivity of 40 bp (1, 2). To explain the ability of UvrD to unwind these long repair tracts, it has been proposed that MutL continually loads UvrD onto the DNA in order to unwind a long distance taking advantage of the processive translocation of UvrD on ssDNA (3). The basic notion is that UvrD molecules that dissociate after unwinding 40-50 bp will be immediately replaced by UvrD molecules processively translocating along the ssDNA behind the leading UvrD dimer. Thus, a long tract of DNA is effectively unwound with many small unwinding efforts.

Recent single-turnover rapid quench kinetic assays have suggested that MutL increases the processivity of UvrD-catalyzed unwinding of dsDNA. To determine the mechanism by which MutL is able to stimulate a single UvrD dimer to unwind long distances, we have utilized the relatively new single molecule FRET (smFRET) technology. Here we describe our novel approach for assaying movement along a DNA strand using FRET and total internal reflection microscopy (TIRM). Details concerning oxygen scavengers and DNA substrates are addressed as are the purification and labeling of UvrD and MutL. This experimental design will be critical in demonstrating the cotranslocation of MutL with UvrD along the DNA during unwinding.

Introduction

Errors arising during DNA replication pose a constant threat to genome integrity in all types of organisms. *Escherichia coli* have developed a post–replication methyl-directed mismatch repair pathway (MMR) to remove IDLs and incorrect base pairing caused by polymerase infidelity (reviewed in (4, 5)). MMR initiates when the MutS homodimer recognizes and binds a mismatched base-pair (or IDL) after passage of the replication fork. The DNA-bound MutS recruits MutL in an ATP-dependent reaction to the mismatch. The endonuclease, MutH, binds the nearest hemi-methylated d(GATC) site and, through an interaction with the MutS/MutL complex, nicks the nascent strand of DNA. The MutL homodimer recruits and loads the UvrD helicase onto the strand with the mismatch 5' to the nicking site to initiate unwinding in a 3' to 5' direction (5, 6).

The processivity of UvrD as an unwinding enzyme is a meager 40 bp whereas translocation on ssDNA is about 3 kb in a single binding event (1, 2). However, MMR repair tracts in excess of 1 kb in length have been reported. Due to these constraints, it is speculated that MutL continually loads UvrD onto the ssDNA allowing the helicase to translocate to the double-stranded portion where it completes a short unwinding event before dissociating. As a result, complete unwinding of a potentially long stretch of dsDNA is accomplished through several short unwinding events from multiple UvrD dimers (reviewed in (6)). The exact mechanism for halting the loading of UvrD is unknown; however, UvrD unwinds approximately 100 bases beyond the mismatch site, and in doing so, presumably displaces the MutS/MutL complex from the repair site. The repair process is complete once polymerase III fills in the gap and the nick is sealed with ligase.

MutL interacts with and stimulates the DNA binding and unwinding activity of UvrD, yet previous experiments have failed to demonstrate a mechanism for this. Bulk biochemical studies on partial duplex substrates show that UvrD unwinds longer substrates more efficiently in a MutL-dependent manner (3, 7). Although very informative, these bulk studies cannot distinguish between the two possibilities of MutL stimulation: (i) MutL loads multiple UvrD molecules to unwind longer substrates or (ii) MutL increases the processivity of UvrD allowing a single dimer to unwind longer substrates.

Recently, experiments were completed to address the nature of MutL stimulated UvrD unwinding utilizing single-turnover rapid quench kinetic assays (8). The advantage of these experiments is that one can look at the unwinding capabilities of a single working dimer of UvrD as opposed to a series of binding and unwinding events by multiple dimers. ATP and DNA are necessary co-factors for the formation of a MutL-UvrD complex, so these experiments were set-up by pre-forming the MutL-UvrD complex in the presence of ATP and DNA but in the absence of $MgCl_2$ (to prevent reaction initiation). To initiate these reactions, $MgCl_2$ and a DNA oligonucleotide were added to the pre-bound MutL-UvrD complex. The oligonucleotide forms a hairpin shape due to its own sequence complementarity and effectively binds all UvrD free in solution. This prevents UvrD from reloading onto another substrate after dissociation from its original DNA substrate molecule, resulting in a single unwinding event.

As expected, UvrD alone was able to unwind 24 bp substrates but could not unwind 60 or 90 bp partial duplex substrates. However, in the presence of MutL, UvrD unwound 24 bp substrates more efficiently and was now able to unwind 60 bp and 90 bp partial duplex substrates. Since the experiment permits only one binding and unwinding event, it was

concluded that one single dimer of UvrD unwound the longer substrates even though they were beyond the limit of the previously determined UvrD unwinding processivity. The results of these experiments effectively demonstrated that MutL is somehow increasing the unwinding processivity of UvrD.

The two models of how this stimulation may occur are as follows: (i) MutL co-translocates with UvrD helping to prevent premature dissociation or (ii) MutL somehow changes the affinity for UvrD to the DNA to prevent dissociation and in effect increase the unwinding processivity of a UvrD dimer. In an attempt to elucidate the precise mechanism employed by MutL to increase the processivity, we have utilized single-molecule Forster resonance energy transfer (smFRET) and total internal reflection microscopy (TIRM) to demonstrate that MutL acts as a clamping protein and co-translocates with UvrD along the DNA preventing UvrD dissociation, thereby increasing processivity.

Materials and Methods

Bacterial strains and plasmids – E. coli BL21(DE3) (F^- *ompT* [lon] *hsd*$S_B r_B^- m_B^-$ galλDE3) was from Novagen. A derivative of this strain, BL21(DE3)*uvrD*::Tn5 *mutL*::Tn10 has previously been described and was transformed with the expression vector pET15b-MutL. The *uvrD* gene was excised from pET11d-uvrD with Nco1 and Sma1 and was ligated into pTYB4-His (9) that had been digested with the same enzymes. Plasmids were transformed into DH5α and verified through sequence analysis. Subsequent transformation and expression in BL21(DE3)*uvrD*::Tn5 *mutL*::Tn10 confirmed UvrD production through SDS-PAGE.

Protein purification – All purification steps were carried out at 4°C. MutL was expressed in BL21(DE3)*uvrD*::Tn5 *mutL*::Tn10 pET15b-MutL. This ensures no contamination of the purified MutL preparation by UvrD. Two liters of cells were grown at 37°C to an A_{600} of 0.8 followed by protein expression induction with 0.5 mM IPTG at 30°C for four hours. The cells were harvested by centrifugation and were suspended in binding buffer (50 mM Hepes-NaOH (pH 7.0), 500 mM NaCl, 5 mM imidazole, 10% (v/v) glycerol) and frozen at –75 °C. Cells were thawed on ice and lysed by the addition of lysozyme to 200 µg/ml followed by incubation at 4 °C for 60 min. The lysate was sonicated briefly to reduce the viscosity and was clarified by centrifugation. The clarified lysate was applied to a TALON metal affinity resin (BD Biosciences; 1 ml of resin/L cells), and extensively washed with binding buffer. The column was subsequently washed with 225 mM NaCl prior to elution to reduce the NaCl concentration (required for the next column in the purification). The TALON column was eluted using 200 mM imidazole in the low NaCl binding buffer. The pooled fractions were diluted 2.5-fold with MonoQ buffer (25 mM Hepes-NaOH (pH 7.0), 0.1 mM EDTA (pH 8.0), 1 mM dithiothreitol, and 10% (v/v) glycerol) containing no NaCl to achieve a final NaCl concentration of ~100 mM and applied to a MonoQ column equilibrated in MonoQ buffer containing 100 mM NaCl. The protein was eluted using a gradient from 100 mM NaCl to 500 mM NaCl in MonoQ buffer.

Following the MonoQ elution, the relevant fractions were pooled as determined by SDS-PAGE. Concentrations ranged from 2-5 mg/ml and an 8 M excess of tetramethylrhodamine-6-isothiocyanate (6-TRITC; R isomer) (Molecular Probes) was dissolved in as little DMSO as possible (usually 10-20 µl of DMSO for 1-5 ml of pooled protein). The TRITC-DMSO solution was added in 2 µl increments followed by gentle

mixing. The labeling reaction was incubated overnight in darkness with gentle agitation followed by binding to and elution from a second TALON column to remove all unreacted TRITC. This second TALON column was completed in the exact manner as the first except only 1 ml of resin was used to bind the protein and the 500 mM NaCl binding buffer was used for all wash and elution steps. The pooled TALON elution fractions were concentrated using solid polyethylene glycol 20,000 and 3500 MW dialysis tubing. The concentrated pool was loaded onto a Superdex 200 column equilibrated with Superdex buffer (50 mM Hepes-NaOH (pH 7.0), 250 mM NaCl, 0.5 mM EDTA (pH 8.0), and 10% (v/v) glycerol). Fractions containing MutL were identified by SDS-PAGE, and MutL eluted at the position expected for a MutL dimer. Final purity was assessed to be >95% by SDS-PAGE. The number of TAMRA molecules on each MutL monomer was calculated to be ~4 according to the degree-of-labeling formula provided by Molecular Probes that is based on the Beers-Lambert Law. Pooled Superdex fractions were dialyzed in MutL storage buffer (25 mM Hepes (pH 7.0), 200 mM NaCl, 0.1 mM EDTA, 1 mM DTT, 50% glycerol v/v) and stored at -20°C.

UvrD was expressed in BL21(DE3)*uvrD*::Tn5 *mutL*::Tn10 under autoinduction conditions (10). Growths and inductions were done at 25°C for 12 hours with a final OD_{600} at ~4-8. Cells were harvested by centrifugation, resuspended in lysis buffer (50 mM Hepes-NaOH (pH 8.0), 10% w/v sucrose, 200 mM NaCl, 5 mM EDTA, 0.5 mM EGTA, 15 mM β-ME) and frozen at -75°C. Cells were thawed on ice, lysozyme was added to 200 µg/ml, and PMSF was added to 0.3 mM. This solution incubated at 4°C for 1 hour followed by the addition of Triton-X 100 to 0.1% and warming to 16°C. The lysate was briefly sonicated to reduce viscosity and the NaCl concentration was increased to 500 mM with the addition of 4 M NaCl. The lysate was clarified by centrifugation followed by a Polymin P precipitation

(final Polymin P concentration of 0.4%). Ammonium sulfate was added to the supernatant to 30% saturation and the pellet recovered after centrifugation was suspended in 30 ml of TALON buffer (50 mM Hepes-NaOH (pH 8.0), 500 mM NaCl, 10% glycerol v/v, 5 mM imidazole). The suspension was batch bound to 2 ml of TALON resin for 1 hour at 4°C. The resin was washed with TALON buffer to baseline and eluted with TALON buffer plus 300 mM imidazole. An 8 M excess of tetramethylrhodamine-6-isothiocyanate (6-TRITC; R isomer) (Molecular Probes) was dissolved in as little DMSO as possible (usually 10-20 µl of DMSO for 1-5 ml of pooled protein). The TRITC-DMSO solution was added in 2 µl increments followed by gentle mixing. The labeling reaction was incubated overnight in darkness with gentle agitation followed by another TALON column to remove all unreacted fluorophore. This second TALON column was completed in the exactly the same manner as the first except only 1 ml of resin was used to bind the protein. Pooled fractions of the second TALON elution were brought to 10 ml with chitin buffer (50 mM Hepes-NaOH (pH 8.0), 500 mM NaCl, 10% glycerol v/v, 1 mM EDTA) and added to 1 ml chitin beads and incubated with very slight agitation for 1 hour at 4°C. The chitin column was washed to baseline followed by a 3 ml wash of chitin buffer plus 50 mM DTT. The column incubated overnight at 4°C to allow intein cleavage. The chitin column was eluted using chitin buffer and the protein purity was assessed by SDS-PAGE analysis. The pooled UvrD was dialyzed in storage buffer (25 mM Hepes-NaOH 8.0, 200 mM NaCl, 50% glycerol v/v, 1 mM EDTA, 0.5 mM EGTA, 25 mM β-ME) and stored at -20°C. The purified protein was judged to be >95% homogeneous as determined by SDS-PAGE. The degree-of-labeling calculations were done as indicated above.

Partial duplex DNA substrates – The 93-bp partial duplex substrate used in the helicase assay was prepared as previously described (9). Oligonucleotides used to generate the smFRET substrate were synthesized by Integrated DNA Technologies (IDT). RQ-60 and dsm4 have no modifications while dsm6 has an internal Cy5 two bases from the 5' end and contains a 3' biotin modification (Table 1). dsm6 (800 pmoles) was 5' phosphorylated using T4 polynucleotide kinase and rATP according to New England Biolob (NEB) instructions. The reaction was halted with a 20 minute incubation at 65°C which effectually denatures PNK. 800 pmoles of both RQ-60 and dsm4 were added to the reaction. The mixture was heated to 95°C for 3 minutes and then allowed to slowly cool to room temperature over 2 hours. T4 Ligase (Invitrogen) was used to ligate the nick between dsm6 and dsm4 according to manufacturer instruction. The substrate was purified on a 10% polyacrylamide gel followed by an overnight electroelution. The smFRET substrate was dialyzed overnight against TEN buffer (10 mM Tris-HCl (pH 8.0), 50 mM NaCl, 0.1 mM EDTA). Concentration was determined through spectrophotometry.

Helicase Assays: Reaction mixtures (20 µl) contained 25 mM Tris-HCl (pH 7.5), 3 mM $MgCl_2$, 20 mM NaCl, 5 mM β-mercaptoethanol, 50 µg/ml bovine serum albumin, 3 mM ATP, a 93-bp partial duplex DNA (final concentration, 2 µM DNA-Pi), 1.25 nM UvrD or UvrD-TAMRA, and a titration of MutL or MutL-TAMRA. The reactions were initiated by the addition of ATP after a 5 minute preincubation at 37° C. After 10 minutes the reaction was stopped with the addition of 10 µl of helicase stop/dye solution (50% (v/v) glycerol, 68 mM EDTA (pH 8.0), 0.022% (w/v) xylene cyanol, 0.022% (w/v) bromphenol blue, 0.3% (w/v) SDS, 44.5 mM Tris base, and 44.5 mM boric acid). The reactions were resolved on a

10% native polyacrylamide gel run in 0.5x TBE and 0.1% (w/v) SDS. Gels were imaged using a phosphor screen (Molecular Dynamics, GE Healthcare) and quantified using ImageQuant on a Storm phosphoimager (Molecular Dynamics, GE Healthcare).

Table 1: Oligonucleotides for smFRET substrate

Oligonucleotide	Oligonucleotide Sequence (5'→3')
RQ-60	CCCCGTGCTGGCCGTTTGCGGTTGTCCTGTACCACTCGAAGTAGGA GGGGTGCTCACCAA
dsm4	TTGGTGAGCACCCCTCCTACTTCGAGTGGTACAGGACAACCGCAAA CGGCC
dsm6	AG(Cy5)CACGGGGTTTTTTTTTTTTTTTTTTTTTTTTTTTTTTTTT TTT(Biotin)

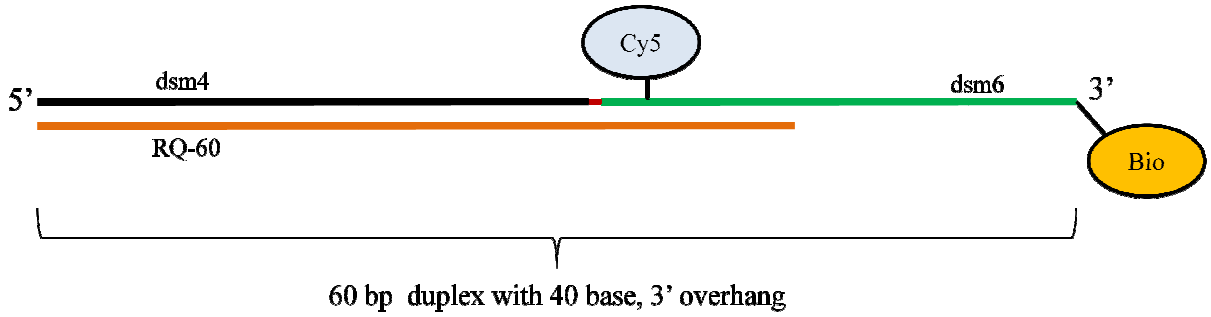

Figure 1: smFRET substrate (not to scale)

Oligonucleotides are labeled and colored as follows: dsm4 is black, dsm6 is green, and RQ-60 is orange. The orange RQ-60 represents the double-stranded region. The ligation is represented with red. The Cy5 and Biotin modifications are shown in blue and yellow, respectively.

Single-molecule experiments: The flow cell channel was created by sandwiching two parallel strips of double-sided tape ¼ inch apart between a quartz slide and cover slip (Fig 2). Two 1 mm holes on opposite sides were previously drilled between the two strips of tape to serve as an inlet and outlet for the sample. 90-second epoxy glue was used to seal the edges (Araldite). A syringe holding the reaction initiation buffer was connected to the inlet hole via tubing and clamped down to the slide with an aluminum clamp (clamp device made in-house) (Fig 2). The experiments were carried out using total internal reflection excitation through a prism with a 532 nm laser and dual view imaging (Optical Insights, Inverted Olympus confocal microscope). Biotin-BSA conjugates (Sigma) were injected into the channel followed by streptavidin (Invitrogen). Reactions were pre-incubated in UvrD buffer containing the indicated DNA substrate and the appropriate concentrations of the indicated proteins (MutL, MutL-TAMRA, UvrD, or UvrD-TAMRA) in the presence of ATP but in the absence of Mg^{+2}. The 3' biotin labeled DNA substrates were immobilized to the streptavidin upon injection. Excess unbound protein and DNA were flushed out with UvrD reaction buffer, ATP, and the enzymatic oxygen scavenging system: 0.4% w/v glucose, glucose oxidase (Type II from *A. niger* Sigma), 1,3,5,7-cyclooctatetraene (COT from Aldrich), catalase (*A. niger* from Sigma) and 1% v/v 2-mercaptoethanol (Sigma). The reaction was initiated with the enzymatic oxygen scavenging system plus 3 mM MgCl and 3 mM ATP. Results were analyzed on a program written in house on MatLab.

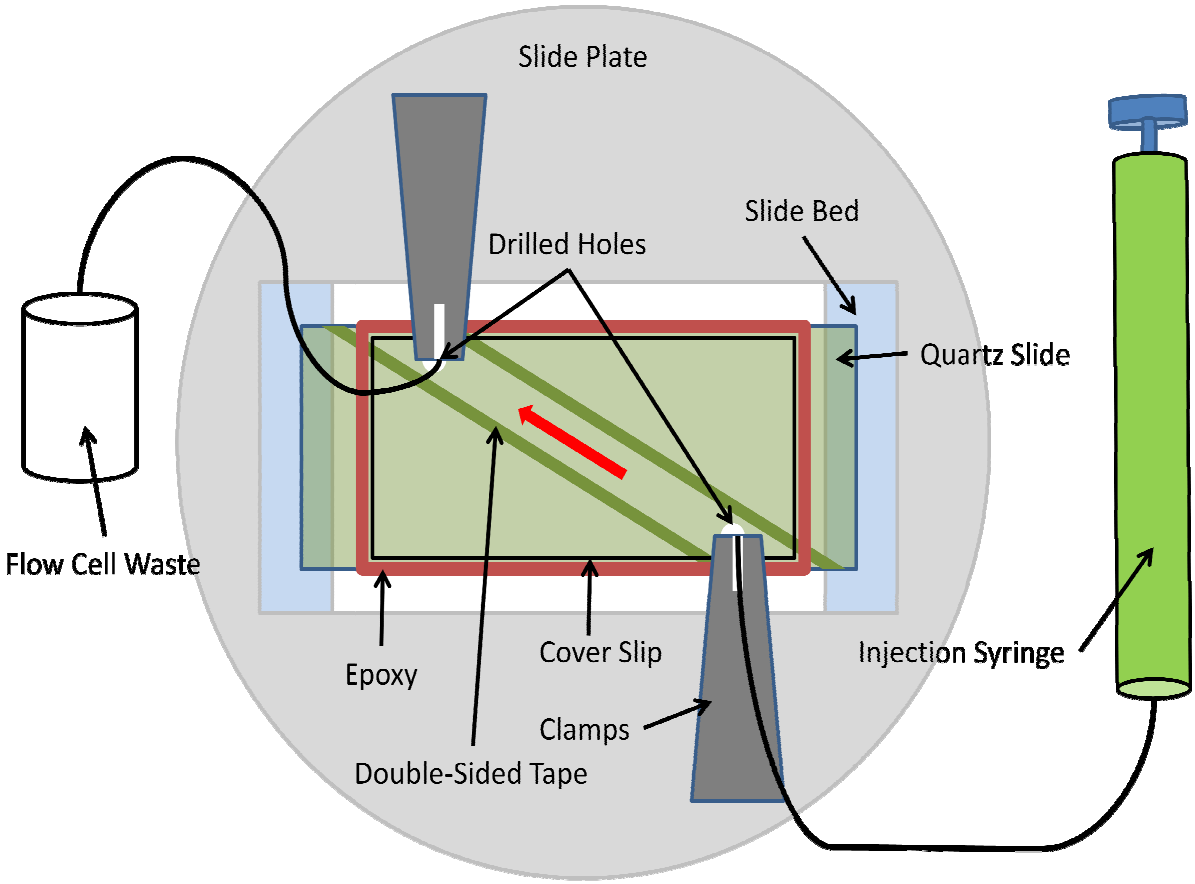

Figure 2: smFRET flow cell design

The flow cell is double-sided tape sandwiched between a cover slip and a quartz slide that has two drilled holes. Epoxy is used to make all the edges air tight. The flow cell is set on a slide plate with adjustable clamps which are used to keep a tight seal between the injection/waste tubes and the quartz slide. The flow area is the region between the two double-sided tape strips and the red arrow indicates the direction of flow.

Results

Purification of TAMRA labeled MutL and UvrD

The *uvrD* gene was cloned into the pTYB4His vector (9) and was expressed using an auto-induction regime as described (10). The induced cells were lysed and the clarified lysate was polymin P precipitated followed by an ammonium sulfate precipitation. The resuspended pellet was bound to a TALON metal affinity column and eluted with imidazole. The pooled TALON elution fractions were labeled with TAMRA using an amine reactive form of the fluorophore (TRITC). The labeled protein was bound to a second TALON column to remove all of the unreacted fluorophore. The pooled elution fraction was bound to chitin resin and incubated overnight in 50 mM DTT to induce cleavage of the intein. Cleavage of the protein from the intein-CBD and his-tags resulted in a TAMRA-labeled UvrD with no purification tags.

MutL was purified using a slightly altered purification scheme described by (11) to permit TAMRA labeling. After the TALON and MonoQ columns, the protein was labeled with TRITC, a TAMRA fluorophore with an amine reactive group. The pH of the reaction partially dictated the location of labeling such that the lower the pH, the higher the likelihood of an amino-terminal label and the higher the pH, the higher the likelihood of surface lysine labels. The number of labels per protein was influenced by both protein concentration and molar excess of the TRITC. Calculations based upon spectrophotometry, the Beers-Lambert Law, and constants provided by Molecular probes estimated that 2-4 fluorophores were present on each MutL monomer.

Both labeled proteins were subjected to an additional metal-affinity column to remove excess fluorophores to complete the purification. MutL-TAMRA was tested for

activity by comparing the stimulatory effect on UvrD-catalyzed unwinding of 93 bp partial duplex substrate with a non-labeled MutL (Fig 3). UvrD-TAMRA was tested in the same assay against unlabeled UvrD for MutL-stimulated unwinding activity (Fig 3). Both proteins' activity was determined to be at wild-type levels and it was concluded that the labels did not interfere with activity (Fig 3).

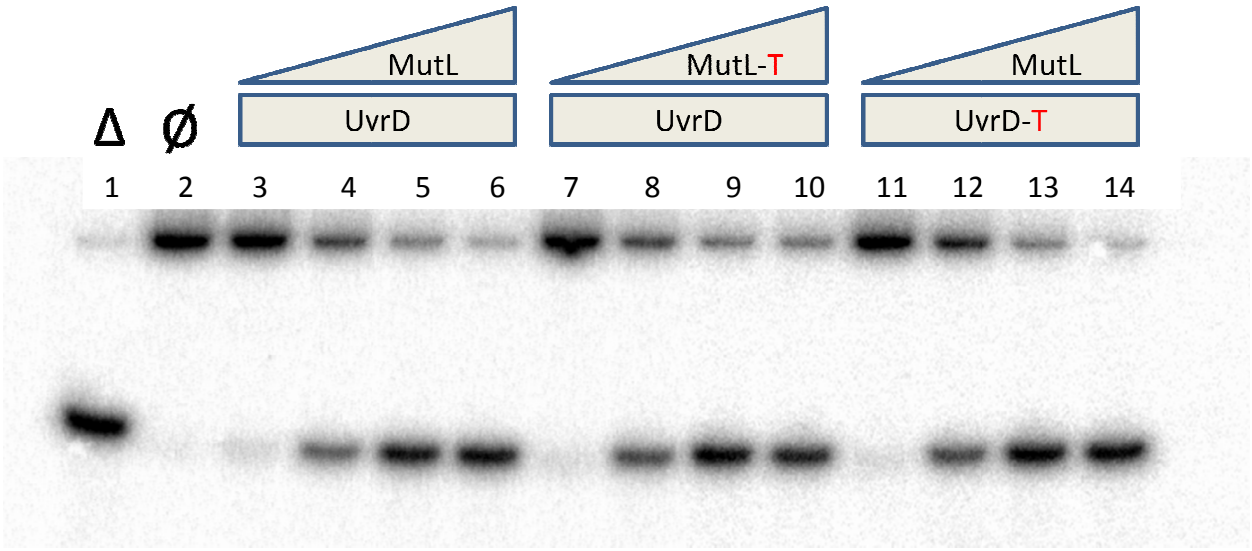

Figure 3: TAMRA labeled UvrD and MutL retain wild type function

Unwinding activity of MutL, UvrD, MutL-TAMRA, and UvrD-TAMRA on a 93 bp partial duplex substrate. Δ, heat denatured 93 bp partial duplex. Ø, no protein added. Lanes 3-6, titration of MutL-stimulated UvrD unwinding. Lanes 7-10, titration of MutL-TAMRA-stimulated UvrD unwinding. Lanes 11-14, titration of MutL-stimulated UvrD-TAMRA unwinding. UvrD concentration was 1.25 nM for all lanes. The range of MutL and MutL-T was 7 nm-132 nM

Unwinding activity in TIRM oxygen scavenging conditions

The TIRM system used in this study requires the detection of fluorophore emittance and FRET. Since photobleaching of fluorophores is greatly affected by the amount of molecular oxygen present in solution, O_2 must be reduced to extend fluorophore lifetime long enough to conduct the experiments (reviewed in (12)). Two so-called "oxygen scavenging systems" have been described which pair chemicals that, when mixed, utilize molecular oxygen which preserves fluorophore lifetime.

The first of these scavenging combinations is the glucose oxidase and catalase system (GOXCAT). When mixed with glucose, glucose oxidase catalyzes the oxidation of glucose to gluconic acid and hydrogen peroxide (reviewed in (12)). To counter-balance the hydrogen peroxide, catalase is added, which converts H_2O_2 to water and molecular oxygen. While this seems like a counter-intuitive mixture, the correct balance reduces molecular oxygen enough to extend fluorophore life and it helps to maintain low levels of hydrogen peroxide. However, if the mixture is not balanced well, there can be an overabundance of oxygen or a harmful accumulation of hydrogen peroxide and reactive oxygen species that can damage the enzyme activity.

The second oxygen scavenging combination pairs protocatechuic acid (PCA) with protocatechuate-3,4-dioxygenase (PCD) (13). In the presence of oxygen, PCD catalyzes the formation of two protons and β-carboxy-cis, cis-muconic acid from PCA and 1 mole of O_2. This reaction doesn't generate harmful biproducts and has previously been shown to be as effective as the GOXCAT system at a smaller concentration. To evaluate the effects of these two oxygen-scavenging systems on MutL-stimulated UvrD unwinding, helicase activity assays were conducted in the presence of the standard working concentrations of each system

(Fig 4). Both oxygen scavenging systems reduce the robustness of the reaction. However, UvrD is still able to unwind the substrate in a MutL-stimulated manner. Because similar results were obtained with both systems, all subsequent smFRET experiments utilize the GOXCAT combination.

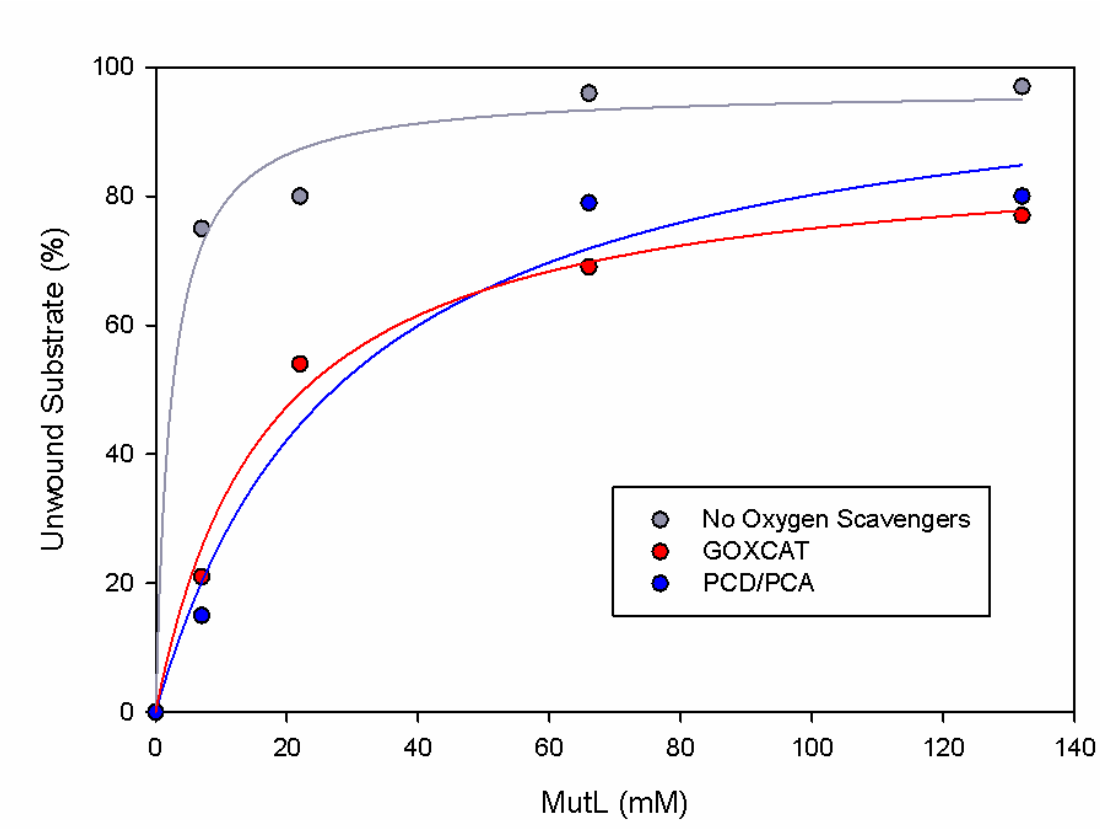

Figure 4: O_2 scavenging systems slightly inhibit MutL-stimulated UvrD unwinding

Helicase activity assays were conducted using the 93 bp partial duplex substrate as described in Materials and Methods. The UvrD concentration was constant at 1.25 nM. Both GOXCAT (red) and PCD/PCA (blue) systems somewhat suppress the efficiency of unwinding compared to standard conditions (grey). Rectangular hyperbolas have been fitted to the data.

Single-molecule FRET substrate and UvrD/MutL colocalization

Traditional single-molecule experiments that utilize optical tweezers in a flow cell require the DNA substrate to be between 5 and 15 kb for visualization and resolution purposes. Since the repair tract in *E. coli* MMR is only as long as 3 kb, using this type of single-molecule approach wasn't practical. smFRET allows the visualization of many single molecules at once from 20-200 bases in size. To demonstrate the cotranslocation of MutL with UvrD, a DNA substrate was needed that was short enough for MutL/UvrD to unwind, yet not so short that UvrD alone could efficiently unwind the duplex region. The DNA would have to have a fluorophore modification and MutL would have to be labeled with a FRET partner. This would allow for assessment of relative distances between the MutL and the stationary DNA fluorophore as MutL moves along the DNA with UvrD.

The smFRET substrate was designed to have a 40 base ssDNA region and a 60 bp double-stranded region. 60 bp is just outside the range of the processivity of UvrD alone and the 40 base ssDNA was for UvrD/MutL loading. Single turnover rapid quench kinetic studies have shown that UvrD alone catalyzes very limited unwinding of a 60 bp partial duplex substrate. The substrate used in smFRET experiments was constructed from three oligonucleotides. The dsm6 oligonucleotide had a 3' biotin modification and an internal Cy5 modification 3 bases from the 5' end. The 5' 9 bases were complementary to the 9 bases at the 5' end of the RQ-60 oligonucleotide to allow annealing. The remaining portion of RQ-60 was complementary to dsm4. After phosphorylation of dsm6, all of the oligonucleotides were annealed together and the nick between dsm4 and dsm6 was sealed with DNA ligase (see Fig 1). Subsequent purification and electroelution from a 10% polyacrylamide gel ensured a single species substrate.

In order to fix the DNA to the slide surface, the flow channels were injected (see Fig 2) with biotin-conjugated BSA (BSA sticks to the surfaces of the flow channel) followed by streptavidin. The 3' biotin modification on the smFRET substrate bound the immobile streptavidin upon injection into the channel and application of oxygen scavengers permitted visualization of the substrate (see Fig 5). A distribution of DNA that was dense enough to allow optimal data points yet sparse enough to prevent fluorescent overlap, was determined to be 50 pM. This concentration of DNA was used in all subsequent experiments.

To determine if UvrD and MutL are bound to the DNA substrate, varied concentrations of TAMRA-labeled MutL and UvrD were pre-incubated with the substrate followed by injection into the flow channel. Co-localization of UvrD-TAMRA and MutL-TAMRA to the smFRET substrate was analyzed by overlaying the two separate fluorescent images of TAMRA and Cy5 and using a mapping function to confirm co-localization. Approximately 10% of the substrate was bound with either MutL-TAMRA or UvrD-TAMRA, however, MutL-TAMRA with UvrD and MutL with UvrD-TAMRA bound more efficiently at 20-30% co-localization (see Fig 6).

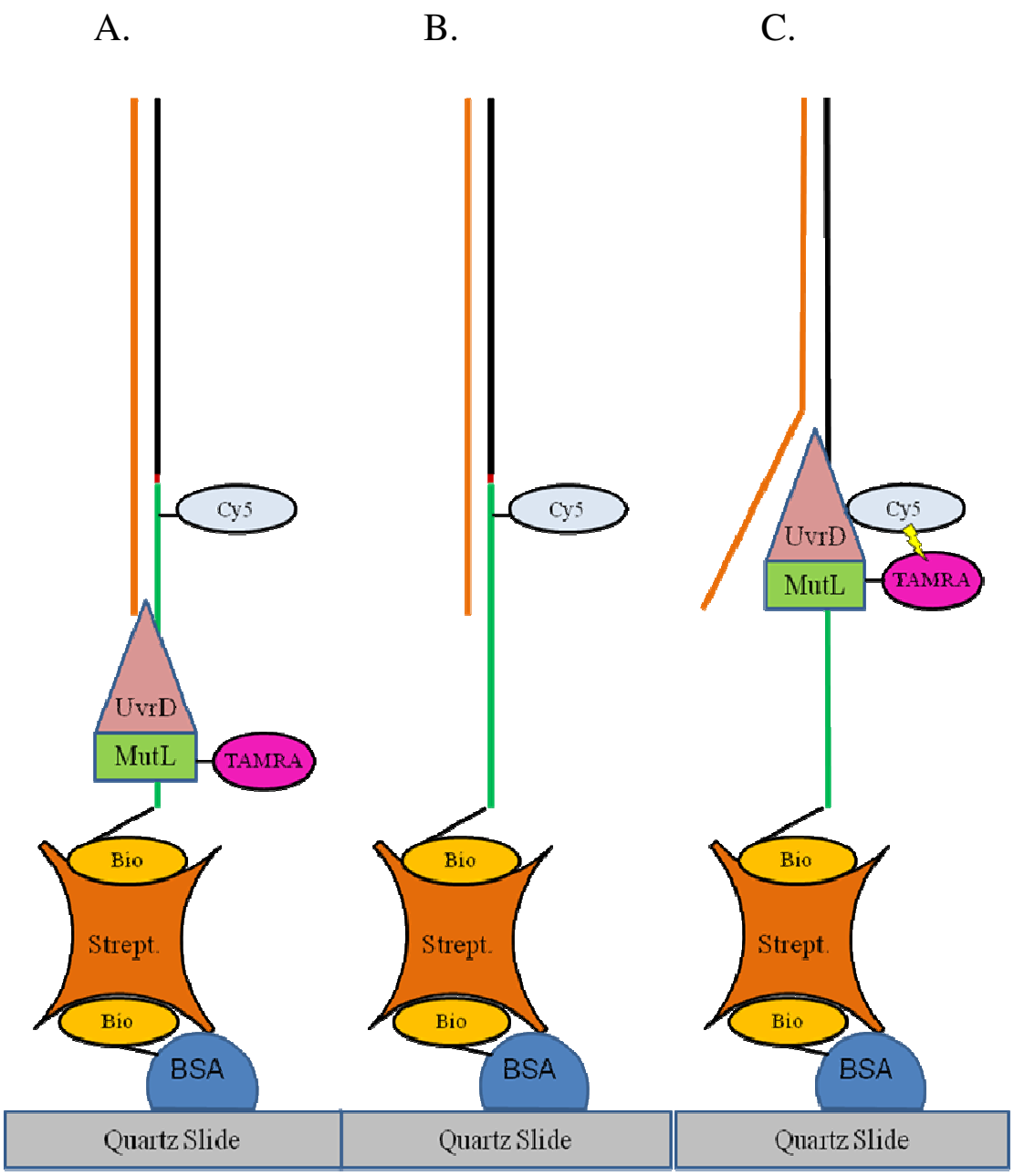

Figure 5: smFRET assay design

A, Representation of the substrate attachment to the slide through biotin-BSA and streptavidin. *B*, The substrate with pre-bound UvrD and MutL-TAMRA at the ssDNA loading site. *C*, Upon initiation, the MutL/UvrD complex begin translocation and as the TAMRA approaches the Cy5, the FRET efficiency increases, and will decrease as the TAMRA passes the Cy5 and gets further away.

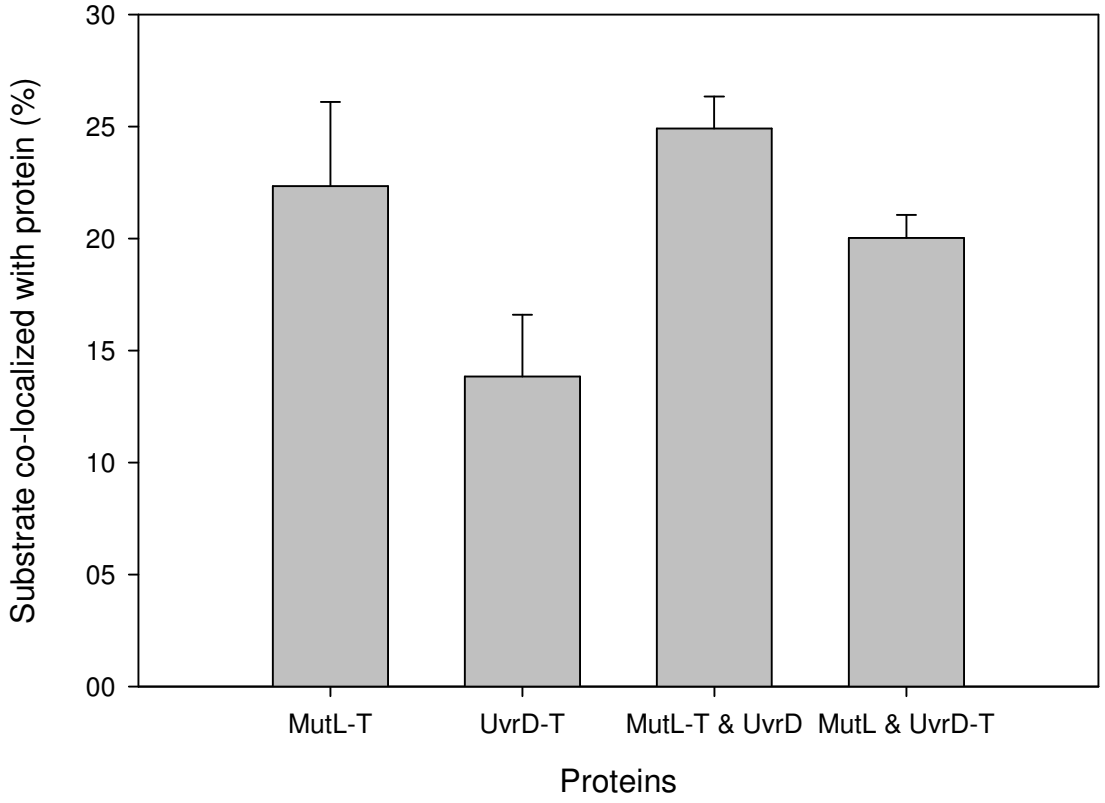

Figure 6: UvrD localizes to the smFRET substrate more efficiently in the presence of MutL

Co-localization data from TIRM analysis showing the percentage of TAMRA-labeled protein bound to the smFRET substrate in the presence and absence of either MutL or UvrD. Error bars represent standard deviation about the mean of six different experiments.

Discussion

The experimental design used here is a novel approach aimed at showing translocation of a UvrD-MutL complex along duplex DNA as it is being unwound. Most smFRET studies to date have shown nucleic acid unwinding and bending based upon doubly-labeled DNA. Our approach is the first to utilize labeled protein and labeled nucleic acid to characterize protein location along a DNA substrate. This chapter represents our initial efforts to set-up a working system in which to assay MutL cotranslocation with UvrD on DNA. We have utilized the relatively new TIRM technology to take advantage of single molecule FRET. An appropriate DNA substrate was designed and constructed to allow analysis of relative distance measurements to assay whether or not MutL translocates along DNA in conjunction with UvrD.

MutL was expressed in *E. coli* and labeled with the TAMRA fluorophore during purification. The amine-reactive form of TAMRA (TRITC) was incubated overnight with MutL mid-purification. Following purification, helicase assays using a 93 bp partial duplex substrate proved that the labeled MutL functioned as well as the unlabeled MutL. UvrD was also purified from *E. coli* but was expressed with a his-tagged chitin binding domain. This simplified the purification of labeled UvrD. UvrD was labeled with TRITC and then helicase assays demonstrated that UvrD-TAMRA retained wild type unwinding activity.

We conducted helicase assays in the presence of two oxygen scavenging systems to determine their effect on the unwinding reaction. Both the GOXCAT and PCD/PCA systems only slightly dampened the efficiency of the MutL-stimulated UvrD unwinding reactions. Because there was no appreciable difference between the two systems, the GOXCAT system was chosen to be the oxygen scavenging system in these experiments due to familiarity.

The experiments proposed to test MutL cotranslocation are now possible with the materials and conditions outlined in this chapter. There are certain controls that need to be completed to demonstrate that the unwinding reaction occurs in the slide channel and not just in a helicase assay. An important control would utilize a smaller substrate to show translocation of UvrD-TAMRA in the absence of MutL.

There are issues concerning FRET pairs that could give poor results. FRET pairs are very particular concerning distance and arrangement when it comes to energy transfer. The proteins are not site-specific labeled and fluorophores are present in different locations on different molecules. The reasoning is that there will be some molecules that will be close enough and aligned correctly to FRET. The most important control of this study is demonstrating that FRET can occur either between the UvrD-TAMRA and the Cy5 DNA or MutL-TAMRA and the Cy5 DNA. In this case, FRET is required to demonstrate that the system is setup and working as intended. Chapter 4 will explore the direction of these experiments and will discuss the alternative options that may be needed to show the mechanism by which MutL stimulates UvrD processivity.

References

1. Fischer CJ, Maluf NK, Lohman TM. Mechanism of ATP-dependent translocation of E.coli UvrD monomers along single-stranded DNA. J Mol Biol. 2004 Dec 10;344(5):1287-309.

2. Maluf NK, Ali JA, Lohman TM. Kinetic mechanism for formation of the active, dimeric UvrD helicase-DNA complex. J Biol Chem. 2003 Aug 22;278(34):31930-40.

3. Mechanic LE, Frankel BA, Matson SW. Escherichia coli MutL loads DNA helicase II onto DNA. J Biol Chem. 2000 Dec 8;275(49):38337-46.

4. Modrich P. Methyl-directed DNA mismatch correction. J Biol Chem. 1989 April 25;264(12):6597-600.

5. Li GM. Mechanisms and functions of DNA mismatch repair. Cell Res. 2008 Jan;18(1):85-98.

6. Matson SW, Robertson AB. The UvrD helicase and its modulation by the mismatch repair protein MutL. Nucleic Acids Res. 2006;34(15):4089-97.

7. Robertson AB, Pattishall SR, Gibbons EA, Matson SW. MutL-catalyzed ATP hydrolysis is required at a post-UvrD loading step in methyl-directed mismatch repair. J Biol Chem. 2006 Jul 21;281(29):19949-59.

8. Shanahan C. Characterization of the interaction between the *escherichia coli* proteins MutL and UvrD in the methyl-directed mismatch repair (MMR) pathway. 2007.

9. Monroe DS,Jr, Leitzel AK, Klein HL, Matson SW. Biochemical and genetic characterization of Hmi1p, a yeast DNA helicase involved in the maintenance of mitochondrial DNA. Yeast. 2005 Dec;22(16):1269-86.

10. Studier FW. Protein production by auto-induction in high density shaking cultures. Protein Expr Purif. 2005 May;41(1):207-34.

11. Runyon GT, Wong I, Lohman TM. Overexpression, purification, DNA binding, and dimerization of the escherichia coli uvrD gene product (helicase II). Biochemistry. 1993 Jan 19;32(2):602-12.

12. Roy R, Hohng S, Ha T. A practical guide to single-molecule FRET. Nat Methods. 2008 Jun;5(6):507-16.

13. Aitken CE, Marshall RA, Puglisi JD. An oxygen scavenging system for improvement of dye stability in single-molecule fluorescence experiments. Biophys J. 2008 Mar 1;94(5):1826-35.

Chapter 4

Concluding Remarks

The research presented in this thesis has provided a greater understanding of the roles and mechanisms of two superfamily 1 helicases; the yeast Hmi1p helicase and the *E. coli* UvrD. Chapter 2 presents genetic and biochemical studies of Hmi1p conducted by Adelaide Leitzel and me (respectively). In Chapter 2 I report the purification of Hmi1p and its biochemical characterization using helicase activity assays and NTPase assays. The data show the purified protein to be an NTP-dependent DNA helicase and a ssDNA-stimulated ATPase as is characteristic of superfamily 1 helicases. Purification and kinetic analyses of Hmi1p point mutants (K32M and K32S) demonstrated that these mutations effectively abolished Hmi1p unwinding activity. However, these mutant proteins were able to partially complement Δ*hmi1* cells, albeit not as well as the wild type protein, suggesting a role of importance but not necessity. Taken together, the results from the genetic and biochemical studies suggested that Hmi1p was not the replicative helicase of yeast mtDNA and a defined role has yet to be determined.

The studies described in Chapter 3 focused on two *E. coli* proteins, MutL and UvrD, and their roles and mechanisms in the *E. coli* MMR pathway. These studies were based upon rapid quench, single-turnover kinetic experiments done previously in the laboratory which suggested that MutL increases the processivity of a UvrD dimer as it traverses and unwinds duplex DNA. In an effort to elucidate the mechanism by which this occurs, a single-

molecule FRET approach was adopted to show MutL translocation along the DNA with UvrD during unwinding of longer DNA tracts. Both UvrD and MutL were successfully labeled and shown to be fully active. Experimental conditions including oxygen scavengers and DNA concentration were established to eventually allow smFRET studies to be conducted.

As with all scientific queries, every question answered presents many new ones. Even though we have greater insight into the roles and mechanisms of these two superfamily 1 helicases, there is much more to be learned to fully understand their precise functions. The following sections will be an analysis of these mechanisms and pathways, and the questions that have yet to be answered. Approaches, experiments, and testable hypotheses will be proposed concerning both MMR and yeast mtDNA maintenance, and the roles that UvrD and Hmi1p play in these important processes in the cell.

The Role of Hmi1p in mtDNA Maintenance

Despite the findings published in 2005 by the Matson and Sedman groups, the specific role of Hmi1p in mtDNA maintenance has yet to be uncovered (1-4). The most interesting result of the studies completed thus far is the ability of the ATP-hydrolysis/helicase negative mutants to partially complement Δ*hmi1* cells. Partial complementation in the context of yeast diploid sporulation refers to the survival and growth of one of the two haploids that receive the ATPase-hydrolysis mutant allele. Sometimes both mutant haploids grow and sometimes neither do. What could cause some cells to survive while others do not? Hmi1p is instrumental in the synthesis of concatemeric mtDNA molecules during replication (3), but by what mechanism is still undefined.

The partial complementation result is enigmatic and an analysis of what this may mean is needed in order to suggest possible roles. It is simplest to think of a partial complementation phenotype as evidence that the protein of interest works sometimes and fails to work at other times. However, this is very hard to imagine mechanistically and it requires a more rigorous review of the facts. First, yeast Δ*hmi1* cells cannot maintain wild type mtDNA, demonstrating that Hmi1p has a significant and indispensable role in mitochondrial genome maintenance. Second, Sedman et al. developed a temperature sensitive allele of *Hmi1* and, upon growth at 37°C, the mtDNA became fragmented and subsequent generations of cells were unable to respire (3). The conclusion drawn from this experiment was that Hmi1p is required for full length synthesis of wild type mtDNA. Lastly, biochemical assays proved that the Hmi1p ATPase point mutants were unable to unwind dsDNA. When these mutant genes were expressed in Δ*hmi1* cells, wild type mtDNA was maintained under metabolic pressure (non-fermentable carbon source) suggesting that Hmi1p is not the replicative helicase. However, in the presence of a fermentable carbon source, these mutant-complemented cells quickly became either ρ^- or ρ^0. Taken as a whole, it is apparent that Hmi1p is essential for wild type mtDNA maintenance and that the helicase activity of the protein is dispensable. If the helicase activity is not required, perhaps Hmi1p plays a structural role in mtDNA maintenance.

A helicase that performs a structural role, absent unwinding activity, is not a novel discovery. The PriA helicase is similar in this regard to Hmi1p in that studies have shown ATPase-deficient PriA mutants are able to carry out necessary roles within the cell (5). PriA is involved in replication restart and primosome assembly in *E. coli* (6-8). Cells devoid of this helicase suffer from numerous phenotypes including fragmented chromosomal DNA and

a consistently induced SOS response. Interestingly, these phenotypes are rescued when the cells are complemented with PriA ATPase-deficient point mutants. PriA presumably plays an integral structural role in primosome assembly at collapsed forks and, in its absence, replication fork restart is impossible and results in double-stranded DNA breaks that compromise cell viability.

Based upon the PriA conclusions and Hmi1p biochemical and genetic data, the most attractive hypothesis is that Hmi1p plays a critical structural role either in assembly or make-up of the mitochondria replisome. One can envision a situation similar to PriA where Hmi1p could bind a specific DNA structure (possibly a primed portion of DNA) and recruit fellow replisome components to assemble and function. Such components could include the replicative polymerase of yeast mitochondria, Mip1p.

Future studies of Hmi1p must include efforts to characterize interactions between Hmi1p and other replisome components. There are two straight-forward approaches that could be used to investigate to this idea: (i) search for interactors within the mitochondria and (ii) specifically target proteins of particular interest based on hypothetical interactions. Both of these methods have their drawbacks but also could provide some very useful information. One of the most widely-used methods for discovering interactors is the two-hybrid assay. Benefits of this include the ability to test a whole library of proteins for possible candidates. This method could return a wide variety of proteins that are involved in mtDNA maintenance and subsequent studies could lend mechanistic insight into yeast mtDNA replication.

Another means of identifying possible interactors is through immunoprecipitation. With an antibody to Hmi1p available, pull down of interacting proteins should be straight-forward and simple. However, isolation of mitochondrial lysates is not trivial and Hmi1p has

never been detected on a Western Blot from whole cell or mitochondrial fractions. Overexpression of Hmi1p directed to the mitochondria may be a feasible option to increase the amount of the protein in cells.

Specifically targeting proteins might also prove to be useful if there is reason to believe an interaction is likely. Experiments testing the affinity of the yeast mtDNA polymerase (Mip1p) and Hmi1p, both with each other and on specific DNA substrates could be very informative. There is the possibility that Hmi1p is a sort of processivity factor for Mip1p such that the interaction provides a better structural association with the DNA. The 80 kb yeast mtDNA is long and Hmi1p may assist in prolonged binding or restart of the replication fork if Mip1 is dissociated. These hypotheses are quite possible considering that the loss of *HMI1* leads to shortened mtDNA concatemers. Broken or fragmented DNA is often the result of failed or incomplete DNA replication, pointing to a role for Hmi1p involving replisome stability and/or replication restart. The unwinding role of Hmi1p may assist in the processivity of the replisome, which could explain why there is a partial complementation phenotype. The cells apparently prefer the presence of active Hmi1p as demonstrated by the loss of mtDNA on fermentable carbon sources. However, it seems that the structural role that Hmi1p plays is usually sufficient for cell viability on non-fermentable carbon sources causing one to wonder how the 80 kb mtDNA genome is unwound for replication.

The search for the so-called replicative helicase of the yeast mtDNA is ongoing and there are no candidates at this time. Could Mip1p, with the assistance of processivity factors, really displace dsDNA strands as long as 80 kb? Maybe Hmi1p is the replicative helicase, in that it helps unwind the duplex while complexed to Mip1p to allow for a more efficient

replication event since cells that have Hmi1p without ATPase activity have a much higher likelihood of losing their mtDNA due to fragmentation and/or incomplete replication. These proposed experiments should help shed light on the role of Hmi1p in mtDNA maintenance. A greater understanding of Hmi1p and its interactors will provide insight into the mechanism of yeast mtDNA replication which has remained elusive after decades of research.

The Mechanism of MutL-stimulated UvrD Unwinding

The novel experimental design outlined in Chapter 3 promises to be very informative concerning the mechanism by which MutL is able to stimulate UvrD-catalyzed unwinding. We were able to purify both MutL and UvrD with TAMRA labels and proved that they both retained wild type biochemical function. The substrate designed for these studies is ideal with reference to base length. The 40-base ssDNA will provide ample room for the loading of the proteins and the dsDNA is too long for efficient unwinding by UvrD alone. The Cy5 fluorophore has been placed in a position that should show a gradient in FRET efficiency relative to protein distance. The overall length of 100 bases permitted the substrate to be constructed from oligonucleotides and is ideal for smFRET.

New studies have demonstrated that the addition of lipids to the surface of the flow chamber can prevent MutL/UvrD binding. Injection of phospholipids after the biotin step, effectively "blocks" the remaining sites available to protein binding. This has been shown to greatly reduce the background fluorescence and would permit a more accurate colocalization estimate. Due to the high degree of background fluorescence, confidence in colocalization is low and could give a false-positive colocalization result. Utilizing this "blocking" method would allow for a more stringent analysis and may show that the reason we have not yet seen

unwinding or FRET is due to a lack of colocalized proteins on the substrate. With the optimal reaction conditions determined and a greater reduction in background fluorescence, controls demonstrating that FRET is attainable in the system remain the priority.

The first control to be done will test the FRET efficiency of UvrD-TAMRA on the dsm6 substrate. This control is important for several reasons. First, since the oligonucleotide is ssDNA, UvrD-TAMRA should completely coat the substrate. This should all but guarantee that FRET is seen since UvrD will be bound at the Cy5. Since a 25% FRET efficiency should be observed between TAMRA and Cy5 at an approximate 19 base separation, the only feasible explanation for failing to observe FRET with UvrD-TAMRA would be quenching of the fluorescence by the UvrD dimer. Protein quenching and enhancement of fluorescence has been shown previously with UvrD which quenches fluorescein fluorescence, but amplifies Cy3 (9, 10). If it were the case that UvrD quenched either the TAMRA (depending on complex orientation) or the Cy5, alternate FRET pairs would have to be chosen and a new substrate constructed.

It is also necessary to show FRET with MutL-TAMRA and UvrD because this control tests the basic premise of the experiment. An experiment with dsm6 bound by MutL-TAMRA and UvrD is expected to yield FRET. However, if we do not see FRET, there are several possible reasons that would have to be addressed. If MutL-TAMRA is bound to UvrD such that the TAMRA fluorophores are too far from the Cy5 or if the UvrD quenches the Cy5 fluorescence, then we should not expect the experiment to work as expected. Again, changing FRET pairs may resolve the issue of UvrD quenching and distance because some FRET pairs have stronger or brighter emissions which could show FRET efficiency over

longer distances. Another option would be labeling MutL with more TAMRA molecules, which could increase the chances of FRET if distance or orientation were the concern.

Once FRET has been established on the simple ssDNA dms6 oligonucleotide, unwinding experiments can be conducted to test the enzymes and their activities in this environment. Chapter 3 showed that both oxygen scavenging options slightly suppressed the unwinding activity of MutL-stimulated UvrD but the reactions were able to proceed nonetheless. Although this is a good indication that the reaction will work in the flow cell, it still needs to be shown. The simplest way to show that UvrD is unwinding the substrate is to set up a reaction in the flow cell that contains UvrD and a shorter smFRET substrate that contains only about 30 bp in the double-stranded region. This substrate would require two FRET pairs to be on opposite strands but within FRET distance of each other. A substrate designed like this would show FRET when the dsDNA is annealed and when the UvrD unwinds the substrate, FRET is lost. This answers the straight-forward question: Can UvrD unwind the substrate under these conditions? If this cannot be shown and the unwinding reaction cannot proceed in the flow channel, tests will have to be done that determine the limit of oxygen scavenger presence (i.e. how low can the concentrations of the oxygen scavenger chemicals be and still function to prolong fluorescence?).

With all of these controls in place, measurements of FRET efficiency between MutL-TAMRA and the Cy5 can be used to evaluate qualitatively whether MutL co-translocates with UvrD to increase unwinding processivity. Obviously there are two possible outcomes to this experiment: MutL does or does not co-translocate with UvrD. If a FRET efficiency gradient is seen between the MutL-TAMRA and the Cy5, it can be concluded that MutL does translocate with UvrD. However, if FRET is not observed, one more control is necessary to

prove that MutL does not co-translocate with UvrD. An experiment that tests the ability of UvrD-TAMRA to unwind the 60 bp dsDNA in the presence of MutL will verify the findings. If UvrD-TAMRA does unwind the substrate in the presence of MutL then MutL must increase the processivity of UvrD by some other mechanism. This might be accomplished by MutL increasing the affinity for UvrD for the DNA. It is difficult to envision a mechanism by which this could occur, but one could imagine a scenario where MutL facilitates UvrD to engage the DNA more tightly than if it were alone.

A positive FRET result, including a FRET efficiency gradient over time, would prove the movement of MutL along the DNA with UvrD. This explanation is feasible based upon our knowledge of MutL structure. Since the dimer of MutL is able to encompass dsDNA in its cleft, the MutL molecule could act similarly to beta-clamp and topologically tether the UvrD dimer to the DNA. This would increase the processivity of UvrD because MutL encircles the DNA and simultaneously binds UvrD, preventing the dissociation of one from the other. This activity would verify the biochemical data and shed new light on the mechanism of repair tract unwinding in MMR.

References

1. Monroe DS,Jr, Leitzel AK, Klein HL, Matson SW. Biochemical and genetic characterization of Hmi1p, a yeast DNA helicase involved in the maintenance of mitochondrial DNA. Yeast. 2005 Dec;22(16):1269-86.

2. Kuusk S, Sedman T, Joers P, Sedman J. Hmi1p from saccharomyces cerevisiae mitochondria is a structure-specific DNA helicase. J Biol Chem. 2005 Jul 1;280(26):24322-9.

3. Sedman T, Joers P, Kuusk S, Sedman J. Helicase Hmi1 stimulates the synthesis of concatemeric mitochondrial DNA molecules in yeast saccharomyces cerevisiae. Curr Genet. 2005 Apr;47(4):213-22.

4. Lee CM, Sedman J, Neupert W, Stuart RA. The DNA helicase, Hmi1p, is transported into mitochondria by a C-terminal cleavable targeting signal. J Biol Chem. 1999 Jul 23;274(30):20937-42.

5. Zavitz KH, Marians KJ. ATPase-deficient mutants of the escherichia coli DNA replication protein PriA are capable of catalyzing the assembly of active primosomes. J Biol Chem. 1992 Apr 5;267(10):6933-40.

6. Jones JM, Nakai H. PriA and phage T4 gp59: Factors that promote DNA replication on forked DNA substrates microreview. Mol Microbiol. 2000 May;36(3):519-27.

7. Heller RC, Marians KJ. Unwinding of the nascent lagging strand by rep and PriA enables the direct restart of stalled replication forks. J Biol Chem. 2005 October 7;280(40):34143-51.

8. Sandler SJ, Marians KJ. Role of PriA in replication fork reactivation in escherichia coli. J Bacteriol. 2000 Jan;182(1):9-13.

9. Lohman TM, Tomko EJ, Wu CG. Non-hexameric DNA helicases and translocases: Mechanisms and regulation. Nat Rev Mol Cell Biol. 2008 May;9(5):391-401.

10. Tomko EJ, Fischer CJ, Niedziela-Majka A, Lohman TM. A nonuniform stepping mechanism for E. coli UvrD monomer translocation along single-stranded DNA. Mol Cell. 2007 May 11;26(3):335-47.